2012

Investigation of electroosmotic flow dynamics and reproducibility in capillary electrophoresis

Funda Kizilkaya
Louisiana State University and Agricultural and Mechanical College

INVESTIGATION OF ELECTROOSMOTIC FLOW DYNAMICS AND REPRODUCIBILITY IN CAPILLARY ELECTROPHORESIS

A Dissertation

Submitted to the Graduate Faculty of the
Louisiana State University and
Agricultural and Mechanical College
in partial fulfillment of the
requirements for the degree of
Doctor of Philosophy

in

The Department of Chemistry

by
Funda Kizilkaya
B.S., 9 Eylul University, 1998
December 2012

DEDICATION

I dedicate this dissertation to my wonderful family, my husband, Orhan, who always encouraged and supported me through the years of research, and to our precious kids, our son Ekrem Eren and our daughter Aliye Rana who are joys of our lives.

ACKNOWLEDGMENTS

I would like to acknowledge and extend my heartfelt gratitude to my parents, my mother Ünzile Kurtbörü, my father Tahsin Kurtbörü and my late grandfather Sıddık Kurt for their endless love and support during my education years.

I would like to thank my advisor, Dr. S. Douglass Gilman for his patience, guidance, support and understanding through my years in the graduate program.

I would like to recognize and thank my dissertation committee members, Dr. Isiah Warner, Dr. Kermit Murray, Dr. Bin Chen and Dr. Jose A. Romagnoli for their valuable comments.

Also, I would like to thank past and present Gilman group members: Yohannes Rezenom, Rattikan Chantiwas, Rachel Henken, Sherrisse K. Bryant, and Suresh Regmi. I appreciate all their help and support during my journey in the graduate school.

I also would like to thank Dr. Kresimir Rupnik and Dr. Catherine Situma for their guidance during my responsibilities as a teaching assistant.

TABLE OF CONTENTS

LIST OF TABLES

Table **Page**

LIST OF FIGURES

Figures **Page**

ABSTRACT

The goal of this dissertation is to investigate electroosmotic flow (EOF) and electric field dynamics during capillary electrophoresis (CE) experiments using methods based on periodic photobleaching of fluorophores added to the separation buffer at nanomolar concentrations. The methods provide time resolved EOF and local electric field information during an experiment, which can be applied to fundamental studies to provide better understanding of CE techniques.

The potential of the EOF monitoring method to improve CE migration reproducibility was investigated in Chapter 2. The EOF monitoring method and four other methods from the literature were applied to the same electrophoretic separations, and their performance for improving reproducibility was compared. The EOF monitoring method significantly improved migration reproducibility, in general; however, much simpler neutral marker method performed nearly well.

Biological sample adsorption is a common cause of EOF variability and poor reproducibility for CE. In Chapter 3, the effects of biological samples on EOF dynamics were investigated. Model compounds representing major components of a biological cell and complex biological samples were introduced into the CE system while EOF was monitored continuously. Due to sample adsorption, EOF rates decreased and vacancy peak widths, used for EOF monitoring, increased. It was found that protein molecules had the greatest impact on EOF.

Discontinuous solutions in a capillary (zones of different pH, ionic strength or composition) result in generation of different EOF and local electric fields down the length of the capillary. The EOF monitoring method was expanded by adding a charged marker (fluorescein), and this improved method was employed to investigate EOF dynamics and local electric field changes during CE with discontinuous solutions, which were generated by introducing a low

ionic strength buffer zone into the capillary. Faster EOF rates in the capillary and faster fluorescein electrophoretic velocities within the sample plug were observed due to high local electric field. Unexpected fluorescein concentration changes were observed during the experiments. These observations led to use of computer simulations in an attempt to understand and reproduce the electrophoresis results. The simulation results, which were obtained using Simul 5.0 indicated the experimental results are consistent with the CE theory.

CHAPTER 1
INTRODUCTION

1.1. Capillary Electrophoresis Reproducibility

Capillary electrophoresis (CE) has become a well-established analytical separation technique, and several research groups have contributed to the development of this widely used method. In 1967, Hjerten developed rotating tube electrophoresis utilizing 1-3 mm internal diameter (i.d.) quartz capillaries and described the results in a report about free zone electrophoresis [1]. Later, Virtanen employed 0.2-0.5 mm i.d. glass capillaries with potentiometric detection [2], and Mikkers et al. reported rapid and highly efficient separations with a 0.2 mm i.d. Polytetrafluoroethylene (PTFE) narrow-bore tube and UV absorbance detection [3]. In 1981 Lukacs and Jorgenson employed 75 μm i.d. glass capillaries with fluorescence detection for amino acid and peptide separations [4]. This report is credited with introducing modern capillary electrophoresis to the scientific community and led to its widespread use.

Capillary electrophoresis can be considered a hybrid separation technique combining aspects of gel electrophoresis separations in a planar format with the column format and detection approaches used for HPLC. In CE, analytes separate based on their electrophoretic mobilities under an applied electric field. Electrophoresis is a very common method for protein separations, but the separation medium is usually a slab gel. The basic mechanism for gel electrophoresis is related to the migration of different sized macromolecules through pores in the gel. The typical problems that occur when using gel electrophoresis such as Joule heating, quantification and long analysis times are greatly reduced when electrophoresis is carried out in a capillary [5-7]. The capillary employed for CE as a separation column typically has an inner diameter of 25-100 μm with two ends of the capillary placed in vials that contain buffered

aqueous solutions. The buffer solution also fills the capillary to provide a conductive separation medium. The vials house two electrodes, which are connected to a high voltage power supply to apply the electrophoretic potential as shown in Figure 1.1.

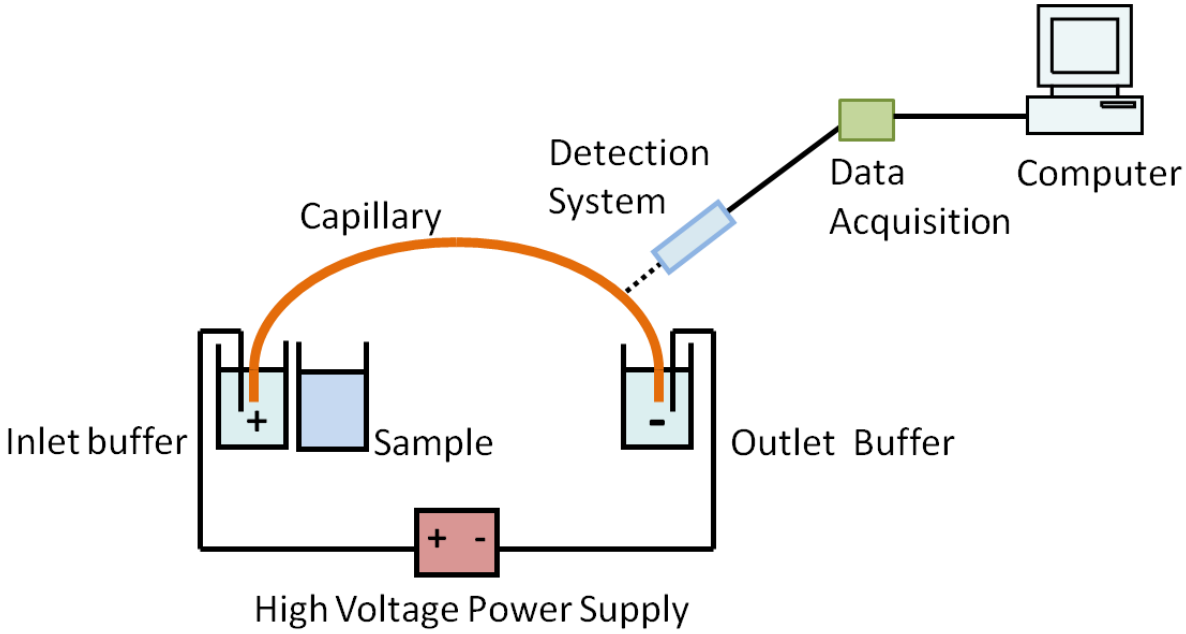

Figure 1.1 Schematic showing components of a basic capillary electrophoresis system.

Since the CE capillary has a high surface-to-volume ratio, problems associated with Joule heating are greatly reduced compared to gel electrophoresis. Additionally, the development of commercial CE instruments has included automation of sample handling and injection, which lessens total analysis times and improves reproducibility. Also, capillary array electrophoresis can further reduce total analysis times through parallel analysis of as many as 384 samples [5, 6, 8]. Many aspects of CE separations, sampling and data treatment are similar to HPLC, including the figures of merit used for characterizing the separation and quantification of analytes.

Separation efficiency is directly related to plate height in chromatography. It can be represented by the van Deemter equation, which describes the relationship between plate height (H) and factors that affect it, as seen in Equation 1.1. One of the main differences and advantages of CE relative to HPLC is that there is no stationary phase for basic CE. As a result, two of the factors that cause band broadening and low separation efficiency in HPLC separations are eliminated. These factors are represented by the multiple path term (A_i), which is affected by the space between the packing material in the column and the mass transfer term (C_s), which is the time required for solutes to equilibrate between the stationary and mobile phase. The flat flow profile of electroosmotic flow (EOF) further reduces band broadening in CE. The plate height equation also takes into consideration the effects of longitudinal diffusion (B), mobile phase term (C_m) and the mobile phase flow rate (v).

$$H = \frac{B}{v} + \sum \left[\frac{1}{(1/A_i)+(1/C_{mi}v)} \right] + C_s v \qquad (1.1)$$

As seen from Equation 1.1, longitudinal diffusion is the only factor that should cause band broadening in CE because of the open tubular nature of the capillary and flat flow profile. This makes CE separations highly efficient with corresponding high peak capacities. Additionally, CE uses small injected sample volumes (typically 1-10 nL), which is important for volume-limited samples.

Because of these advantages, CE has been applied to a broad range of scientific problems extending from biology to the environment [7, 9-11]. The most commonly used detection method for CE is UV absorbance. With this detection method, limits of detection (LOD) and limits of quantification (LOQ) in CE are generally higher (10^{-5}-10^{-6} M) than for HPLC because of the relatively short optical path (50-100 μm) compared with HPLC (10 mm) [12]. There are several strategies used to improve detection limits for CE with UV absorbance detection, such as

sample stacking, using a bubble cell, increasing the capillary diameter and injection volume, and adjusting the detection wavelength to eliminate the background signal that is increased by the buffer's absorbance [13]. In addition, the linear dynamic range of UV absorbance detection for CE is more restrictive than the range for HPLC because of the circular geometry of the capillary used for detection, which increases scattered light.

The LODs in CE are better for fluorescence detection. It is possible to detect even a single molecule [14, 15]. The typical LOD values for CE/MS (low micromolar range) are similar to the values for UV absorbance detection [16]; however, with the development of more sophisticated approaches, the LOD can be reduced to the low nanomolar range [17]. Derivatization of the analyte is another way to increase the number of options for CE detection [18, 19]. In addition, indirect detection can be used [20, 21]. When utilizing indirect detection, the background buffer absorbs or fluoresces at the detection wavelength, and the analytes, which do not absorb or fluoresce, are detected as negative peaks. The LOD values for indirect detection methods are typically around 10^{-6} M [16].

It has been recognized since the early days of CE development that reproducibility (migration time and peak quantification) is a significant limitation for CE compared to other separation techniques, particularly HPLC [6, 16, 22-26]. The performance of HPLC and CE has been compared directly in some quantitative studies. In a bioassay, better precision for HPLC (2.7% RSD) than for CE (6.0% RSD) was reported [24]. For the determination of parabens in a cosmetic product, repeatability values of 0.4-1.1% RSD for HPLC and 0.8-2.2% RSD for CE (for five consecutive runs) was noted [27]. In another study, the performances of HPLC and CE were compared for determination of diazepam in pharmaceutical tablets, and RSD values of 0.4-1.0 % for HPLC and 0.9-1.6 % for CE in ten successive experiments were obtained [28].

Quantitative determination of ketoconazole in pharmaceutical products was performed with both methods, and HPLC provided better precision (0.2-1.2% RSD) than CE (2.2-3.0% RSD) [29]. One of the main reasons for CE not being utilized as extensively as HPLC in industry or as an approved separation method for analysis is its relatively poor reproducibility.

Capillary electrophoresis is also carried out in channels based on microchip technology, which provides even smaller i.d. separation channels, reduced reagent consumption, low waste production, portability and fast separation times [7]. Reproducibility issues are also common in microchip electrophoresis and the fundamental causes of poor reproducibility and basic separation mechanisms are the same in capillaries and microchips. However, it is often preferable to carry out fundamental investigations of CE reproducibility in a capillary electrophoresis system, since capillaries are less expensive and simpler to use.

1.2. Causes of Poor CE Reproducibility

Relatively poor reproducibility for CE is a problem for both migration times and analyte quantification. Migration time reproducibility is important because it is crucial for the correct identification of peaks. This is particularly true for complex electropherograms, which are produced for complex biological and environmental samples. Analyte quantification typically is based on peak area, which is proportional to the sample concentration. The accurate determination of an analyte's concentration in a sample mixture is critical for applications such as reporting drug impurity levels [30], determination of the quantity of an analyte in a commercial product [31-34], quantification of DNA in organelles [35], enzyme studies [36], proteomics [37] and quantification of an analyte in biological fluids [38]. There are several factors affecting CE reproducibility, which will be described in following sections of this chapter.

1.2.1. Migration Time Reproducibility

When an electric field is applied to a capillary filled with a buffered solution, ions in the capillary migrate in the field depending on their electrophoretic mobilities (μ_{ep}). Only molecules with a net charge have electrophoretic mobility, and neutral species do not migrate electrophoretically. However, the phenomenon called electroosmotic flow (EOF) makes migration of all species in the solution possible, regardless of their charge (Figure 1.2).

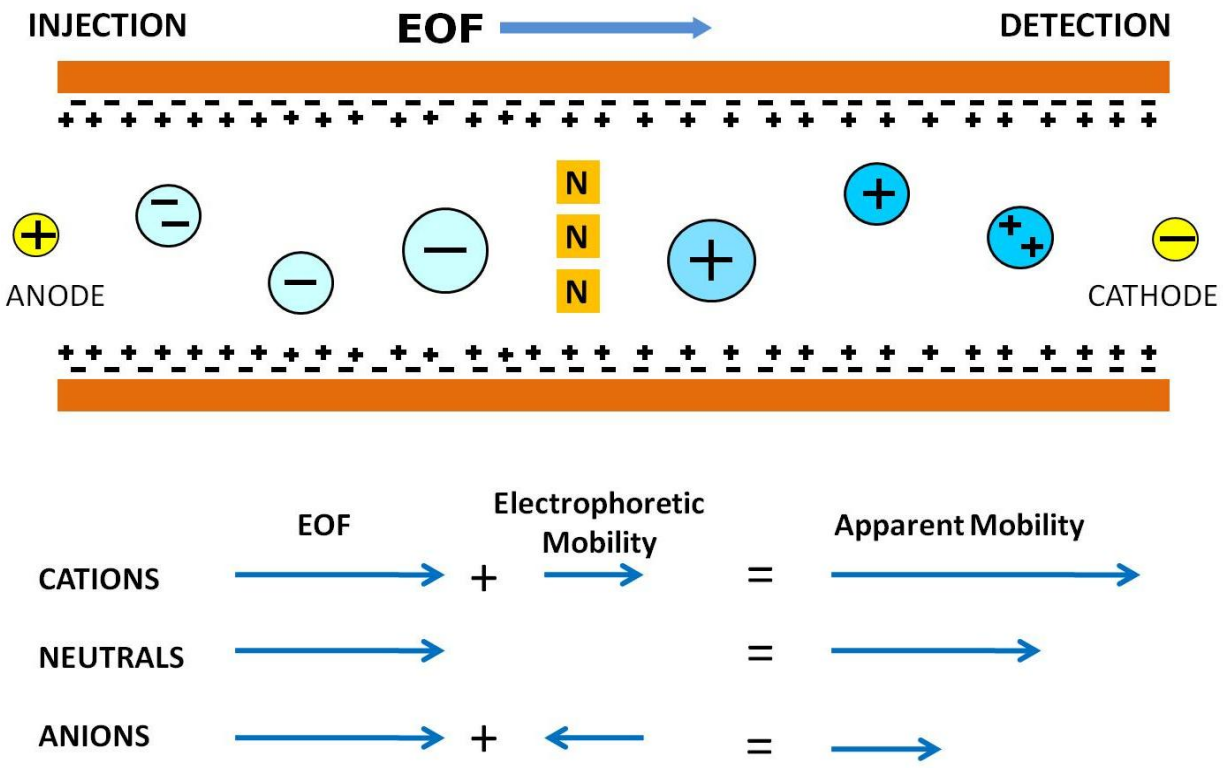

Figure 1.2 Schematic representations of the mechanism of CE separations. As illustrated at the top of the figure, cations and anions separate based on their electrophoretic mobilities, which are related to their charge-to-size ratios. Neutral molecules do not have electrophoretic mobility. They move with EOF. Apparent mobilities include the influence of EOF as indicated in the figure.

The EOF is one of the important advantages of CE separations. In the presence of strong EOF, all ionic species, as well as neutral species, migrate in one direction due to a combination of electrophoresis and EOF. For typical CE separations, cations arrive at the detection window first, due to the combination of EOF and the molecules' electrophoretic migration towards the cathode at the detection end of the capillary. Anion electrophoretic mobility is toward the anode, which is opposite to the detection point; however, the EOF typically is strong enough to transport anions toward the cathode. Anions reach the detection window last, since their mobility is the sum of the EOF and μ_{ep}. All neutral molecules move toward the detector at the rate of the EOF. The migration time (t), which is the time that it takes for an analyte to pass the detection point after its injection, is related to the analyte electrophoretic mobility (μ_{ep}), electroosmotic mobility (μ_{eof}), the total capillary length (L_t), the length to the detector (L_d) and the applied voltage (V). This relationship is summarized by the following equation:

$$t = \frac{L_d L_t}{(\mu_{ep} + \mu_{eof})V} \tag{1.2}$$

Changes in the applied voltage, electrophoretic mobility and electroosmotic mobility affect the overall migration time of an analyte. The electrophoretic mobility (μ_{ep}) and electroosmotic mobility (μ_{eof}) are described by the following equations:

$$\mu_{ep} = \frac{q}{6\pi\eta r} \tag{1.3}$$

$$\mu_{eof} = \frac{\varepsilon\zeta}{4\pi\eta} \tag{1.4}$$

In equations (1.3) and (1.4), q is charge of the analyte, η is viscosity of the buffer solution, r is analyte's hydrodynamic radius, ε is dielectric constant of the buffer solution, and ζ is zeta potential. Electrophoretic mobility is affected by temperature changes due to its relation to the

viscosity of the solution. During a CE separation, the analyte charge and hydrodynamic radius are constant as long as the separation solution remains the same. Any change in solution pH can change the charge on the analyte.

Electroosmotic mobility is also influenced by temperature changes, as well as changes in the surface chemistry of the capillary inner wall and the chemistry of the solution. This is due to the zeta potential dependency of electroosmotic mobility as indicated in Equation 1.4. The migration time reproducibility is highly affected by changes in EOF [39-43]. In some cases, the migration times of the analytes can change by 10-20% in a regular laboratory setting during a single day [41, 44].

Migration time reproducibility is important for accurate analyte identification. Migration time reproducibility is mainly affected by EOF and temperature fluctuations which also influence the EOF. Additionally, the capillary, sample and buffer are important factors as well, since they have significant effects on EOF due to their relation to the zeta potential. These factors and their effects on separations in CE and migration times are discussed in the following sections.

1.2.1.1. Electroosmotic Flow

There are approximately three to seven ionizable silanol groups per square nanometer on a capillary wall [7]. The silanol groups on the capillary wall are negatively charged when the capillary is filled with buffer solution at pH values between 3 and 10. The amount of negatively charged groups differs depending on the pH and ionic strength of the separation buffer. A double layer occurs at the surface of the capillary wall due to coulombic attraction between positively charged ions from the buffer and the negatively charged silanol groups. This double layer has two regions, a fixed (Stern) layer and a diffuse layer (Figure 1.3). The fixed layer is immobile

even with an applied electric field. At the boundary plane (plane of shear) between the fixed layer and the diffuse layer, an electrical potential develops, which is called the zeta potential (ζ).

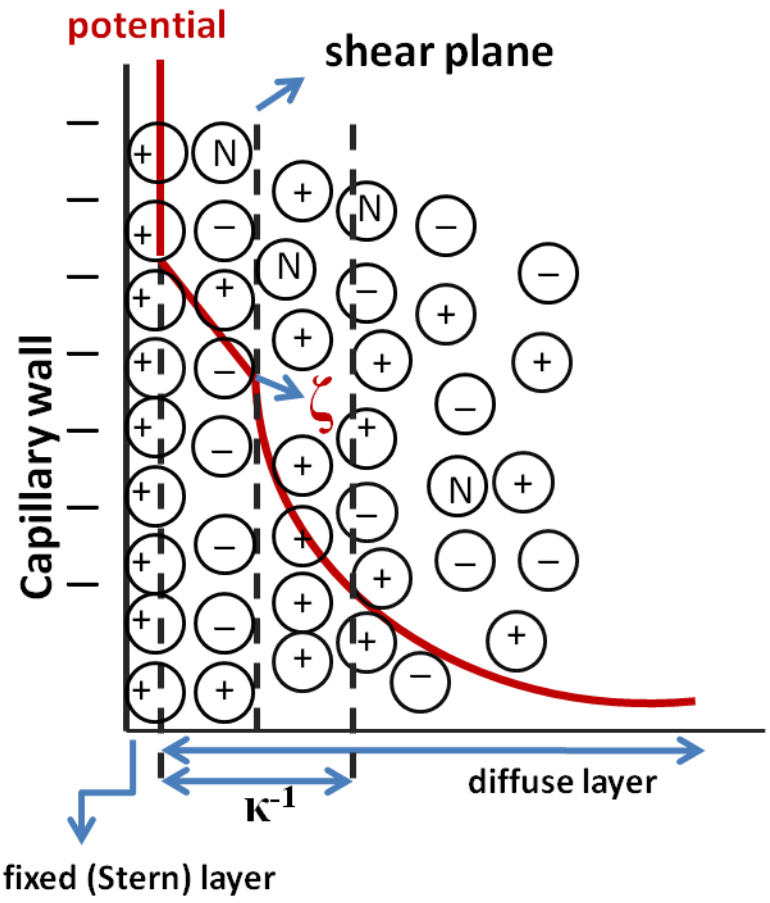

Figure 1.3 Schematic representation of the electric double layer at the capillary wall. The red line represents the potential drop across the capillary wall.

The zeta potential is a complex quantity that depends on the surface potential of the capillary wall and the composition of the electrolyte solution. It can be represented by Equation (1.5) where δ is the thickness of the double layer, e is the total excess charge in solution per unit area and ε is the dielectric constant of the separation buffer.

$$\zeta = \frac{4\pi\delta e}{\varepsilon} \tag{1.5}$$

The double layer thickness (δ) is the reciprocal of the Debye-Huckel parameter (κ) and can be expressed using Equation 1.6 where ε_0 is the permittivity of the vacuum, ε is the dielectric constant, R is the universal gas constant, T is the absolute temperature, F is the Faraday constant, and I is the ionic strength.

$$\delta = \sqrt{\frac{\varepsilon_0 \varepsilon RT}{IF^2}} \tag{1.6}$$

The zeta potential drops exponentially to zero from the interface through the diffuse layer (Figure 1.3). The distance over which the zeta potential drops to zero is the thickness of the double layer, which typically is around 100 Å. Due to the applied field, the solvated cations in the diffuse double layer start to move toward the cathode, and they drag solvent with them. This phenomenon is called electroosmotic flow (EOF) which acts like a pump in HPLC but without the mechanical complexity of an HPLC pump [45]. One advantage of EOF relative to pressure-driven flow is that the flow profile is relatively flat across the capillary diameter. This flow profile results in highly efficient separations for CE relative to HPLC [45]; however, EOF is a double-edged sword. It is very sensitive to chemical changes at the capillary surface and changes in the separation buffer as indicated in Equation 1.4, where μ_{eof} is the electroosmotic mobility and η is the viscosity of the solution. The surface chemistry of the silica surface, which is represented by the double layer thickness (δ) and charge in solution per unit area (e), affect the zeta potential. Interactions of sample molecules with the capillary wall, and differences in ionic strength of the buffer used cause a nonuniform zeta potential down the length of a CE capillary. In addition, temperature fluctuations play an important role in EOF, since temperature has an impact on the double layer thickness, as well as the viscosity of the solution. Due to its

sensitivity to changes in these factors, EOF is one of the main causes of poor reproducibility for CE [6].

1.2.1.1.1. Capillary

The capillary is an essential part of a CE experiment. Its surface chemistry is the main reason for the EOF in CE. The capillary structure is not as complex as an HPLC column, but the interactions of the capillary with the electrolyte solution and analyte molecules have significant effects on CE separations and reproducibility. Fused-silica capillary used for CE is produced in batches by drawing the preform, which is a larger fused silica tube, through an oven at a certain drawing speed [46]. There are reports that indicate a concern about the batch to batch reproducibility of capillary production[46, 47]. Unfortunately, the capillary dimensions are not completely under the control of the operator. The inner diameter of the capillary, as reported by the manufacturer, is only a mean value and can vary significantly over several meters of capillary [24, 41]. The capillary is generally cut from the batch to a desired length. The edges of the capillary should be carefully trimmed to ensure that they are straight, which prevents the effects of sample carryover, diffusion and droplet formation [46]. The tip shape can also cause distortions in the shape of the sample zone and EOF, as well as baseline shifts, zone broadening and poor resolution [24, 48-50].

Charge characteristic of the inner wall of the capillary, which depend on the pH and chemical composition of the separation electrolyte, are essential to a CE separation. The capillary commonly is conditioned with NaOH, water and separation buffer before being used for the first time and before changing to a new buffer solution. The conditioning steps and amount of solution used should be the same for every conditioning [25]. As a general principle, the capillary should be rinsed with the separation buffer in between runs [51]. In addition, it may

be necessary to recondition or regenerate the capillary wall surface to maintain the same charge characteristics between the runs for experiments with adsorbing species [7, 25, 48, 51].

The inner wall of the capillary can be dynamically or permanently coated with molecules such as polymers to prevent sample adsorption to the inner wall for some applications [52, 53]. The permanent wall coating acts as a capillary wall, and it is important to have the same chemical structure for long periods of time for reproducible results. This coating can degrade over time and be more susceptible to adsorption of sample molecules, which impacts the quality of separation. For dynamic coatings, it is important to have a routine application and rinsing process in order to maintain the same coating quality between the runs.

1.2.1.1.2. Sample

Capillary electrophoresis is commonly used for biological applications. Biological samples such as proteins, DNA, biological fluids, cells, and tissue are common. The multiple charge sites on the molecules of these samples can result in adsorption to the capillary wall due to the columbic attraction between the molecule and negatively charged silanol groups on the capillary wall, even if the overall charge of the molecule is neutral. This adsorption changes the zeta potential at the shear plane, and it can cause charge reversal and magnitude increase [54]. Nonuniform zeta potential consequently affects the EOF and migration times of the analytes [25, 45, 55-57]. Researchers have developed several strategies to prevent this problem such as working at extreme pHs [58], rinsing before and after each run [59], using buffer additives, and using dynamically or permanently coated capillaries [55].

1.2.1.1.3. Buffer

The buffer solution filling the capillary during electrophoresis, which is also referred to as the background electrolyte, is a crucial component of a CE separation. It provides a separation

medium with constant pH, since the buffer solution can resist pH changes. The reproducibility is seriously affected by the changes in the pH and concentration of the buffer. The pH change affects the charge of the sample species and the magnitude of EOF [60-62]. Any fluctuation in the buffer concentration alters the double layer thickness and thus the zeta potential and EOF. Because of these detrimental impacts on the reproducibility, considerable care should be given to choosing and using a buffer solution for CE separations [63].

Changes in pH can be caused by buffer depletion over time due to the electrolysis of water that takes place at the electrodes. This causes OH^- ions to form at the cathode and H^+ ions at the anode. According to Faraday's Law, the quantity of the ions generated or consumed in electrolysis is proportional to the quantity of electricity transferred, which is the product of the electrolytic current and the elapsed time [64]. This leads to the buffer at the anode becoming more acidic and the buffer at the cathode becoming more alkaline as electrophoresis takes place [23, 61, 62, 64]. The buffer salts and modifiers are also subject to electrolysis, which results in the formation of degradation products that can influence the EOF by changing the composition of the electric double layer. Utilizing high voltage, high ionic strength buffers and long run times enhance the buffer depletion, which cause pH drift at the electrodes [59, 60]. The degree of electrolysis and its impact depend on the buffer capacity [64], the volume of the buffer vials [61], duration of the run and applied voltage [62]. Most importantly, high current generation causes Joule heating, which leads to formation of nonuniform temperature gradients and zone broadening.

Low concentration buffers are not appropriate for eliminating the electrolysis effects, since they do not have enough buffer capacity to compensate for pH changes. One solution to this problem is the use of low mobility zwitterionic buffer solutions, which contain large

minimally charged ions, such as tris-(hydoxymethyl)methylamine (Tris) and 2-(N-morpholino)ethanesulponic acid (MES) [61]. Zwitterionic buffers contain both positively and negatively charged groups; therefore, at the buffer pI value, the buffering ions will not migrate toward the electrodes and carry little or no current. These buffers allow for a ten-fold increase in buffer concentration without generation of excessive Joule heating [61, 65, 66]. One way to minimize the run-to-run changes in pH and EOF due to the electrode reactions is to use fresh buffer for each run [60, 64]. Replacing the buffer solution frequently makes separations more reliable and the capillary surface uniformly charged. Some adjustments such as replacing the buffer vials and rinsing the capillary with the fresh buffer can be included in the sequence of an instrument program [61].

Buffer concentration can change during CE experiments due to evaporation, which leads to poor reproducibility [67]. It is mainly caused by high temperatures in the room or in the autosampler tray. Evaporation is worsened by uncapped buffer vials and long run times. Recent instrumental developments included using capped vials and thermostated trays [24]. Also a thin layer of mineral oil can be placed on the surface of the buffer solution [68, 69].

One of the buffer related problems is buffer contamination during sample injection. Sample carryover, which is caused by adsorbed sample molecules on the outer capillary surface, can be problematic because it can cause contamination of the solutions, sample and buffer. This can be avoided by washing the capillary with water before the injection and injecting a water plug after the injection, removing the polyimide coating from the tip of the capillary, rinsing the capillary tip by dipping it into a fresh buffer solution [70] and renewing the electrolyte solutions regularly [24]. Using two buffer containers (one for conditioning, one for separation) is useful for more reproducible results [67].

1.2.1.2. Temperature Fluctuations

Inevitably, heat is generated when an electric field is applied to a capillary tube filled with a conducting solution. This heating is known as Joule heating. As Joule heating occurs in the capillary when the electric field is first applied, the electrical conductivity and current increase. Consequently, the temperature rises both radially and axially until a steady state is reached when the heat generation is balanced by the conduction of heat to the surroundings [45, 71]. The heat generation is equal to the electrical power generated per unit length of the capillary as seen in Equation 1.7:

$$P/_L = KCr_c^2E^2 \tag{1.7}$$

where P is the power, K is the molar conductance of the buffer, r_c is the capillary radius and E is electric field [45, 72]. Based on this equation, there is less thermal load which must be dissipated by the CE system when smaller capillary radius is employed, which provides a higher surface area to volume ratio and enhanced heat dissipation ability.

$$\eta = 2.761 \times 10^{-3}(e^{\frac{1713}{T}}) \tag{1.8}$$

Viscosity is related to temperature according to Equation 1.8, where η is viscosity and T is temperature. [71]. The viscosity decreases with increasing temperature, which increases μ_{eof} and μ_{ep} as indicated in Equations 1.3 and 1.4. The electrophoretic mobility of an analyte can change 2% per °C because of the relationship of buffer viscosity to the mobilities [23]. In addition, temperature significantly affects the zeta potential as indicated by the following equation:

$$\zeta = -\frac{2RT}{F} sinh^{-1}\left(\frac{\sigma_w}{8RT\varepsilon_0\varepsilon\, c^{\frac{1}{2}}}\right) \tag{1.9}$$

where σ_w is the charge density on the capillary wall and c is the buffer concentration. The magnitude of the zeta potential increases with increasing temperature [73]. When these factors

are taken into account, it is clear that temperature has a significant effect on the migration time of an analyte [25, 74].

In addition to its effect on the capillary wall chemistry, high temperatures in the capillary can cause superheating, boiling of the buffer and formation of microbubbles. Additionally, changes in pH and charge characteristics occur as a result of temperature increase. Depending on the structure of an analyte, the high temperatures can change the analytes' net charge and configuration. This effect can be even more significant for bioanalytical applications since temperature increases could affect the stability of the analyte and cause protein denaturation. Consequently, temperature fluctuations affect both migration time and analyte quantification reproducibility [23, 24, 74, 75]. These affects can be prevented by lowering the electrophoretic current and enhancing the heat dissipation. Several approaches to achieve this are decreasing the ionic strength or conductivity of the buffer, using a smaller ID capillary, using a larger OD capillary and applying a lower separation voltage [24, 76, 77]. For commercial instruments, capillary thermostating using liquid cooling or forced air convection, offers a good solution to this problem [24, 74, 76, 78].

1.2.2. Reproducibility of Analyte Quantitation

In CE, the procedures used to perform quantitative analysis are similar to HPLC methods [79]. Standard addition or construction of calibration curves are based on the detection response from the analyte and employed to determine its concentration. Usually, peak areas are used to construct the calibration curve instead of peak heights. It has been reported that the linear range of a calibration curve set up based on the peak heights is small, especially at high concentrations, due to peak broadening [6, 13, 22, 23, 47].

Reproducibility of analyte quantification in CE has been a subject of several review papers [16, 23, 24, 79, 80]. Generally, HPLC provides better precision than CE. For example, HPLC offers 0.8% RSD for analyte peak areas whereas CE offers 1.6% RSD for quantification of insulin [69]. In the following sections in this chapter, the major factors that affect quantitative reproducibility for CE are discussed.

1.2.2.1. Injection

Quantitative reproducibility is closely related to the reproducibility of the sample injection [23, 25, 68]. Non-ideal injections can cause irreproducible results. Typical RSD values for an HPLC injection are about 1% due to the well controlled loop-fill type of injection with volumes on the order of 5-50 µL. On the other hand, for a CE instrument, 5-50 nL injection volumes are common, and loop injectors are not suitable for these small volumes which are typical in CE experiments due to small capillary size [6, 45, 68]. It is preferable to have small sample volumes in order to decrease band broadening; however, small sample volumes result in poor reproducibility. Precise control of the injection device is difficult and might be a problem for hydrodynamic injections, especially when using short injection times (~1 s). Diffusion of the analyte in and out of the capillary is problematic, resulting in reduced reproducibility. It has been reported in the literature [81] that solution can enter into a capillary after a brief contact, and this affects the separation efficiency by causing zone broadening. The nature of diffusion for the different sample molecules makes it hard to control; however, increasing the electrolyte viscosity is helpful. Reproducible and short delay times for the capillary end to move from one vial to another vial can be applied to control this effect. The diffusion effect is even more pronounced at shorter injection times and for smaller molecules, since they have higher diffusion coefficients than larger molecules [24, 82]. Longer injection times (~5 s) can be employed to overcome this

problem [59]; however, long injection lengths are undesirable due to problems with sample overloading such as peak distortion, low separation efficiency and poor precision. Therefore, the injection length should be short. Using a capillary with a larger i.d. can increase the sample volume [24, 83].

Moving the capillary tip from one solution to another during the sample introduction and electrophoresis processes causes exposure to air which can result in problems for the separation [59] such as evaporation, droplet formation, siphoning and sample movement on the outside of the capillary [68]. Sample evaporation can be problematic, especially when using an organic solvent to prepare the sample. An evaporation rate of 0.05 nL/s was observed for sample volumes about 5 µl [80]. Usually, the sample and buffer vials are not capped during the experiments to allow the capillary to go into the vial. Therefore, the solvent can evaporate and this changes the concentration. Vial caps can be placed on the vials and also a thin layer of mineral oil can be placed on the surface of the buffer solution as in the case for the separation buffer [50, 68, 69]. Droplet formation at the capillary tip when the capillary is removed from the sample solution is another cause of irreproducibility. It can be prevented or controlled by having a straight edged capillary, removal of the polyimide coating at the capillary tip, capillary surface roughness modification and reducing the noise and vibration within and around the instrument [24]. Furthermore, unwanted siphoning should be avoided since it causes variable injection volumes and band broadening [59, 68]. Siphoning is caused having height differences between the capillary tips at the inlet and outlet vials and by having different liquid levels at the inlet and outlet vials. The effects of siphoning can be reduced by taking some precautions such as leveling the liquid heights [82], usage of restrictors at the ends of capillaries [83], or using a viscous background electrolyte [82].

Several methods were developed to improve injection performance such as using a split injector [84], auto sampler [85], on-column fracture/electrokinetic injection [86]. The two most commonly used sample introduction methods are hydrodynamic (HD) and electrokinetic (EK) injections [23, 85, 87].

1.2.2.1.1. Electrokinetic Injection

An electrokinetic injection is performed by applying an electric field to a sample solution, and the analyte molecules enter into the capillary by electrophoretic migration and EOF. The amount of sample injected by electrokinetic injection is expressed by Equation 1.10;

$$Q = \left(\mu_{ep} + \mu_{eof}\right) U t_i \pi r^2 c_s L^{-1} \qquad (1.10)$$

where Q is the injected volume, c_s is the sample concentration, U is the injection voltage, t_i is the injection time, L is the capillary length, and r is the capillary inner radius. As seen in Equation (1.10), the factors affecting the EOF also affect the amount of sample injected and thus affect the reproducibility. The electrophoretic mobilities of analytes depend on analyte charge. Consequently, cationic species will be injected more compared to anionic species. This effect is referred to as injection bias and has been recognized since the early publications of CE [4, 88, 89]. A second type of bias is due to the differences between the separation buffer and sample buffer [88]. The injected sample amount is dependent upon the nature of the sample matrix since the mobility of sample ions and EOF depend on pH and conductivity of the sample solution. Differences in sample matrices limit the comparability of peak areas of analytes, even though the sample concentration is constant. Thus, hydrodynamic injection is preferred over electrokinetic injection, especially when analyzing biological samples like plasma or urine with varying composition and conductivity [24]. Hydrodynamic injection provides reproducibility values of 0.2-2 % for migration times and 2-5% for peak areas [88]. Additionally, as the current flows

through the sample during electrokinetic injection, an electrochemical reaction might occur, resulting in some products being formed, which will lead to the sample being contaminated and damaged, especially when one uses small sample volumes [85].

1.2.2.1.2. Hydrodynamic Injection

Hydrodynamic injection utilizes pressure to inject the sample into the capillary. There are two ways to accomplish hydrodynamic injection. One is to use a pump to generate pressure or vacuum in the capillary, and another method is siphoning or gravity injection where the height difference between inlet and outlet vials is increased [45, 88]. Hydrodynamic injection is unbiased to the different components of the sample solution, so it is assumed to be the most reliable sampling method. It is affected if the viscosity of the buffer changes due to temperature differences between the buffer vial and the capillary caused by poor thermostating, as seen in the Equation (1.11) where Δp is pressure difference.

$$Q = \frac{\Delta p \pi d^4 t_i}{128 \eta L} c_s \tag{1.11}$$

In addition, this injection method's reproducibility is crucially dependent on the t_i and Δp and thus, a precise mechanism to control pressure is necessitated [45]. This usually requires the addition of complicated equipment to a very simple separation system. The hydrodynamic injection process causes large RSD values for short injection times [59]. Reproducibility values of 0.1-0.5% for migration times and 0.5-3% for peak areas were obtained by using this type of injection [88]. Additionally, the parabolic flow profile of the sample zone causes peak broadening and consequently difficult peak integrations due to low signal-to-noise ratios.

1.2.2.2. Peak Integration

The precision of peak quantification for CE is related to the reproducibility of the peak integration. This could be more problematic when the electropherogram has asymmetric and

triangular shaped peaks [25]. Usually commercial CE instruments are available with built-in software for data analysis and system control. As a result, every commercial instrument uses its own software. This can be problematic when reporting figures of merit such as LOD and signal-to-noise (S/N) ratio, and transferring a method for CE experiments between laboratories. Faller et al. [25] compared several commercial CE instruments' software for precision in analyte quantification. These programs were grouped based on their generation. First generation software for CE instruments was initially used for HPLC instruments. Therefore, they do not take into account some specific situations for CE applications, such as small signal heights due to short detection path length and triangular shaped peaks. The new generation software was designed for CE instruments exclusively with the adjustments for integration and peak identification algorithms. The software that was specifically designed for CE produced lower RSD values compared to those designed for HPLC. All newer software produced similar RSD values within their group. The RSD values were very high when the sample concentrations were close to the LOD for all of the instruments. Additionally, it is essential to use a detection system with an optimum data sampling rate, since inadequate data sampling rates can lead to increased error in peak area determination [23].

1.3. Solutions to Poor CE Reproducibility

1.3.1. Migration Time Reproducibility

Improving the migration time reproducibility has been an important goal for CE practitioners since the beginning of CE. A number of methods have been proposed to address this issue and make CE a more widely used analytical separation method. In the following sections, these methods are discussed.

1.3.1.1. Markers

Electroosmotic flow must be measured in addition to migration time in order to report analyte migration as electrophoretic mobility. The neutral marker method is the simplest and most commonly used technique to determine EOF to calculate μ_{ep} [72, 90]. A neutral compound is injected with the sample, and electroosmotic flow is the only factor that affects the migration time of this neutral marker. Based on the migration time of the neutral marker peak, the average EOF rate can be determined. The neutral marker method has some fundamental limitations. For analytes migrating after the neutral marker (typically negatively charged compounds), any changes in EOF after the neutral marker peak is detected will not be accounted for in the calculation of analyte electrophoretic mobility. Likewise, for peaks migrating faster than the EOF, the average value of the EOF will include any flow changes after detection of the analyte until the neutral marker peak is detected.

The neutral marker method only reduces the effects of variation of the EOF. Therefore, additional markers haven been employed. Vespalec et al. [42] have reported a method which permits the determination of the "actual mobility" of the unknown. This can be determined from its migration time and the migration times of the two reference standards in the same electrophoresis run. The actual mobilities of the two reference standards, under a given set of conditions, must be known, as indicated in Equation 1.12, where μ_A and μ_B are mobilities of two standards, while t_A and t_B are migration times of the standards. This approach produces reproducible results under a variety of conditions and is reported to be independent of temperature.

$$\mu_x = \mu_A + (\mu_B - \mu_A)\frac{t_B}{t_x}\frac{t_A - t_x}{t_A - t_B} \qquad (1.12)$$

The standard mobilities must be known to correct for the migration changes in the experiments. This presents one of the challenges for the application of markers. Koller et al. [91] corrected the migration time of the analyte based on the migration times of two standards by using the following equations;

$$t_{corrected,x} = [\frac{1}{t_{m1,s}} - \frac{1}{\gamma}(\frac{1}{t_{m1}} - \frac{1}{t_x}]^{-1} \quad (1.13)$$

$$\gamma = \frac{\left(\frac{1}{t_{m1}}\right) - (\frac{1}{t_{m2}})}{\left(\frac{1}{t_{m1,s}}\right) - (\frac{1}{t_{m2,s}})} \quad (1.14)$$

where $t_{m1,s}$ and $t_{m2,s}$ are the migration times of two markers in a standard electropherogram while t_x, t_{m1}, and t_{m2} are migration times of the sample, and two markers under non-standard conditions. Improvements in qualitative and quantitative reproducibility were noted.

Jumppanen et al. employed 2, 3 and 4 marker compounds with known electrophoretic mobilities to correct the electrophoretic mobility of the analytes [92]. The chosen marker compounds were fully disassociated at the pH of the separation buffer, and their migration times covered the total run time of an electropherogram. In this method, electric field strength is assumed to be constant. For each marker technique, the time dependence of EOF was in a different approximation. For instance, for the two-marker technique, it is constant during the run, and it linearly increases for the three-marker technique. However, the acceleration is non-linear for the four-marker technique. The electrophoretic mobilities of analytes are solved based on various equations which change for each marker technique which are two-marker, three-marker and four-marker techniques. The coefficients of these equations were determined from the marker compounds' electrophoretic mobilities and migration times. Excellent reproducibility

was obtained with their technique (0.01-0.03 %); however, identifying three or four suitable marker compounds could be a challenge for some applications.

1.3.1.2. Migration Parameters

Several migration parameters have been introduced as a means to minimize irreproducibility for CE separations. These parameters were proposed to be employed to identify the analytes and be used as communication tools between different laboratories. Several migration parameters were compared by Lacunza et al. [40] to accurately assign bands of EPO isoforms separated by CE: migration time, migration time relative to an internal standard, migration time relative to the EOF marker (relative migration time) and electrophoretic mobility (μ_{ep}). It was mentioned that as the migration time difference between the analyte and the internal standard increased, the improvement in the reproducibility worsened for the internal standard method. They obtained very similar results for the relative migration time and μ_{ep} which provided the best reproducibility. In a study by Palmer et al. [41] the reproducibility of the migration time, relative migration time (based on a migration time of a charged standard), electrophoretic mobility, relative mobility (by using one neutral and one charged standard) and actual mobility (by using two charged standard) were compared. The main reproducibility problems arose due to fluctuations in EOF and temperature. The relative mobility and actual mobility presented the greatest performance for providing more reproducible results. They are independent of all parameters which the user does not control [41]. In the following sections, several parameters will be introduced and discussed.

1.3.1.2.1. Electrophoretic Mobility

The relatively poor reproducibility of migration time for CE makes it an unsuitable value to be used to transfer data between different labs [39-43]. A quantitative parameter which is

more reproducible is necessary to permit transfer of methodology. Such a parameter should depend only on the buffer composition and analyte properties and should be independent of temperature, applied field, capillary dimensions and EOF [41]. The electrophoretic mobility is dependent on the characteristics of the analyte, buffer and temperature, but it is free from the effects of zeta potential changes as seen in Equation 1.2. Therefore, it is preferred as a migration parameter by many CE users [23, 43].

Boone et al. used corrected effective mobility as a new identification parameter for CE [39, 93]. They corrected the μ_{ep} of analytes by interpolation between reference and measured μ_{ep} values of standards. They compared intra- and interinstrument reproducibility obtained with different mobility parameters and demonstrated that μ_{ep} is much more reproducible than the migration times and the use of corrected effective mobility did not improve reproducibility more than μ_{ep}.

1.3.1.2.2. Migration Time Ratio

Usually, a neutral compound added to a sample or the migration time of the solvent is used to determine the EOF. Since EOF is the main reason for poor migration reproducibility for CE, elimination of its effects on the migration times has been attempted. Chen et al. introduced the relative migration time, where the analyte's migration time is divided by the EOF marker's migration time ($t_{analyte}\backslash t_{marker}$) [94]. They demonstrated that the RSD values improved to 0.45% by using this parameter when the RSD's of the analyte migration times and EOF were 3.4% and 3.9%, respectively. A similar approach, using a mobility and migration time ratio, was introduced by Yang et al. [44]. The mobilities of the analyte and reference standard were divided, and the same procedure was repeated for the migration times as well. For their method,

the reference standard compound can be charged or neutral. In this report [44], a neutral compound (mesityl oxide) was used.

1.3.1.2.3. Migration Indices

Lee and Young introduced two parameters to express the migration of an analyte, migration index (MI) and adjusted migration index (AMI) [95]. The MI for an analyte is calculated by integration of i/L as a function of time, where i denotes current density (ratio of current to cross sectional area of the capillary) and L is the capillary length. By applying this index, it is possible to correct the fluctuations that occur in the temperature and electric field in the capillary; however, it requires use of capillaries with the identical zeta potentials which is very hard to control. Batch-to-batch differences occur for capillary characteristics even when the capillary is from the same manufacturer [46, 47]. For this reason, a second parameter, AMI, was further developed to include the MI of neutral marker in the calculations to eliminate the effect of EOF changes. This study reported reproducibility values as low as 0.05% by using AMI. This approach requires that the internal diameters of the capillaries be known within 0.5%, which presents a significant problem in the light of current capillary manufacturing technology [95].

1.3.1.3. Electropherogram Transformation

Normally in a CE electropherogram, migration times of the analytes are represented. As mentioned in sections above, migration time of an analyte includes the influence of the EOF; hence, it has poor reproducibility. In order to reduce the migration time fluctuations, there are some reports to use different parameters in the axis of abscissa instead of time. Transforming the migration time axis to the mobility axis has been proposed [96-100]. Schmitt et al. presented the migration data based on electrophoretic mobility on the x axis [99]. They were able to improve the results qualitatively and quantitatively. With this method, direct comparison of complete

electropherograms was possible. Ikuta et al. used two conversion methods, one based on the temperature coefficient and another based on the delay time and the temperature coefficient [100]. They were able to eliminate hardware dependent parameters such as E, V, L_d, L_t and v_{eof} and obtain very low RSD values (0.3%) for the mobilities of the analytes.

Iwata et al. made use of migration indices as reported by Lee and Yeung [95] by plotting the electropherograms as a function of quantity of electric charge (Q), which is product of migration index and volume of the capillary [101]. The RSD values of the migration times when this method was applied were between 0.9-4.1%. For the peak areas, the RSD values were between 4.7-9.4%. The authors indicated that voltage and temperature dependence of migration times and peak areas were eliminated by using the Q-electropherogram. In addition to aforementioned methods, Mammen et al. proposed to use *1/time* instead of migration time on the *x* axis. They demonstrated that this presentation was useful since it presented information that would have otherwise been overlooked in a regular time domain plot [102].

1.3.1.4. EOF Monitoring

Another approach to account for EOF fluctuations during a CE separation is to measure EOF during the entire separation and use this data to correct the electropherogram accordingly. Several approaches to measure EOF as a function of time have been reported in the literature. The heat index flow monitoring method is based on measuring a change in refractive index when a small heated volume enters the probe region [103, 104]. The heated zone is generated in a repetitive fashion by a laser [103] or by a heating coil [104]. The heated zone migrates with the EOF, thus the time it takes for this zone to travel within the capillary provides the EOF rate. However, the authors did not apply the EOF data to correct migration times in these reports. Saito et al. developed another method based on a heating zone generation in the capillary [105].

The permanent change of composition in the electrolyte, which is referred as a thermal mark, is recorded by a contactless conductivity detector and used to monitor the EOF. This method was used to correct for the mobilities of analytes and RSD values smaller than 1% were obtained. In a recent study, Seiman et al. applied the thermal marks method to investigate EOF rates for non-aqueous capillary electrophoresis in the presence of ionic liquids and obtained good reproducibility with a 1.3% RSD value [106].

Lee and Zare [107] monitored EOF by delivering a known amount of fluorescent dye to the buffer flowing out of the CE capillary, so that the dilution of the fluorophore was proportional to the EOF. They were able to detect flow changes as small as a 1% and obtain reproducible electrophoretic mobilities (2% RSD).

Gilman and coworkers introduced a method that measures EOF rates continuously based on periodic photobleaching of a neutral dye, which provides precise measurements of EOF over an entire separation, with a time resolution of ~1 s [108, 109]. In this method, the neutral fluorophore is added to the sample and separation buffer at nanomolar concentrations. It is photobleached periodically by a laser beam, which is blocked by a computer controlled shutter (Figure 1.4). When the shutter is opened, a photobleached zone is generated at position F1, and light is collected by an optical fiber and directed to a photomultiplier tube. A positive peak is generated when the shutter is opened, and this is used to mark the beginning time for an individual EOF measurement. The photobleached zone migrates with the EOF and is detected as a negative peak at position F2 (Figures 1.4 and 1.5). The time difference for this zone to travel from the photobleaching point (F1) to the detection point (F2) is used to calculate the EOF rate. This procedure is repeated as many as times as desired during an experiment. It is possible to monitor the EOF rates and obtain a precise EOF profile (0.2-1.8%) for an entire CE run with a

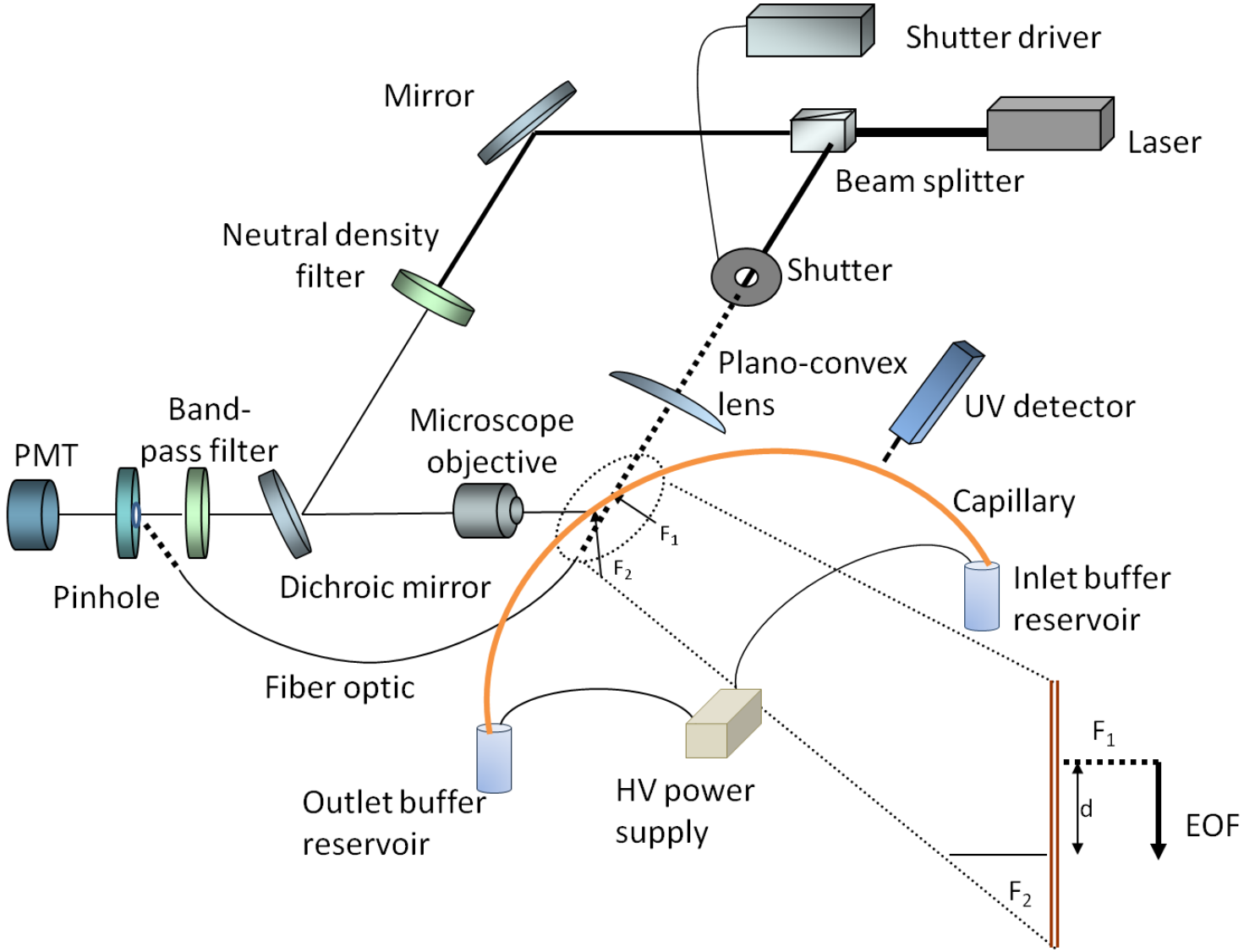

Figure 1.4 Schematic of the instrumentation for continuous EOF monitoring. The laser beam is focused at two different points on the capillary, F_1 and F_2. The first point, F_1, is where photobleaching takes place, and the second one, F_2, is where detection occurs.

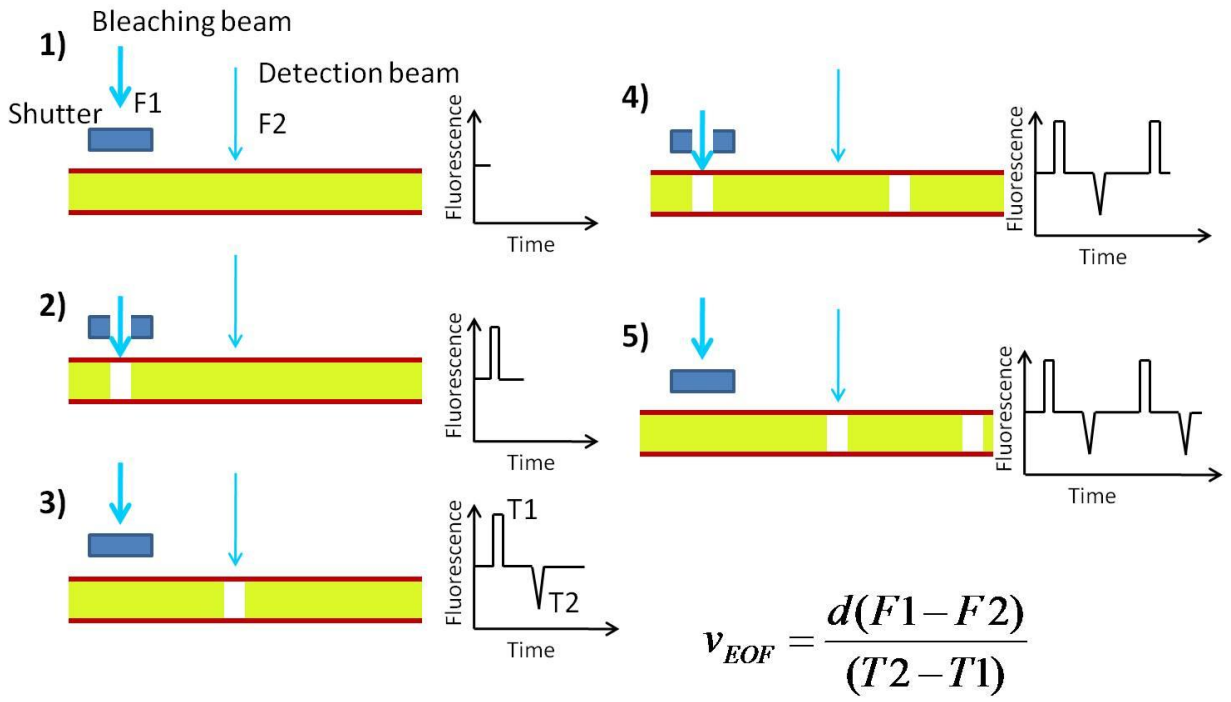

Figure 1.5 Schematic of the continuous EOF monitoring method. 1) The capillary is filled with neutral dye, and the shutter is closed. 2) The shutter is opened, and a photobleached zone is generated at F_1. A fiber optic collects the scattered light which is detected as a positive peak. 3) The photobleached zone migrates with the EOF and is detected at F_2 as a negative peak. 4 and 5) The procedure in steps 2 and 3 is repeated throughout the CE experiment. The EOF rate is calculated by dividing the distance between F_1 and F_2 by the time difference between the positive and negative peaks.

time resolution of 1 s using this method. This technique has been applied for fundamental studies of EOF dynamics [110, 111]. It has been demonstrated that this method can be applied simultaneously with other detection methods and does not affect the separation or detection. Figure 1.4 shows a UV absorbance detector in addition to the EOF monitoring CE system. There is potential to improve the reproducibility of CE using this method, since it is able to provide precise, time-resolved EOF information for an entire CE separation.

1.3.2. Analyte Quantification Reproducibility

1.3.2.1. Peak Area Corrections

Analytes travel and pass the detection window in CE at different rates in contrast to HPLC, where all the molecules have the same velocity after leaving the analytical column. The difference causes inaccurate peak areas because the slower analytes stay in the detection window for a longer period of time, and consequently, peak areas are overestimated [89, 112]. One way to overcome this effect is to normalize the peak areas by dividing them by their migration times[23, 30, 79, 89], as shown in the equation 1.15, where A_c is the corrected peak area, A_i is the peak area of an analyte, and t_i is the migration time of the analyte.

$$A_c = \frac{A_i}{t_i} \tag{1.15}$$

This correction is called the peak normalization or migration time-corrected peak area method. This quantity which is preferred over using peak area or peak heights because of its better precision, is also proportional to the sample concentration [24]. This method is required for cases where a significant drift in migration times exists, since the quantification will be inaccurate. It is common to compare results between HPLC and CE in order to report impurity levels in pharmaceuticals. Altria [30] reported that in order to have a good correlation between two separation methods, normalization of peak areas is crucial, especially when reporting the amount of drug impurities. In the case of peak tailing or fronting, application of an integration algorithm which uses a weighted integration system provides better RSD values than the regular peak area correction [25].

Most biological samples have solutions with different compositions than the separation medium. This decreases precision for electrokinetic injections due to differences in conductivity between the sample and the buffer. Leube et al. developed a calibration by regression using

matrix corrected peak areas (COPA) [113]. They aimed to compensate for all changes in the sample matrix using a normalized bias factor (F_{Mxi}), which describes the change of peak area of an analyte in a sample matrix of similar analyte concentration according to Equation (1.16):

$$F_{Mxi} = \frac{PA_{xi}}{PA_{cali}} \tag{1.16}$$

$$COPA_{xi} = \frac{PA_{xi}}{F_{Mxi}} \tag{1.17}$$

where PA_{xi} is the peak area of the analyte *i* in the sample matrix *x*, and PA_{cali} is the peak area of the analyte *i* in the sample solution used for calibration. Then matrix-corrected peak areas can be determined from the raw peak area data according to the Equation 1.17, where $COPA_{xi}$ is the matrix-corrected peak area of the analyte *i* in the sample matrix *x*, PA_{rxi} is the actual raw peak area data of the analyte *i* in the sample matrix *x*, and F_{Mxi} is the respective matrix factor calculated based on the Equation 1.17. By applying this method, the authors were able to improve precision and accuracy so that they were comparable to values obtained with hydrodynamic injection [113].

1.3.2.2. Internal Standards

Employing internal standards to improve precision is frequently used for CE as it is for HPLC [47, 68, 79, 114, 115]. The reproducibility problems related to quantification are caused by poor injection reproducibility (spontaneous injection, short injection time, inappropriate injection procedure, and pressure variations), temperature variations, sample evaporation and carryover [68]. An internal standard is added to the sample mixture, and it is affected by the same experimental conditions as the analyte molecules in the sample. The analytes' peak areas are corrected based on the internal standard peak areas by simply taking the ratio of the peak area of the analyte and the internal standard as was demonstrated by Fujiwara et al. [115] to

determine cinnamic acid. When using a single internal standard, it may be difficult to find a compound that has a migration time that is distinct from those of the analytes, but ideally the migration behavior of the internal standard should be similar to those of the analytes. Precision decreases as the difference between the migration time of the analyte and the internal standard increases [40, 68]. Using two internal standards is proposed to overcome this problem; however, it is desirable to have the migration times of the analytes fall between the migration times of the internal standards. This requirement makes it difficult to find proper standards and often increases the run times of the experiments. Additionally an internal standard should not be found in samples (before the internal standard is added). Also, the addition of the internal standard can affect the sample properties resulting in reduced accuracy and precision.

The Zare group employed an internal standard method to quantify low molecular weight carboxylic acids by conductivity detection [116]. They used Equation 1.18 to determine the concentration (*C*) of lactate based on the internal standard's peak area (*A*), concentration (*C*) and migration time (*t*).

$$\left[C_{analyte}\right] = \left[C_{standard}\right] \frac{A_{analyte}}{A_{standard}} \frac{t_{analyte}}{t_{standard}} \qquad (1.18)$$

Choosing an internal standard for a CE experiment is easier when compared to HPLC, since elution times of each candidate for an internal standard should be determined first, which requires additional runs [68]. Since, the internal standard should migrate close to the analyte, in CE it should have a charge-to-size ratio similar to that of the analyte [47, 68], which is easier to predict for CE. The main requirement however, is that the standard should be well resolved from the analyte peaks. It should be stable in the solvents used for sample preparation and at the pH that is being used. As a general prerequisite, toxicity levels should be minimal. The internal standard should produce a high signal S/N (≥ 30 [69]), and, therefore, its absorbance (for UV

absorbance detection) and emission wavelengths (for fluorescence detection) should be suitable for the detection system used for the target analytes.

As was mentioned before, using an internal standard is a common practice in HPLC. Several groups have compared CE to HPLC in terms of precision and sensitivity by employing internal standards [69, 117]. Kunkel et al. [69] were able to improve the precision for insulin analysis using CE to 0.5% RSD with internal standards. Williams et al. [117] demonstrated that CE was able to produce RSD values around 0.5% for the analysis of anthraquinone sulphonates.

Dose et al. [118] investigated the application of an internal standard method to improve the quantitative reproducibility for both hydrodynamic and electrokinetic injection. They defined response ratios R_i/R_A and R_i/R_B from a single calibration run, where R_i is the response factor of the analyte, R_A and R_B are response factors of the first and second internal standards, respectively. Equation 1.19 was used to calculate the ratios, where A_i and C_i are the peak area and concentration of the analyte, A_A and A_B are peak areas of the internal standards, and C_A and C_B are the concentrations of internal standards.

$$\frac{R_i}{R_A} = \frac{A_i C_A}{A_A C_i} \text{ and } \frac{R_i}{R_B} = \frac{A_i C_B}{A_B C_i} \tag{1.19}$$

Then, these were used to calculate the concentration, $C_{i,}$ of the analyte based on Equation 1.20. In the equation, t_i is the migration time of the analyte, F_i is the interpolation factor, and t_A and t_B are the migration times of the internal standards.

$$C_i = \frac{A_i}{R_i t_i [F_i \frac{A_A}{R_A C_A t_A} + (1-F_i) \frac{A_B}{R_B C_B t_B}]} \tag{1.20}$$

They were able to observe that using one internal standard for hydrodynamic injection is sufficient for good precision. The RSD values decreased from 5-6% for raw peak areas to 1% for corrected peak areas with one internal standard. However, for the electrokinetic injections, the

RSD values improved only slightly with one internal standard from 6.8% to 3.2 %. When a second internal standard was use, the improvement was significantly better (0.8 % RSD for two standards). It was also noted that larger RSD values were observed when the migration times of the analyte and the standard increased. They concluded that two internal standards are required to correct for the electrokinetic injection related errors, whereas for hydrodynamic injection, using a second internal standard might add systematic error to the analysis.

Peak normalization or migration time-corrected peak area method is a common practice as mentioned in Section 1.2.2.1. Some groups have compared its performance to improve precision with the internal standard method [69, 117, 119]. Kunkel et al. [69] obtained 1.6% RSD for normalized peak areas and 1.3% RSD with internal standard correction. In another study, Williams et al. [117] reported 1.9-2.2% RSD values for peak normalization and 0.4-0.9% RSD values using an internal standard. For clenbuterol analysis, 0.8-2.1% RSD values were obtained when peak normalization was applied, whereas the internal standard correction yielded 0.2-0.9% RSD values [119]. These reports indicate that while the normalization method offers acceptable precision values, the internal standard method improves the precision more.

1.4. Questions To Answer

1.4.1. Method Comparison

Reproducibility is a fundamental requirement for all analytical techniques that are used in research or industrial laboratories. Capillary electrophoresis has been limited by its poor reproducibility relative to HPLC. As mentioned in the previous sections, many approaches have been developed to reduce or eliminate this problem; however, more direct comparisons of these approaches should be performed to better evaluate their relative ability to improve CE reproducibility. There are simple methods such as the neutral marker method, where the

correction is based on the migration time of the EOF marker. Also, there are complicated methods such as the heat index flow monitoring method, where time-resolved EOF data are provided. Comparison of these methods would provide insight as to what approaches CE users should consider for their experiments.

1.5. Goals of This Research

Electroosmotic flow is a major component of any CE experiment. It is sensitive to the changes in the CE system. Often, it is suppressed to avoid reproducibility problems. The dynamics of EOF during CE experiments are not completely understood. A method has been developed by the Gilman group [108, 109] to continuously monitor EOF during a CE experiment. It provides precise and time resolved EOF information throughout a CE experiment. This method has the potential to bring insight into EOF dynamics.

The overall objective of this dissertation is to investigate EOF dynamics in capillary electrophoresis by using the continuous EOF monitoring method. The relationship between the research explained in Chapters 2-4 to the overall goal is described below.

Chapter 2. A continuous monitoring of EOF method was developed based on periodic photobleaching of a dilute neutral fluorophore by the Gilman group [108, 109]. In Chapter 2, this method was applied to correct CE migration times for EOF fluctuations in order to improve migration reproducibility. This approach for improving reproducibility for CE also was directly compared to methods in the literature that utilize a single neutral marker [90], multiple markers [92], a migration time ratio [44] and an adjusted migration index [95].

Chapter 3. Capillary electrophoresis is a common technique to analyze biological samples. In Chapter 2, it was observed that basic protein molecules adsorb on the capillary wall, and consequently change the surface chemistry of the wall and the EOF. In Chapter 3, the sample

adsorption and changes in the capillary surface were investigated by introducing biological cell components (proteins, lipids, carbohydrates and DNA) to the CE system at different buffer pHs (neutral and basic) and at different concentrations. The continuous EOF monitoring method was used to observe the changes in EOF due to these cell components.

Chapter 4. Discontinuous systems have been used in CE to concentrate sample solutions and carry out online enzyme reactions. EOF dynamics in sample stacking conditions were investigated by Pittman et al. [110] using the continuous EOF monitoring method. In Chapter 4, another marker, fluorescein, has been added to the EOF monitoring technique to monitor electric field changes in addition to EOF. Discontinuous systems were generated by using solutions that were prepared in a lower concentration buffer than the separation buffer. Computer simulations were performed in order to further investigate the results.

CHAPTER 2
IMPROVING MIGRATION REPRODUCIBILITY IN CAPILLARY ELECTROPHORESIS: A QUANTITATIVE COMPARISON OF TECHNIQUES

2.1. Introduction

Capillary electrophoresis (CE) offers several important advantages compared to other common analytical separation techniques, including high separation efficiency, fast analysis times, and low sample volumes [6, 7]. Capillary electrophoresis has been applied to a broad range of scientific problems stretching from biology to the environment[6, 7]; however, it has been recognized since the early days of CE development that reproducibility (migration time and peak quantification) is a significant limitation for CE compared to other separation techniques, particularly HPLC [6, 24, 25, 44, 51, 80, 95, 120, 121]. There are various factors such as temperature fluctuations, analyte-wall interactions, and injection and detection methods that can contribute to poor precision for migration times and quantification [6, 24, 25, 51, 73, 80, 121]. Changes in electroosmotic flow (EOF) between experiments and during a separation are believed to be the most common cause of poor migration time reproducibility for CE [51, 80, 120]. The capillary surface chemistry, the chemistry of the solution filling the capillary as well as temperature and the potential field, all impact EOF and can be sources of EOF variability.

The migration time of an analyte for CE results from a combination of electrophoretic migration and electroosmotic flow as given by Equation 1.2 in Chapter 1. Electrophoretic mobility, like electroosmotic mobility is affected by temperature changes, solution chemistry and the applied potential, but not by the capillary surface chemistry as seen in Equations 1.3 and 1.4. Therefore, electrophoretic mobility is more reproducible than electroosmotic mobility. Analyte migration is often reported as electrophoretic mobility rather than migration time since the migration time is affected by the relatively poor reproducibility of EOF [24, 51, 95, 97, 98, 122].

Electroosmotic flow must be measured in addition to migration time in order to calculate the electrophoretic mobility. The neutral marker method is the simplest and most commonly used technique to determine EOF in order to calculate μ_{ep} [90, 120, 123]. A neutral compound is injected with the sample, and electroosmotic flow alone affects the migration time of the neutral marker. Based on the migration time of the neutral marker, the average EOF rate can be determined [90, 120, 123]. The neutral marker method has some fundamental limitations. For analytes migrating after the neutral marker (typically negatively charged compounds), any changes in EOF after the neutral marker peak is detected will not be accounted for in the calculation of analyte electrophoretic mobility. Likewise, for peaks migrating faster than EOF, the average value of EOF will include any flow changes after detection of the analyte until the neutral marker peak is detected.

An alternative to the neutral marker method for improving CE migration reproducibility is to use more than one marker compound, including charged standards with known electrophoretic mobilities [122, 124]. Jumppanen et al. employed 2, 3 and 4 marker compounds with known electrophoretic mobilities to correct the electrophoretic mobility of analytes [92]. The chosen marker compounds were fully disassociated at the pH of the separation buffer, and their migration times spanned the expected analyte migration times. Excellent reproducibility was obtained with their technique (0.01-0.03%); however, they did not directly compare their results with the results obtained using a single neutral marker under the same conditions. In addition, identifying three or four suitable marker compounds that don't interfere with sample peaks can be challenging for many applications.

In order to improve migration reproducibility, Lee and Young introduced two parameters to express the migration of an analyte, migration index (MI) and adjusted migration index (AMI)

[95]. The MI for an analyte is calculated by integration of i/L_t as a function of time, where i denotes current density (ratio of current to cross sectional area of the capillary) and L_t is capillary length. By applying this index, it is possible to correct for fluctuations that occur in the temperature and electric field in the capillary. The second parameter, AMI, was further developed to include the MI of a neutral marker in the calculations to eliminate the effect of EOF changes. This study reported reproducibility values as low as 0.05% using the AMI. Iwata et al. reported a related method based on the work of Lee and Yeung [101]. Hage and coworkers developed a simple method for improving CE migration reproducibility based on plotting the ratio of migration times of analyte peaks divided by the migration time of a neutral marker. They reported RSD values of 0.7% for this ratio for analyte peaks [44].

A more comprehensive experimental approach to correct CE migration data for EOF changes during a CE separation would be to continuously measure EOF during the entire separation and use this data to correct the electropherogram accordingly. Several approaches to measure EOF as a function of time have been reported in the literature [103, 104, 107, 109, 125]. Lee et al. monitored EOF by diluting a fluorophore solution with the effluent from the CE capillary [107]. They were able to correct for changes in EOF and obtain reproducible electrophoretic mobilities (2% RSD). Gilman and coworkers developed a technique to measure EOF continuously based on periodic photobleaching of a neutral fluorescent dye [109]. This technique provides precise measurements of EOF (0.2-1.8%) over an entire separation with a time resolution of ~1 s [108]. This technique has been applied for fundamental studies of EOF dynamics in capillaries and microfluidic devices [108, 110, 111, 126].

In this chapter, we report the application of the technique developed by Gilman et al. for continuous monitoring of EOF to correct CE migration times for EOF fluctuations in order to

improve migration reproducibility. In principle, this approach should provide improved results compared to methods based on single or multiple marker compounds by providing a more complete record of EOF during the entire separation. Results obtained using this approach for improving migration reproducibility for CE have also been compared directly to methods in the literature that based on a single neutral marker [90, 123], multiple markers [92], migration time ratio [44] and adjusted migration index [95].

2.2. Material and Methods

2.2.1. Chemicals

Laser grade coumarin 334 was obtained from Acros Organics (Morris Plains, NJ). Benzoic acid (BA), α-lactalbumin (from bovine milk), β-lactoglobulin (from bovine milk), lysozyme (from chicken egg white), myoglobin (from equine skeletal muscle), carbonic anhydrase (from bovine erythrocytes), sodium phosphate monobasic, diphenylacetic acid (DPAA) and triphenyl acetic acid (TPAA) were purchased from Sigma-Aldrich (St. Louis, MO). Sodium hydroxide and methanol were purchased from Fisher Scientific (Pittsburg, PA). Mesityl oxide was obtained from Alfa Aesar (Ward Hill, MA).

2.2.2. Capillary Electrophoresis

The instrument for CE with EOF monitoring and simultaneous UV absorbance detection was similar to that described previously [108, 110] (Figure 1.4). Fused-silica capillary (50-μm i.d./360-μm o.d.) was purchased from Polymicro (Phoenix, AZ) and cut to 127.1 cm. The polyimide coating was burned (~1 cm) to make detection windows at 45.2 cm (EOF monitoring by LIF) and at 86.8 cm (absorbance detection). The electrophoretic potential was applied with a Spellman CZE 1000R high voltage power supply (Hauppauge, NY).

The 457.9-nm laser line from an Ar^+ laser (Coherent Innova 90C-5; Santa Clara, CA) was used as the light source for EOF monitoring. The laser beam passed through a beamsplitter, and the resulting two beams were focused on the capillary at two different positions. The first beam (31.1 mW) was used to bleach the neutral fluorophore (coumarin 334) at position F1 on the capillary (see Figures 1.4 and 2.1). The second beam (9.0 mW) was used for LIF excitation, and the emission was detected by a photomultiplier tube (PMT) (Hamamatsu HC 170; Bridgewater, NJ) biased at 750 V. The shutter (Uniblitz LS6Z2; Rochester, NY) was opened for 50 ms every 1.0 s to generate the photobleached zones, and a small portion of the light from the bleaching beam was directed to the PMT by an optical fiber to indicate when the shutter was opened. The distance between the bleaching and detection points (d_{F1-F2}) was determined to be 604.9 ± 0.6 μm as described previously [109]. For UV absorbance detection, a Linear Instruments UVIS-200 detector (Thermo Electron Corporation, Waltham, MA) with an on-column capillary cell was used. A program written in LabView 5.0 (National Instruments, Austin, TX) was used to control the shutter and for data collection. The PMT signal was filtered with a 250 Hz low-pass filter. All data (UV and LIF detection) were collected using a National Instruments PCI-6024E (Austin, TX) data acquisition board at 1000 Hz.

New capillaries were conditioned by rinsing with 0.10 mL of 1.0 M NaOH, 0.25 mL water, and 0.25 mL separation buffer (10.1 mM phosphate buffer at pH 7.51). Next the capillary was flushed with the separation buffer electrokinetically for 30 min. All stock solutions (except coumarin 334) were prepared by dissolving samples in ultrapure water (> 18 MΩcm, ModuLab water system, United States Corp.; Palm Desert, CA) and were stored at 4 °C. The separation buffer was prepared in the ultrapure water, adjusted to the desired pH with NaOH, and filtered with a 0.2 μm nylon filter (Whatman, Oregon). Coumarin 334 was dissolved in methanol and

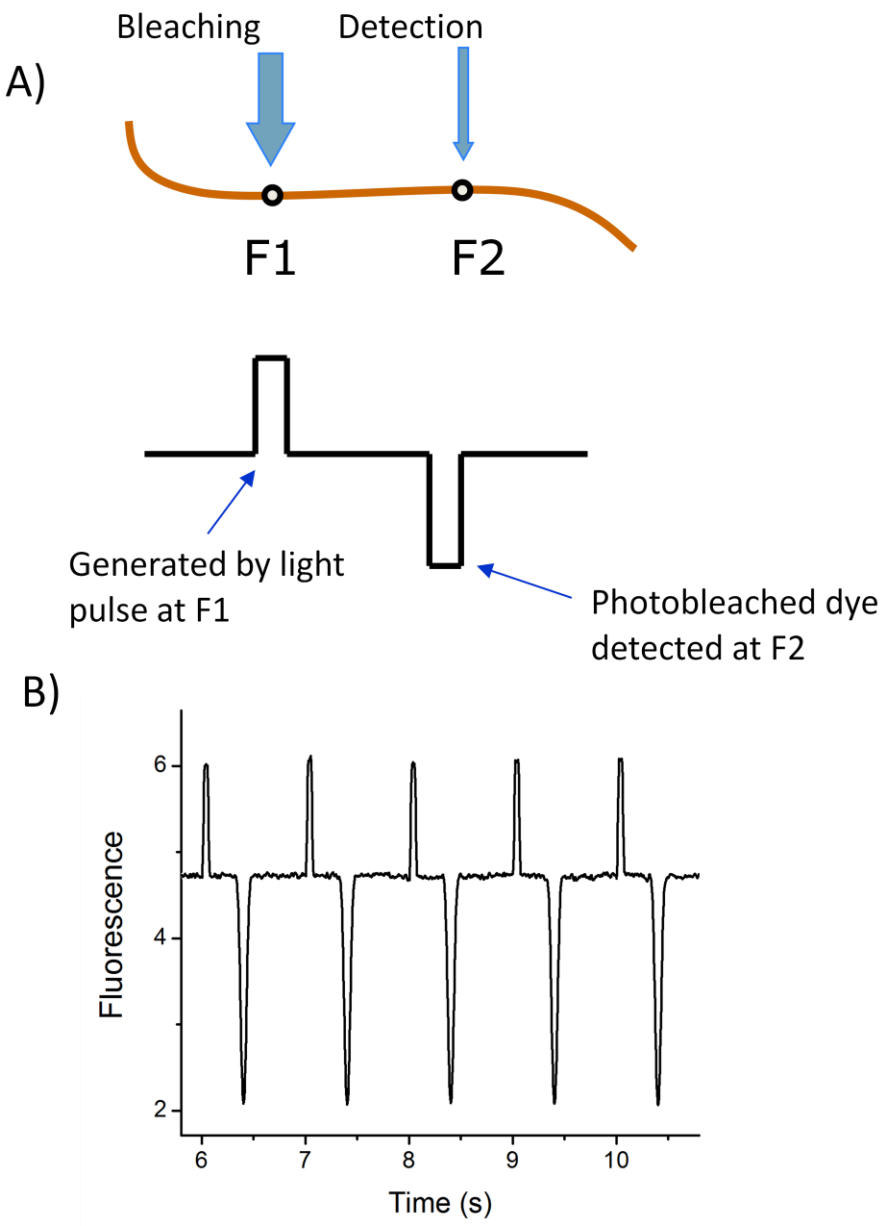

Figure 2.1. A) The bleaching beam was focused on the capillary at F1, and the detection beam was focused on the capillary at F2. When the shutter opened to create a light pulse, the bleaching beam hit the capillary at F1, and a photobleached zone was generated. Light from the bleaching beam was directed by a fiber optic to the PMT (see Figure 1.4) and detected as a positive peak. The photobleached zone traveled with the EOF and was detected as a negative peak at F2. B) A sample of the EOF monitoring data where the capillary was filled with 25.0 nM coumarin 334, and the shutter was opened for 50 ms every 1.0 s. The time difference between each pair of positive and negative peaks was used to calculate EOF each second during a CE run. Other details are as listed in Section 2.2.2.

diluted with ultrapure water to 0.41 mM, and a working stock solution was prepared by diluting this solution with the separation buffer. The sample mixture (analytes and marker compounds) was prepared in separation buffer. Mesityl oxide was used as a neutral marker (absorbance detection) for all experiments. For the EOF monitoring experiments, 25 nM coumarin 334 was added to the sample mixture and to the separation buffer. All injections were electrokinetic (30.0 kV, 236 V/cm) for 3.0 s. A separation potential of 30.0 kV (236 V/cm) was used for all CE experiments, and the electrophoretic current typically was 7.8 μA.

2.2.3. Data Analysis

Data for EOF monitoring experiments were analyzed with a program written in Matlab 6.1 (Natick, MA), which was used for data smoothing, baseline subtraction, peak picking, and calculation of EOF rates for the EOF monitoring experiments. The program also determined FWHM values for the EOF monitoring peaks (Figure 2.1). Absorbance data were plotted using Origin 7.5 (Northampton, MA), and migration times of the analytes were determined using the peak picking function in this program. Calculations for the multiple marker method were performed using Mathematica 7 (Champaign, IL). Microsoft Excel (Microsoft Corp., Redmond, WA) was used to calculate migration time ratios, adjusted migration indices and to analyze the multiple marker data.

2.3. Results and Discussion

The initial objective of this work was to apply an EOF monitoring method [108-110] to improve the migration reproducibility of CE separations by correcting for changes in EOF that occurred throughout each run. The EOF monitoring technique based on periodic photobleaching of a dilute, neutral fluorophore has been shown to be capable of precisely measuring EOF (0.2-1.8%) with a time resolution of ~1 s [108]. We hypothesized that this approach should be

superior to the neutral marker method for correction of CE migration data and that it might offer advantages relative to other published methods for correction of CE migration data based on multiple markers [92], migration time ratios [44] and adjusted migration indices of analytes [95]. In this study, several of these techniques were compared directly for the same electropherograms to determine which techniques provided the best results, in practice.

2.3.1. Separation

A mixture of proteins (myoglobin, carbonic anhydrase, α-lactalbumin, and β-lactoglobulin) and small molecules (TPAA, DPAA, and BA) were separated and detected by CE with UV absorbance detection at 220 nm. During the separations, the EOF rates were monitored as discussed in Section 3.2. Five consecutive separations were performed (Figure 2.2), and these runs included the neutral marker, mesityl oxide. The capillary was rinsed with the separation buffer between each of the five runs for 10 min electrokinetically. The proteins used in this experiment all have p*I* values below the pH of the separation buffer (pH 7.51). These proteins will all have a net negative charge at this pH and are less likely to adsorb to the capillary wall compared to neutral or cationic species. The migration times and electrophoretic mobilities for the analytes were highly reproducible under these conditions with RSD values (average RSD for all 8 peaks) of less than 1.4% and 0.2% (calculated with the neutral marker method), respectively. The EOF monitoring data could be used to correct the data for these separations, but the results would be misleading. Excellent reproducibility values would be obtained after correcting the data for EOF changes, but similar values also would be obtained without correction. A less reproducible separation is required in order to more thoroughly test the new method for improving CE migration reproducibility and compare it to other techniques in the literature.

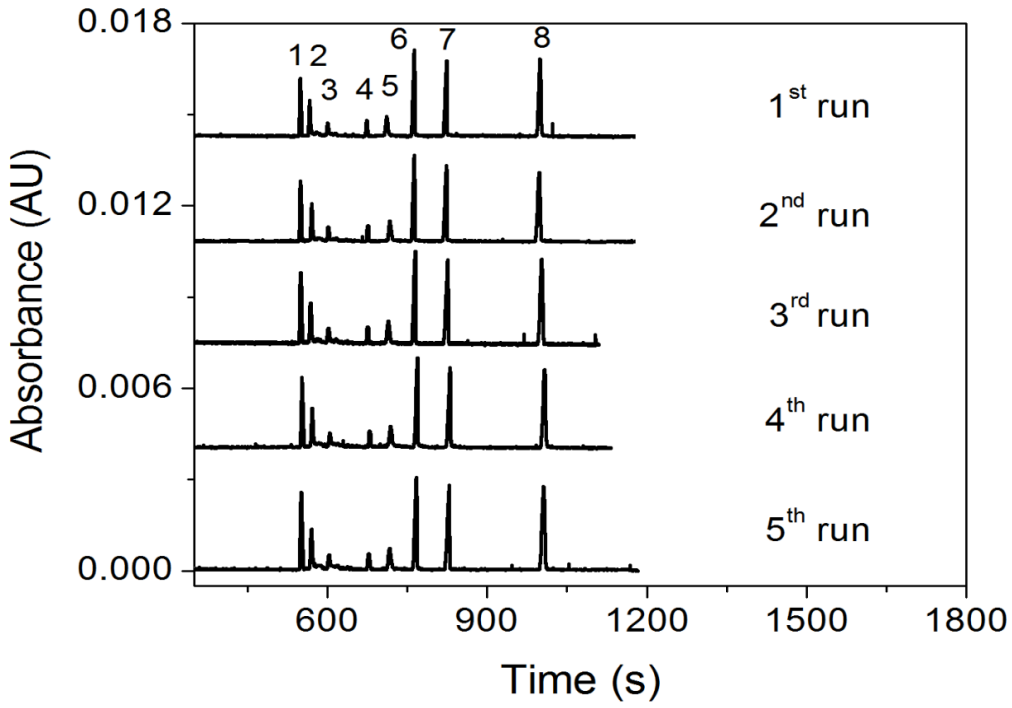

Figure 2.2. Electropherograms of the mixture of molecules used in this study. 1- mesityl oxide, 2- myoglobin, 3- carbonic anhydrase, 4- α-lactalbumin, 5- β-lactoglobulin, 6- triphenyl acetic acid, 7- diphenyl acetic acid, 8- benzoic acid. Electropherograms for runs 1-4 were offset artificially (y-axis) so they could be viewed in one graph.

To reduce the migration time reproducibility due to changes in EOF during the separation, a more basic protein, lysozyme (*pI* = 11.3), was added to the sample mixture at 0.5 mg/ml. Figure 2.3 shows electropherograms from a series of five consecutive separations for this sample. The capillary was not rinsed between consecutive runs. With the addition of lysozyme, the migration times of the analytes increased for each run, and relative peak broadening is apparent. The adsorption of lysozyme to the capillary wall results in an uneven zeta potential down the length of the capillary, which leads to a parabolic flow profile and band broadening [56, 110]. A peak for lysozyme was not observed in the electropherograms, presumably due to strong adsorption to the capillary surface [56]. An additional series of CE separations were

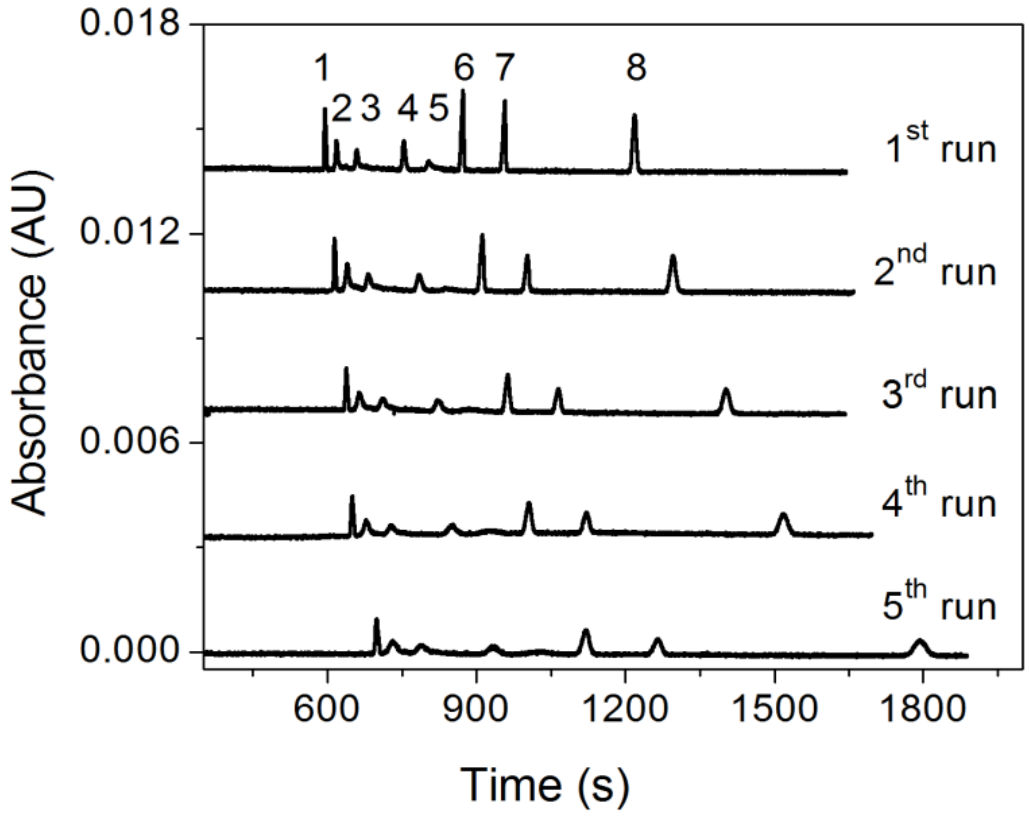

Figure 2.3. Electrophoretic separation of a mixture of proteins and small molecules by CE with UV absorbance detection. 1-mesityl oxide, 2- myoglobin, 3- carbonic anhydrase, 4- α-lactalbumin, 5- β-lactoglobulin, 6- TPAA, 7- DPAA, 8- benzoic acid .Lysozyme, was added to the mixture (0.5 mg/mL) but did not produce a peak. Electropherograms for runs 1-4 have been artificially offset (y-axis) so they can be plotted in one graph. The graph shows five consecutive runs.

carried out using a sample containing 2.0 mg/ml lysozyme. The first three electropherograms for these experiments are presented in Figure 2.4. After three runs with this sample, the photobleaching peaks became so broad that it became impractical to analyze the EOF monitoring data. This broadening is caused by the same process that broadens analyte peaks detected by UV absorbance (uneven zeta potential, parabolic flow profile). The addition of lysozyme to the samples dramatically decreased the migration reproducibility for the other analytes. The

migration time RSD (average for all 8 peaks) increased to 10% in the runs with 0.5 mg/ml lysozyme addition from 1.4% (uncorrected data) without lysozyme.

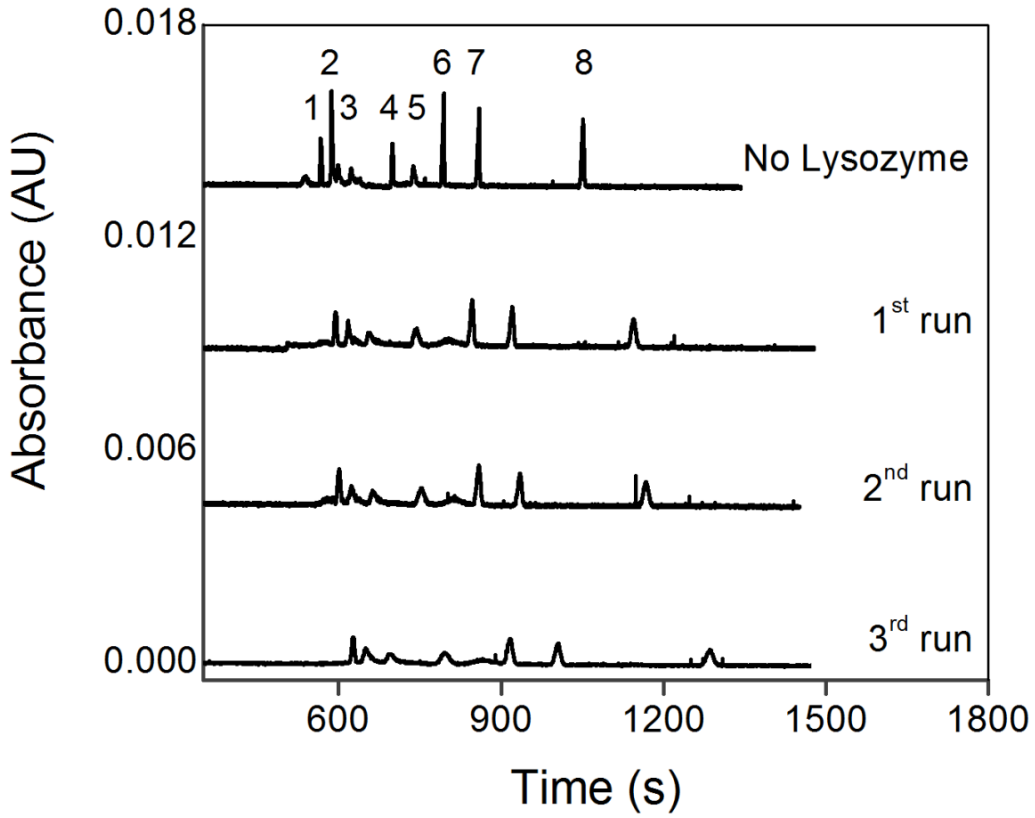

Figure 2.4. Electropherograms of the mixture of molecules with 2.0 mg/ml lysozyme added. Peak identities are the same as in Figure 2.2. Electropherograms for runs 1-4 were offset artificially (y-axis) so they could be viewed in one graph.

2.3.2. Electroosmotic Flow Monitoring

Electroosmotic flow was monitored during the separations presented in Figures 2.2, 2.3 and 2.4 using the technique based on periodic photobleaching of a dilute, neutral fluorophore, coumarin 334 [110]. Coumarin 334 was added to the sample mixture and separation buffer at 25 nM, and it was photobleached every 1.0 s for 50 ms throughout the separations. The EOF rate was determined from the time difference between the shutter opening at F1 (positive peak) and

the detection of the photobleached peak at F2 (negative vacancy peak), and this procedure was repeated every 1.0 s during the run (Figure 2.1). The sample compounds were detected by UV absorbance detection (at 86.8 cm) while EOF was monitored (at 45.2 cm). Previous studies demonstrated that the low concentration of fluorophore does not interfere with absorbance detection of analytes at higher concentrations [108, 110].

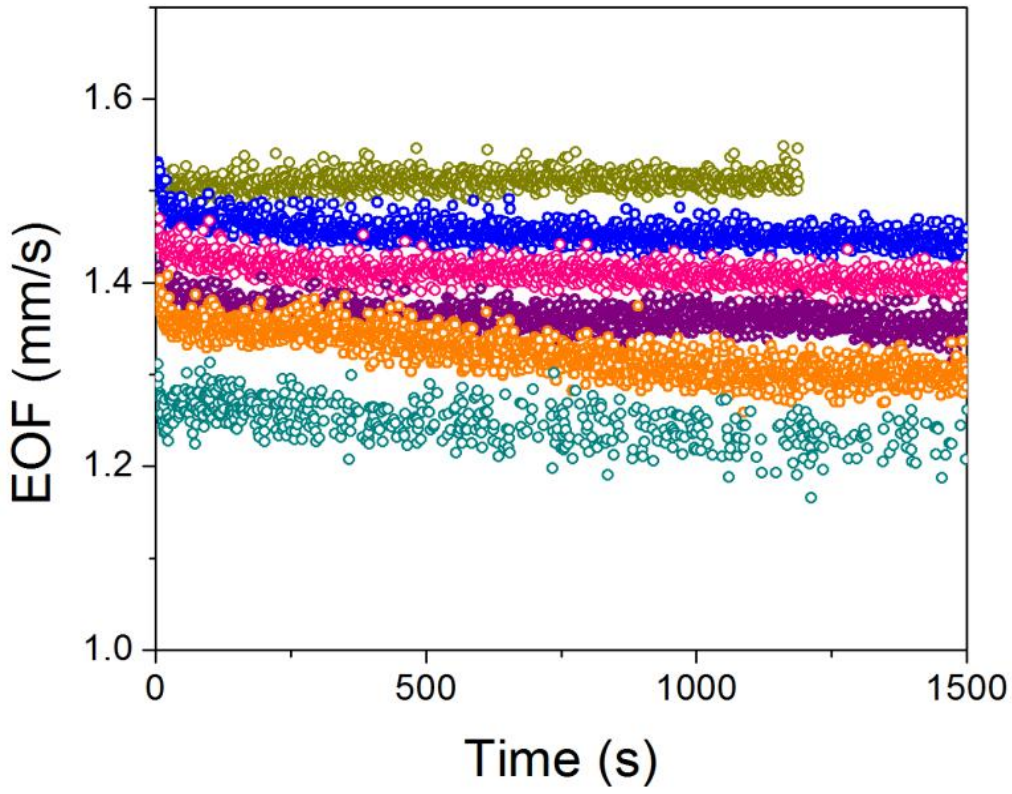

Figure 2.5. EOF vs. time for separations with 0.5 mg/mL lysozyme added to the sample mixture (Figure 2.3). The top trace is from the sample containing only the analyte mixture (no lysozyme, Figure 2.2). Each point is from a distinct EOF measurement made during the run (Figure 2.3).

Figure 2.5 presents EOF measurements vs. time for one representative separation without lysozyme (all 5 separations are presented in Figure 2.2) and five consecutive separations with 0.5 mg/mL lysozyme added to the sample (Figure 2.3). For the separations without lysozyme (top trace in Figure 2.5), the EOF remained constant throughout the runs with an RSD value of 0.7%

(average RSD for all 5 runs). This stable EOF is consistent with the observed migration time reproducibility for these separations, which ranged from 1.0 to 1.9% RSD for the different analyte peaks. For the five consecutive separations with the addition of 0.5 mg/ml lysozyme, the EOF decreased during each separation, and the initial EOF rate for the next separation was lower than that for the preceding separation. The EOF rate decreased 3.7% during the first run and a total of 18.3% over five runs. During each separation, the EOF decreased more rapidly during the first 40 s of the separation, due to adsorption of positively charged lysozyme to the capillary wall [56]. The vacancy (photobleached) peaks for coumarin 334 broadened 11% (FWHM) during the first run and a total of 97% over five runs as the EOF decreased. This result is consistent with adsorption of protein on the capillary surface causing an uneven zeta potential down the length of the capillary and a parabolic flow profile [56, 110]. Similar results were observed for the experiments with addition of 2.0 mg/ml lysozyme to the samples (Figure 2.6). The EOF rates decreased during the initial 140 s of the separation, and then they became relatively constant for the rest of the separation. The EOF rate decreased 4.0% during the first run and a total of 12% over three runs. The corresponding decrease over 3 runs for separations with 0.5 mg/mL lysozyme added was 10%.

2.3.3. Comparison of Techniques to Improve Migration Time Reproducibility

The primary objective of this work was to test the hypothesis that continuous EOF monitoring will be effective for improving migration time reproducibility for CE (Section 2.3.2). In order to objectively evaluate the effectiveness this technique, it was directly compared to four other methods in the literature for improving CE migration reproducibility in addition to comparing it to the uncorrected electropherograms. These selected methods can all be applied to

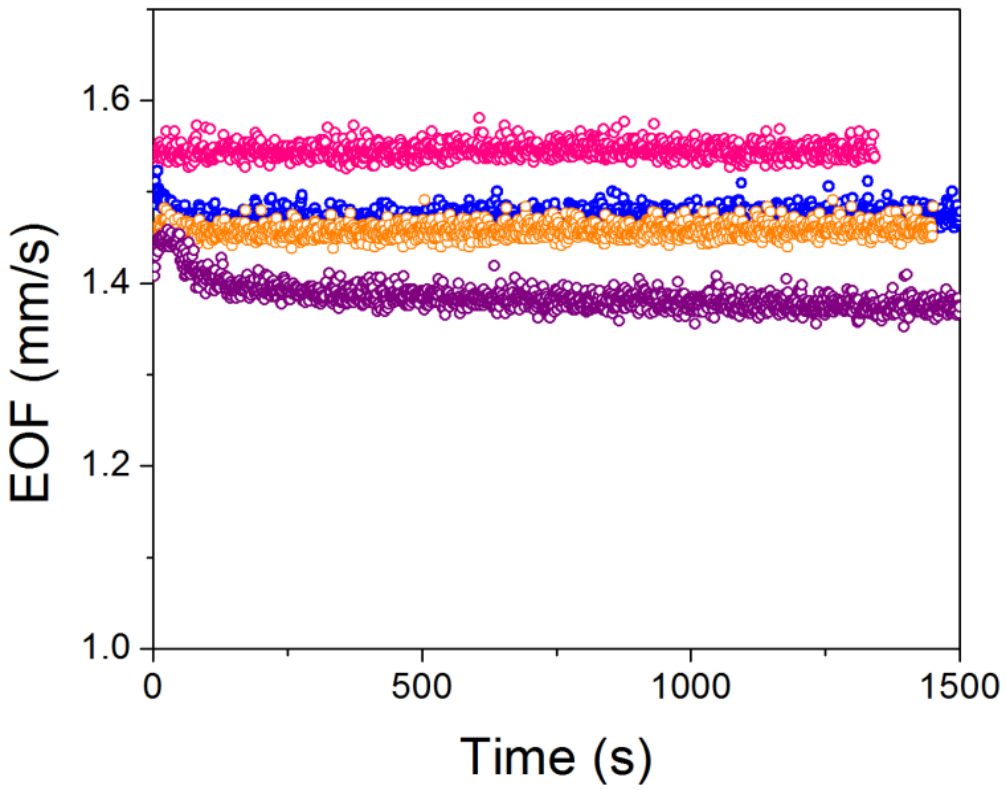

Figure 2.6. EOF vs time for separations with 2.0 mg/mL lysozyme added to the sample mixture. The top trace shows results from the sample mixture without lysozyme added (Figure 2.2). The lower 3 traces present changes in EOF rates with lysozyme added to the sample (Figure 2.4).

the same electropherograms. The neutral marker method is the most routinely used technique by CE practitioners. In addition to that method, the multiple marker, migration time ratio, migration index and continuous EOF monitoring methods were applied, and their performance for improving the reproducibility of CE runs was compared. The migration reproducibility results for four analyte peaks obtained using each of the correction methods and for uncorrected data are presented in Figures 2.7-2.9 and. Tables 2.1-2.3 include the RSD values presented in Figures 2.7-2.9 and the conversion of these values to time values.

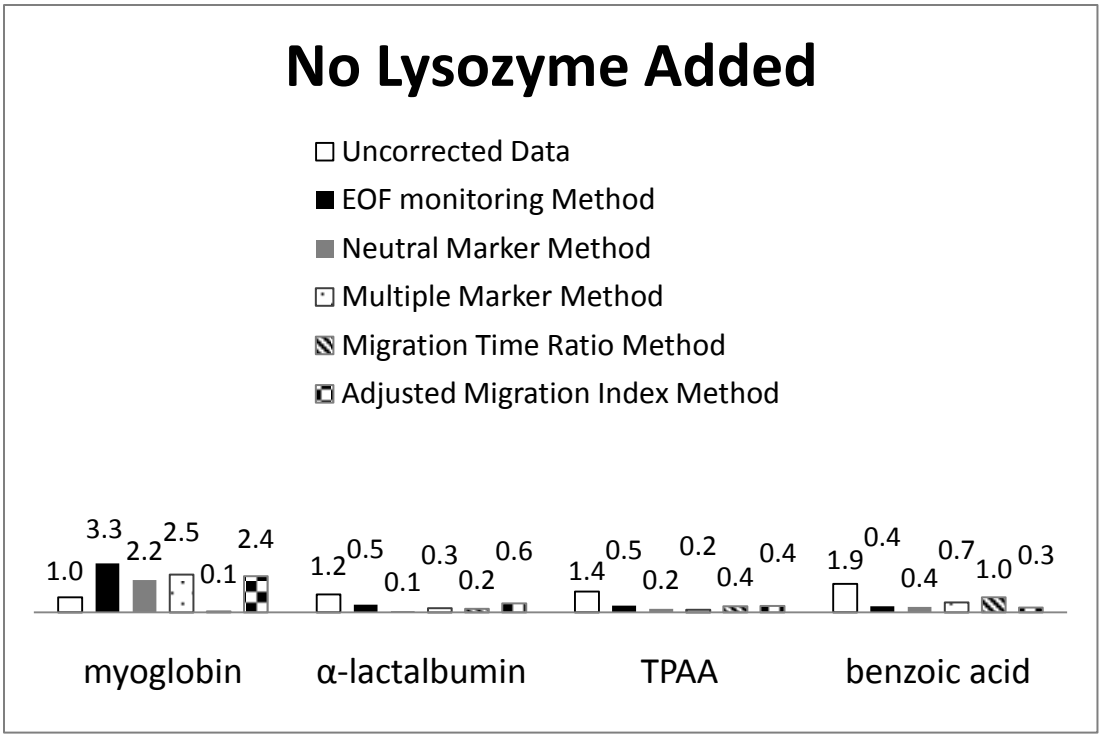

Figure 2.7. Values for reproducibility (RSD) obtained with the five correction methods for the separations without lysozyme added to the sample. The RSD values for uncorrected data are calculated based on the migration times of the analytes. The migration time ratio method is unitless and adjusted migration index method provides RSD values with different units.

Each of the five methods examined in this work uses a different approach to correct the fluctuations in analyte migration times. The equations used for application of these methods are provided in the Supplementary Content. The neutral marker method employs a single neutral compound in order to calculate the average EOF and the electrophoretic mobilities of the analyte [90, 120, 123]. The multiple marker method makes use of more than one compound of known electrophoretic mobility to determine the electrophoretic mobilities of the analytes. When using this technique, the compounds need to be chosen such that their migration times span the range of the analytes' migration times [92]. The migration time ratio method uses the migration times

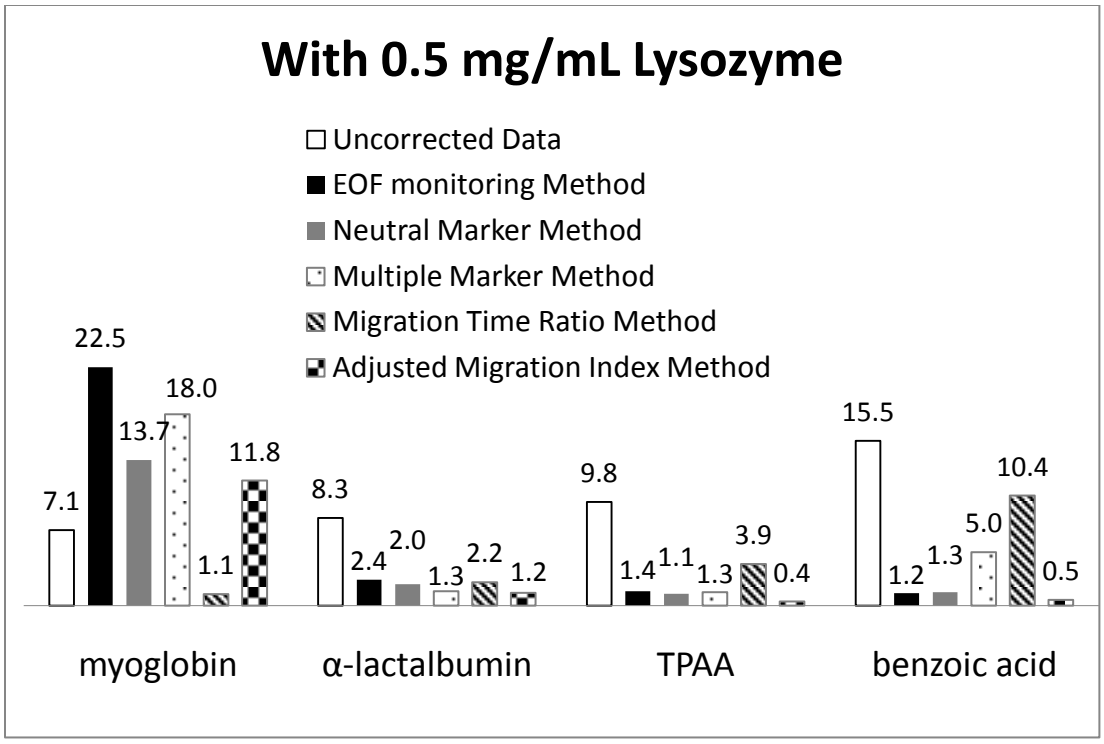

Figure 2.8. Values for reproducibility (RSD) obtained with the five correction methods for the separations with 0.5 mg/mL lysozyme added to the sample. The RSD values for uncorrected data are calculated based on the migration times of the analytes. The migration time ratio method is unitless and adjusted migration index method provides RSD values with different units.

of the neutral marker and each analyte. The migration time ratio is calculated by dividing the migration time of the EOF marker by the migration time of the analyte [44]. The adjusted migration index method utilizes migration indices of the analytes and the EOF marker [95]. The migration index is calculated by integrating i/L_t over time for each analyte, where i is current density (ratio of current to cross sectional area of the capillary) and L_t is capillary length. The new method presented in this chapter is based on measuring EOF continually throughout the CE separation [108, 109]. It provides a precise (0.7% RSD) EOF measurement every second, which takes into account any changes in EOF that occur throughout the CE separation.

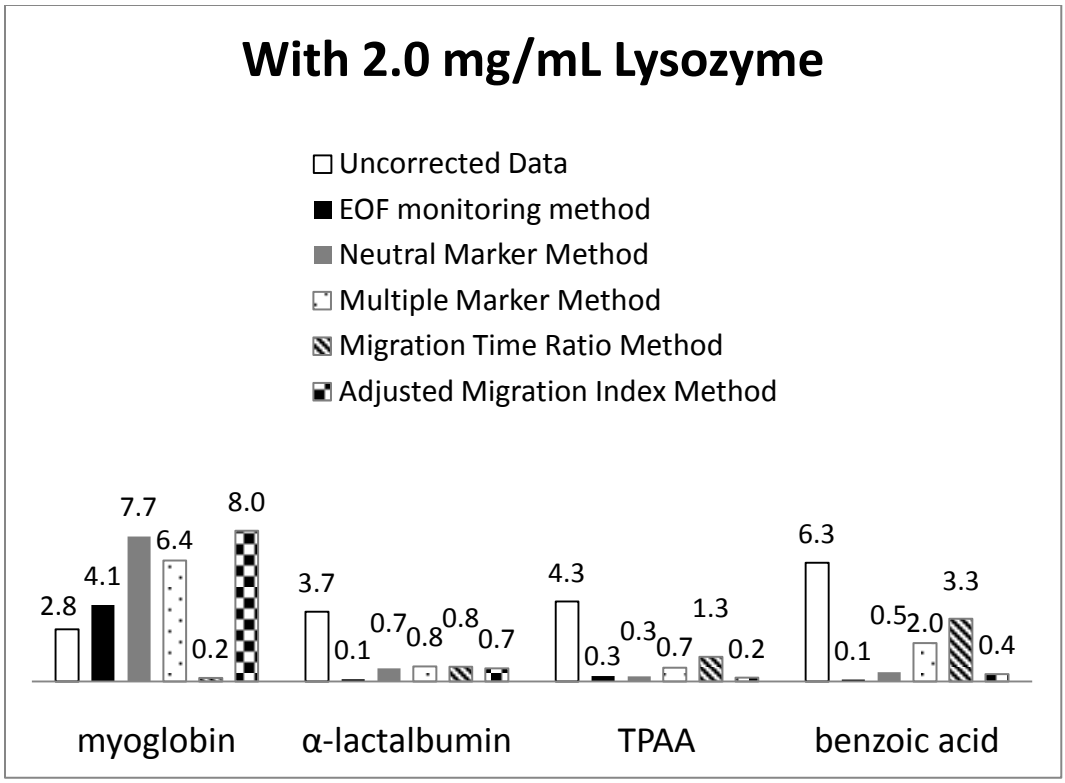

Figure 2.9. Values for reproducibility (RSD) obtained with the five correction methods for the separations with 2.0 mg/mL lysozyme added to the sample. The RSD values for uncorrected data are calculated based on the migration times of the analytes. The migration time ratio method is unitless and adjusted migration index method provides RSD values with different units

Each method used here required marker compounds to be added to the sample mixture. Mesityl oxide was added to all sample mixtures, (with or without lysozyme) and was used for the neutral marker method, the migration time ratio and migration index methods. For the multiple marker method, carbonic anhydrase, β-lactoglobulin, and DPAA were chosen as the marker compounds since their migration times spanned the migration times of most of the other compounds in the mixture, which are referred to as the analytes. The migration times of myoglobin and benzoic acid (categorized as analytes for this work) fall outside the range

Table 2.1. Values for μ_{ep} reproducibility (RSD), time difference and percent error values obtained with the five correction methods for the separations without lysozyme added to the sample

	myoglobin			α-lactalbumin			TPAA			benzoic acid		
	RSD_M[a]	Er_{time}[b]	$\%Er_{time}$[c]	RSD_M[a]	Er_{time}[b]	$\%Er_{time}$[c]	RSD_M[a]	Er_{time}[b]	$\%Er_{time}$[c]	RSD_M[a]	Er_{time}[b]	$\%Er_{time}$[c]
Uncorrected Data	-	11.6	1.0	-	17.1	1.2	-	22.4	1.4	-	43.1	1.9
EOF monitoring Method	3.3	1.4	0.2	0.5	1.8	0.3	0.5	3.2	0.4	0.4	8.5	0.8
Neutral Marker Method	2.2	0.9	0.2	0.1	0.3	0.0	0.2	1.7	0.2	0.4	7.6	0.7
Multiple Marker Method	2.5	1.1	0.2	0.3	1.0	0.1	0.2	1.2	0.1	0.7	13.6	1.3
Migration Time Ratio Method	0.1	0.9	0.1	0.2	3.7	0.5	0.4	8.9	0.8	1.0	34.8	2.0

[a] Relative standard deviation value of electrophoretic mobility of analyte

[b] Error in time that is converted from RSD_M

[c] Percent error of Er_{time}

Table 2.2. Values for μ_{ep} reproducibility (RSD), time difference and percent error values obtained with the five correction methods for the separations with 0.5 mg/mL lysozyme added to the sample

	myoglobin			α-lactalbumin			TPAA			benzoic acid		
	RSD_M[a]	Er_{time}[b]	$\%Er_{time}$[c]	RSD_M[a]	Er_{time}[b]	$\%Er_{time}$[c]	RSD_M[a]	Er_{time}[b]	$\%Er_{time}$[c]	RSD_M[a]	Er_{time}[b]	$\%Er_{time}$[c]
Uncorrected Data	-	95.2	7.1	-	136.8	8.3	-	190.7	9.8	-	449.3	15.5
EOF monitoring Method	22.5	13.8	2.1	2.4	11.7	1.4	1.4	13.5	1.4	1.2	39.1	2.8
Neutral Marker Method	13.7	8.3	1.3	2.0	9.7	1.2	1.1	11.2	1.2	1.3	44.6	3.1
Multiple Marker Method	18.0	12.8	2.0	1.3	5.9	0.8	1.3	11.4	1.3	5.0	203.8	14.4
Migration Time Ratio Method	1.1	14.1	2.1	2.2	39.6	4.3	3.9	102.8	7.6	10.4	460.7	19.4

[a] Relative standard deviation value of electrophoretic mobility of analyte

[b] Error in time that is converted from RSD_M

[c] Percent error of Er_{time}

Table 2.3. Values for μ_{ep} reproducibility (RSD), time difference and percent error values obtained with the five correction methods for the separations with 2.0 mg/mL lysozyme added to the sample

	myoglobin			α-lactalbumin			TPAA			benzoic acid		
	RSD_M[a]	Er_{time}[b]	$\%Er_{time}$[c]	RSD_M[a]	Er_{time}[b]	$\%Er_{time}$[c]	RSD_M[a]	Er_{time}[b]	$\%Er_{time}$[c]	RSD_M[a]	Er_{time}[b]	$\%Er_{time}$[c]
Uncorrected Data	-	34.9	2.8	-	56.5	3.7	-	74.4	4.3	-	151.2	6.3
EOF monitoring method	4.1	2.1	0.3	0.1	0.5	0.1	0.3	2.2	0.3	0.1	2.3	0.2
Neutral Marker Method	7.7	3.6	0.6	0.7	2.7	0.4	0.3	2.1	0.2	0.5	11.6	1.0
Multiple Marker Method	6.4	4.5	0.7	0.8	2.9	0.4	0.7	5.5	0.7	2.0	87.1	6.2
Migration Time Ratio Method	0.2	2.4	0.4	0.8	13.1	1.6	1.3	31.0	2.6	3.3	123.3	6.6

[a] Relative standard deviation value of electrophoretic mobility of analyte

[b] Error in time that is converted from RSD_M

[c] Percent error of Er_{time}

spanned by the selected marker compounds and are useful for probing the effects of this extrapolation. The electrophoretic mobilities of the marker compounds were calculated based on the neutral marker migration time in preliminary runs, and the electrophoretic mobilities were used to determine the analytes' mobilities. The neutral fluorophore, coumarin 334, was added to the sample mixture and to the separation buffer at 25.0 nM for the continuous EOF monitoring method.

The EOF monitoring method provided an EOF value for each second of the separation as shown in Figures 2.5 and 2.6. The EOF data were used to calculate μ_{ep} for each analyte based on the average EOF value from the application of the separation potential to the detection of the analyte peak. Changes in EOF after the elution of the neutral marker were included, and EOF data after the detection of a particular analyte were excluded. The RSD values for the uncorrected migration times presented in Figures 2.7-2.9 show that reproducibility decreased as migration times of the analytes increased both with and without lysozyme added to the samples. For □-lactalbumin, TPAA and benzoic acid, the new EOF monitoring method resulted in low RSD values for μ_{ep} with and without lysozyme added to the sample (Figures 2.7-2.9). For separations without lysozyme (Figure 2.7) an average 3 fold improvement in migration reproducibility (μ_{ep}) was obtained for these three analytes relative to the uncorrected data (migration time). The average improvements when lysozyme was added at 0.5 mg/mL (Figure 2.8) and 2.0 mg/mL (Figure 2.9) were 6-fold and 22-fold, respectively. Clearly this new method for improving migration reproducibility is effective for these analytes and separation conditions.

While a comparison of the migration reproducibility obtained with the EOF monitoring method to the uncorrected migration data demonstrates that this new technique is effective, it is essential to directly compare this new method to other techniques in the literature for correcting

CE migration data. Such comparisons with competing techniques have seldom been made in the literature when new methods have been introduced for improving CE reproducibility [93, 95, 99]. The most obvious technique to compare to is the neutral marker method because it is experimentally simple and widely used. The migration time of the neutral compound, mesityl oxide, was used to calculate, μ_{eof} for each separation (see Equation A2 in Appendix). The analyte migration time (t) and, μ_{eof} can then be used to calculate the electrophoretic mobility μ_{ep} for each analyte and separation (See Equations 1.2 in Chapter 1, and A3, A4 and A5 in Appendix). When the RSD values of μ_{ep} obtained with the neutral marker method are compared to those obtained with the EOF monitoring method, the improvements compared to uncorrected data are similar for the two methods. The average RSD values (for α-lactalbumin, TPAA and benzoic acid) obtained with the neutral marker method were 0.2%, 1.5% and 0.5% for the runs without lysozyme, with 0.5 mg/mL lysozyme added and with 2.0 mg/mL lysozyme added, respectively. The corresponding values obtained with the EOF monitoring method were 0.5%, 1.7% and 0.2%. The neutral marker method provided slightly lower RSD values than the EOF monitoring method for the experiments without lysozyme and with 0.5 mg/mL lysozyme added; however, the EOF monitoring method produced lower RSD values for the runs with 2.0 mg/mL lysozyme added, when the capillary wall was affected the most by lysozyme adsorption. Overall, while the EOF monitoring method is effective for correcting CE migration data to account for EOF dynamics, the much older and simpler neutral marker method performs comparably well.

The multiple marker technique was applied to the same data in order to evaluate its performance for improving reproducibility and to compare it to the other methods. Carbonic anhydrase, β-lactoglobulin, and DPAA were chosen as the marker compounds. The electrophoretic mobilities of the marker compounds were calculated from preliminary runs to

determine the coefficients for the multiple marker technique as described by Jumppanen et al. [92]. These coefficients were used to calculate μ_{ep} for each analyte and to calculate an EOF profile for the separation. This method provided average RSD values (for α-lactalbumin, TPAA and benzoic acid) of 0.4%, 2.5% and 1.2% for the separations with no lysozyme, 0.5 mg/ml lysozyme added, and 2.0 mg/ml lysozyme added, respectively. This method also is substantially more complicated than the neutral marker method. While it did improve the reproducibility of the separation, it did not outperform the neutral marker method or the EOF monitoring method. The neutral marker method provided better results both with and without lysozyme added to the sample. The multiple marker method performed similar to the EOF monitoring method when no lysozyme was added to the sample. Additionally, the RSD values for benzoic acid are substantially higher compared to the other two techniques, presumably due to lack of a marker compound after benzoic acid.

Another relatively simple method for improving migration reproducibility uses a migration parameter for each analyte based on the ratio of the migration times of a neutral marker and that of the analyte. The migration time ratio for each analyte was calculated as described by Yang and Hage [44]. This method provided average RSD values of 0.5%, 5.5% and 1.8% for separations with no lysozyme, 0.5 mg/ml lysozyme added, and 2.0 mg/ml lysozyme added, respectively. Additionally, the RSD values obtained with this method increased with the analyte elution time for all conditions. While this method does improve migration reproducibility, its performance was generally worse than the three techniques discussed above, including the similarly simple neutral marker method.

The last method applied to these separations was the adjusted migration index method reported by Lee and Yeung [95]. Following their method, migration indices first were calculated

for each analyte and the neutral marker (mesityl oxide). Then, the adjusted migration index was determined using these migration indices for each analyte. Overall, the migration index method's performance was similar to the neutral marker and the EOF monitoring methods. For separations without lysozyme it provided an average RSD 0.5% (for α-lactalbumin, TPAA and benzoic acid), which is close to the values provided by the other methods with the exception of the neutral marker method (0.2%). The adjusted migration index method provided the best average RSD value (0.7%) for the separations with 0.5 mg/ml lysozyme added. For the separations with 2.0 mg/ml lysozyme addition, the average RSD was 0.4%, which was only surpassed by the EOF monitoring method. The migration index method employs only a neutral compound as the neutral marker method does, and it does not require extra instrumentation like the EOF monitoring method does. The calculations of MI and AMI are not especially difficult, but they are not as simple as those for the neutral marker method.

The preceding comparison of the methods for improving CE reproducibility does not include the results for myoglobin, which are presented in Figures 2.7-2.9. Surprisingly, the corrected RSD values for myoglobin are higher than for the uncorrected migration times using all of these methods except for migration time ratio method. This surprising outcome for myoglobin results from the way in which migration reproducibility is reported. For the neutral marker, multiple marker and EOF monitoring methods μ_{ep} for each analyte is used to evaluate migration reproducibility, but the uncorrected migration data are reported in time units (s). The value for μ_{ep} is obtained from the difference between net mobility (μ_{net}) and EOF mobility (μ_{eof}) as shown in Equation 2.1

$$\mu_{net} = \mu_{eof} + \mu_{ep} \tag{2.1}$$

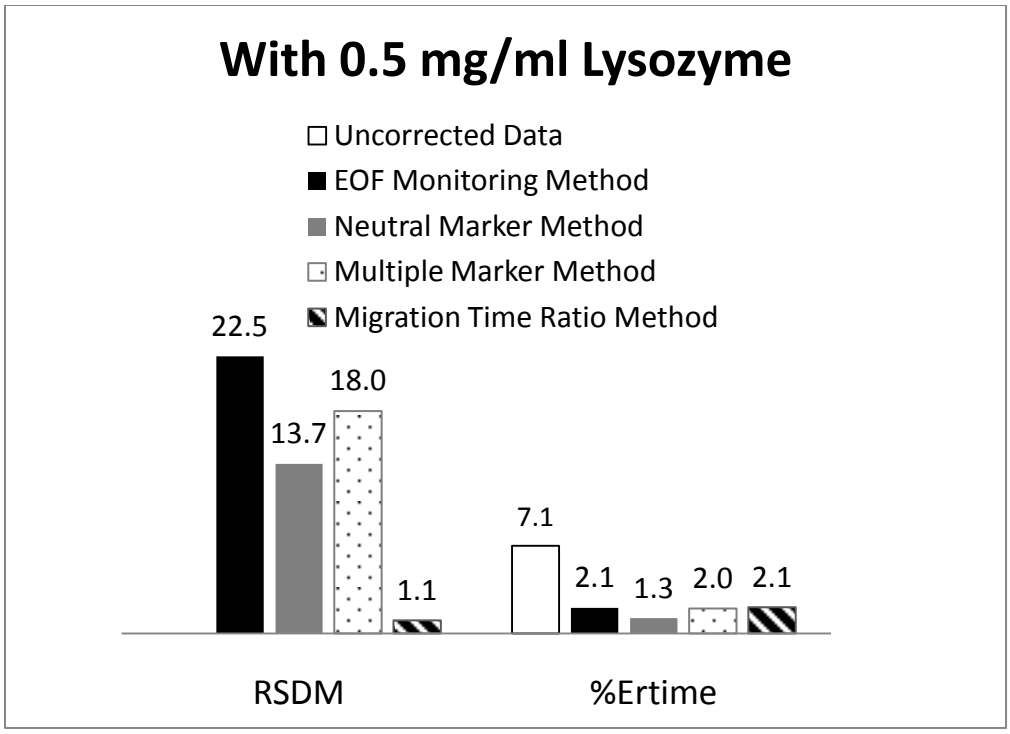

Figure 2.10. Comparison of different representations (RSD_M and $\%Er_{time}$) of four methods' performance to improve reproducibility of myoglobin.

In the case of myoglobin, the absolute magnitude of μ_{ep} is small (approaching 0) compared to the other analytes, and the total error for μ_{ep} becomes relatively large as indicated by the relatively high RSD values for myoglobin (Figures 2.7-2.9).

The error values reported in Figures 2.7-2.9 can be converted from electrophoretic mobility (cm^2/Vs) to migration time (s) using Equation 1.2 in Chapter 1. Figure 2.10 presents the RSD values for separations with myoglobin with 0.5 mg/mL lysozyme in units of both electrophoretic mobility and time for the EOF monitoring method, the neutral marker method, the multiple marker method, and the migration time ratio method. The uncorrected data can only be expressed in units of time. As shown in Figure 2.10, all of these methods actually improve migration reproducibility for myoglobin 7 to 11 fold when considered in units of time. It is important to note that the mobility values produced by the migration ratio method are actually

are unitless, not electrophoretic mobility (cm^2/Vs); however, these ratios can be easily converted back to time units. The data from the adjusted migration index method are not presented in Figure 2.10. The values obtained from the adjusted migration index method cannot be readily converted back to migration times. In fact, it is difficult to compare the results obtained with the adjusted migration index in a meaningful way to any of the other methods tested. Tables 2.1-2.3 present all of the data presented in Figures 2.7-2.9 converted to units of time with the exception of the adjusted migration index method. For myoglobin, the migration ratio method provides the biggest improvements in migration reproducibility when compared to the other methods in time.

In an effort to better understand the relative performance of each technique for improving CE migration reproducibility, the EOF profiles measured or assumed by the EOF monitoring method, the neutral marker method and the multiple marker method (using three markers) have been plotted and compared. The migration time ratio and adjusted migration index methods are based on the same EOF profile as the neutral marker method, so only the plot for the neutral marker method is considered. The EOF rates from a separation with 2.0 mg/ml lysozyme addition are presented in Figure 2.11 since the capillary surface and EOF were most affected by injection of this sample. The neutral marker method (also migration time ratio and migration index methods) assumes a constant EOF during the entire separation as shown in Figure 2.11. The multiple marker method assumes different EOF profiles depending on the number of marker compounds used [92]. This method assumes a constant EOF for the two-marker technique, a linearly accelerating EOF profile for the three-marker technique and a nonlinearly accelerating EOF for the four-marker technique. In our study, the three-marker technique was used, which resulted in an EOF profile that is linearly accelerating as shown in Figure 2.11. Equations A7,

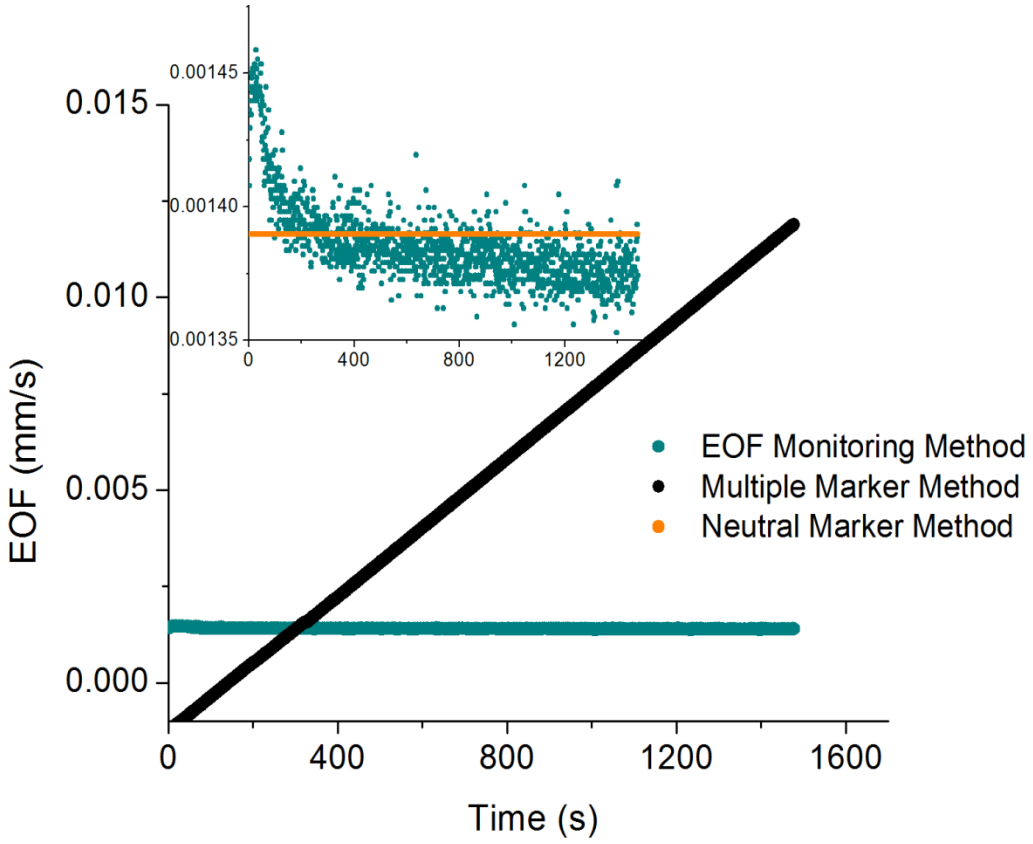

Figure 2.11. Electroosmotic flow profiles of the methods used to improve CE migration reproducibility for a separation with 2.0 mg/mL lysozyme added to the sample. The inset shows and expanded view of the EOF profile for the EOF monitoring method and neutral marker method, which represents the other three method's EOF profile as indicated in the text. Other data for the same experimental conditions are presented in Figures2.4, 2.6, and 2.9.

A8, and A11 in Appendix were used to obtain the EOF profile for the multiple marker method [92]. The EOF profile obtained with the EOF monitoring method showed that the EOF rates decreased over the first 140 s, then stabilized for the rest of the run. The neutral marker method provides a profile that is relatively close to the real, measured EOF. The EOF profile assumed by the multiple marker method clearly is not an accurate representation of the EOF during the separation although the method still improves migration time reproducibility for these experiments.

Interestingly, the continuous EOF monitoring method provided the best RSD values for the separations with 2.0 mg/ml lysozyme added to the samples (average RSD of 0.2% RSD). The EOF monitoring method clearly offers superior reproducibility results when the capillary wall surface has been affected by concentrated protein samples (2.0 mg/ml lysozyme). The EOF changes in those runs are very striking as seen in Figures 2.5 and 2.6. The change in EOF occurred over longer times for the runs with more concentrated protein. During experiments with the less concentrated protein, the EOF rates became stable after 40 s, whereas it took 140 s for the rates to become constant for the more concentrated protein addition. The EOF monitoring method has the ability to observe the changes in EOF throughout a run, and especially when the capillary wall is affected by the sample. Additionally, the method is capable of correcting the mobilities of the analytes when the change in the chemistry of the capillary wall is very dramatic.

2.4. Conclusion

This study demonstrates that the continuous EOF monitoring method can be used to significantly improve migration reproducibility for CE experiments; however, based on direct experimental comparison, this new technique does not provide results that are superior to several other techniques in the literature for correcting CE migration times. The EOF monitoring method still provides a real-time EOF profile and can be a useful tool to observe and study changes in capillary surface that may occur during the CE separations. While this central hypothesis of the study (the EOF monitoring method would provide superior results) was not supported by these results, the direct experimental comparison between several methods for improving migration CE migration reproducibility is novel and valuable for CE practitioners. Perhaps the most important and surprising conclusion from this study is that for most of the separation conditions studied in this work, the neutral marker method [90, 123] provides results that are comparable to

those obtained with several more complicated and sophisticated techniques for improving CE migration reproducibility.

CHAPTER 3
INVESTIGATION OF ELECTROOSMOTIC FLOW DYNAMICS IN RESPONSE TO BIOLOGICAL SAMPLE INTRODUCTION FOR CAPILLARY ELECTROPHORESIS

3.1. Introduction

Capillary electrophoresis (CE) is widely used for bioanalytical applications, particularly those applications that require small sample volumes and rapid, highly efficient separations [7, 10]. Capillary electrophoresis separations typically are carried out in aqueous solutions near physiological pH values, and often biological samples can be injected directly into a CE capillary for analysis with minimal sample preparation [10, 127]. Early in the development of CE, the technique was applied to the analysis of single cells as well as biological fluids such as serum and urine [128-133]. The use and development of CE for such applications continues today in both capillaries and microchip devices [9, 134].

A major drawback for biological sample analysis with CE is unwanted adsorption of sample components to the capillary wall, which impacts the capillary surface charge, thereby altering electroosmotic flow (EOF) [56, 135-138]. Such sample-induced changes in EOF have long been recognized as a problem for CE [55, 56, 139]. Unwanted sample adsorption is one of the main causes of irreproducible migration times, sample loss, and compromised separation efficiency for CE [22, 56]. Equation 1.2 in Chapter 1 shows the relationship between electrophoretic mobility, electroosmotic mobility and migration velocity. Clearly changes in EOF will impact the migration times of all analytes, and variation during and between runs will impact migration reproducibility. Equation 1.4 in Chapter 1 shows the relationship between electroosmotic mobility and the zeta potential, ζ, which is related to the double layer structure on the capillary surface as indicated in Equation 1.5. When molecules from the sample adsorb to the capillary surface, they alter the surface charge, which affects the double layer and local zeta

potential [138]. This leads to changes in EOF, band broadening and degraded migration reproducibility [56, 137-139].

There have been a handful of studies exploring how sample adsorption impacts EOF and CE separations, dating back to the early years of CE [56, 107]. Towns and Regnier experimentally confirmed that the sample adsorption affected the zeta potential and EOF [56]. They demonstrated that injections of basic protein molecules into a CE system caused sample adsorption, low sample recovery percentages, low separation efficiencies and irreproducible migration times. These studies suggest that EOF may be changing continuously from the time a sample is first introduced in the capillary until and perhaps even after sample components detected as peaks have eluted from the capillary. Ghosal [140] performed theoretical calculations for the experimental conditions that Towns and Regnier used in their report and confirmed the generation of space- and time-dependent zeta potential distribution while the sample zone travels through the capillary. Zare group observed similar EOF changes during experiments where human serum was injected at various dilutions [107]. In a more recent study, Fang et al. [141] investigated the adsorption properties of an autofluorescent protein by CE experiments, fluorescence microscopy and computer simulations. Electrophoretic mobility data (from the simulations and CE experiments) and calculations of capacity factor (based on the experiments and imaging) were compared to understand adsorption process and the basic separation mechanism of CE. In addition, adsorption characteristics of sample molecules have been investigated in microchips by using an enzyme-linked immunosorbent assay (ELISA) technique [142], fluorescence microscopy [143], and radiolabeling [144, 145] with various microchip materials. A study by Salim et al. [146] presented results confirming that the EOF rates are very sensitive to protein adsorption on the channel wall, which could result in reversed EOF.

In order to understand the dynamics of these processes, it is necessary to measure EOF as a function of time. Zare and coworkers monitored the EOF by delivering a known amount of a fluorescent dye to the flow stream, where the dilution of the dye by EOF resulted in a change in fluorescence signal intensity proportional to the EOF rate [107].

They were able to detect flow changes as small as 1% and correct for the changes in electric field to calculate electrophoretic mobilities of the analytes when the sample (serum sample) had adsorbing species that altered EOF. Another EOF monitoring approach is based on measuring a change in refractive index when a small heated volume of solution travels over a short, defined distance. The generation of the heated zone is performed periodically by a laser [103] or by a heating coil [104]. The migration of the heated zone is due to the EOF, thus its migration behavior provides the EOF rates. Heated zone generation was employed in another study to change the electrolyte composition permanently, which was called a thermal mark, to monitor the EOF by contactless conductivity detection [105]. In a recent study, Seiman et al. applied the thermal marks method to investigate EOF rates for non-aqueous capillary electrophoresis in the presence of ionic liquids [106].

The aforementioned techniques have measured the EOF as a function of time; however, they have rarely been applied to fundamental studies of EOF dynamics, which have potential to provide useful insights into CE separations and events related to EOF occurring during CE experiments. Gilman and coworkers developed a technique for studying EOF dynamics based on periodic photobleaching of a dilute, neutral fluorophore [108, 109] and later applied this technique to study EOF dynamics in capillaries and microchips. This technique can monitor EOF with a time resolution of ~1 s and with a precision below 1% [108]. Because the added neutral fluorophore is used at nanomolar concentrations, the method can be used with UV absorbance

detection of nonfluorescent analytes at higher concentrations [110]. The continuous EOF monitoring method was used to investigate EOF during sample stacking in capillaries and how the current monitoring method affects EOF in microchips. Frederick and coworkers applied this technique to detect deviations from ideal plug flow during the course of a CE experiment [126] and to investigate the stability of polyelectrolyte multilayer (PEM) coatings and their responses to different pH conditions based on observed changes in the EOF [147].

In this study, we investigated the effects of biological samples on EOF dynamics in order to gain a better understanding of the interactions between the sample molecules and the capillary wall and their impact on CE separations. The continuous EOF monitoring method based on periodic photobleaching of a neutral dye was used for this work [108, 110]. Sample adsorption and its deleterious effects on CE separations have been observed during analysis of serum samples and even single cell analysis with CE [139]; however, it is not known which sample component or components most affect EOF and consequently, CE separations. Samples of pure molecules representing proteins, carbohydrates, lipids and DNA were studied individually along with lysed whole cells and serum samples.

3.2. Materials and Methods

3.2.1. Chemicals

Lysozyme (chicken albumin), cytochrome *c* (horse heart), ribonuclease A (bovine pancreas), myoglobin (equine skeletal muscle), sodium phosphate monobasic, sodium chloride, methanol, sodium decodecyl sulfate (SDS), *d*-galactose, *d*-cellobiose, maltoheptaose, cholesterol, tetrahydrofuran, acetonitrile, chloroform, DNA (calf thymus), nuclease free water, and fetal bovine serum (FBS) were purchased from Sigma-Aldrich (St. Louis, MO). Dipalmitoyl-L-α-phosphatidylcholine (DPPC), dipalmitoyl-L-α-phosphatidylgycerol (sodium salt) (DPPG), and

1,2-dioleoyl-3-trimethylammonium-propane (DOTAP) were obtained from Avanti Polar Lipids (Alabaster, AL). Boric acid and sodium hydroxide were obtained from Fisher Scientific (Fair Lawn, New Jersey). Laser grade coumarin 334 was from Acros Organics (Morris Plains, NJ).

3.2.2. Capillary Electrophoresis and EOF Monitoring

The general design for the CE system was described previously [108, 110]. Fused-silica capillary (50-μm i.d./360-μm o.d.) was purchased from Polymicro (Phoenix, AZ) and cut to 72.0 cm. The polyimide coating was removed (~1 cm) to make a detection window at 49.1 cm. The separation buffers (20.1 mM phosphate buffer at pH 6.91 and 20.0 mM borate buffer at pH 9.1) were prepared in ultrapure water (> 18 MΩ-cm, ModuLab water purification system, United States Filter Corp., Palm Desert, CA), adjusted to the desired pH with NaOH, and filtered with a 0.2 μm nylon filter (Whatman, Oregon). Coumarin 334 was dissolved in methanol (0.41 mM) and diluted with ultrapure water, and a working stock solution was prepared by diluting this solution with the separation buffer. In order to monitor EOF, 50 nM coumarin 334 was added to the sample mixture and to the separation buffer for all samples. All injections were electrokinetic at 20.0 kV (278 V/cm) for 5.0 s. An electrophoretic potential of 20.0 kV (278 V/cm) was applied with a Spellman CZE 1000R high voltage power supply (Hauppauge, NY). The electrophoretic current was typically 5.4 μA for the phosphate buffer, and 17.8 μA for the borate buffer.

The instrument for CE with EOF monitoring is similar to an instrument reported previously [108, 110]. The 488.0-nm line of an argon ion laser (Melles Griot 543-AP-A01; Carlsbad, CA) was used as the light source. The laser beam was split with a broadband cubic beam splitter, and then the beams were focused on the capillary at two different positions, F1 and F2. The bleaching portion of the beam (54.2 mW) was directed by a computer controlled shutter (Uniblitz LS6Z2; Rochester, NY) and focused on the capillary at position F1. The shutter was opened for 50 ms

every 1.0 s to generate photobleached zones. Additionally, a small portion of the light was directed to a photomultiplier tube (PMT) (Hamamatsu HC 170; Bridgewater, NJ) by a fiber optic to mark the beginning of each individual flow measurement. The detection portion of the beam (10.0 mW) was used for fluorescence excitation. The beam was directed toward to the capillary by a dichroic mirror (505DRLPXR; Omega Optical; Brattleboro, VT) and was focused onto the capillary through a 20 x microscope objective (0.4 NA) at position F2. The fluorescence emission was collected at 180^{o} and residual scattering from the capillary was reduced by a band-pass filter (520BP10; Omega Optical; Brattleboro, VT). Scattering light was spatially reduced by a pinhole (1.0 mm). The distance between the bleaching and detection points (d_{F1-F2}) was determined to be 692.5 ± 0.6 μm using a method that was described previously [108, 109]. The emitted light was detected by the PMT biased at 850 V. The PMT signal was filtered with a 250 Hz low-pass filter. A program written in LabView (National Instruments, Austin, TX) was used to control the shutter and to collect the data using a National Instruments PCI-6299 (Austin, TX) data acquisition board at a 300 Hz scan rate.

3.2.3. Sample Preparation for Model Compounds, Cell Lysates and FBS

The stock solutions of compounds for protein and carbohydrate studies were prepared by dissolving samples in ultrapure water and were stored at 4 °C. Cholesterol was dissolved in tetrahydrofuran (THF) (62.5%), mixed with acetonitrile (ACN) (37.5%) and stored at 4 °C. DPPC/DPPG and DOTAP liposomes were prepared according to Burns et al. [148] and Bordi et al. [149], respectively, and the stock solutions were stored at 4 °C. Digital images of liposomes were taken with Nikon Microphot-FX-A optical microscope and with TEM (JEOL 100CX) instrument for size determination. DNA was dissolved in nuclease free water overnight and stored at -20 °C. The cultured human adipocyte cells were lysed using a freeze-thaw method

[150]. Separation buffer and coumarin 334 were added to the cell lysate for CE experiments. The fetal bovine serum was stored at 4 °C and diluted with separation buffer containing 50 nM coumarin 334 to the desired concentration for CE experiments. The following regeneration procedure for the capillary was applied after each protein, cell lysate and FBS injections. The capillary was rinsed with 0.10 ml of 1 M NaOH, 0.25 ml water, and 0.25 ml buffer by syringe pump. Then the capillary was rinsed electrokinetically with buffer for 30 min and with 60 mM SDS solution in buffer for 2 hr. Finally, the capillary was regenerated by injection of 0.25 ml water and 0.25 ml buffer by syringe pump and 30 min buffer by electrokinetic injection.

3.2.4. Data Analysis

Data for the EOF monitoring experiments were analyzed with a program written in Matlab 6.1 (Natick, MA), which was used for data smoothing, baseline subtraction, peak picking, and calculation of EOF rates for the EOF monitoring runs. The program also determined FWHM values for the photobleached peaks. Microsoft Excel (Microsoft Corp., Redmond, WA) and Origin 7.5 (Northampton, MA) were used to present the results of the study.

3.3. Results and Discussion

The goal of this study was to understand how adsorption of biological sample components impacts EOF dynamics during a CE separation. Cultured cells and serum were studied as examples of biological samples that are known to cause reproducibility problems for CE analysis, presumably due to sample adsorption and EOF changes [56, 107, 128, 139, 151]. In addition, pure compounds representative of major components of a biological cell, were studied to determine how each class of biological molecule impacts EOF dynamics. The biological model compounds studied were proteins, carbohydrates, lipids and DNA. The experiments were carried out at two pH values (6.91 and 9.1) with a range of sample concentrations.

Electroosmotic flow dynamics were measured during CE after sample injection using a previously reported method that can measure EOF with a precision of less than 1% [109] and at a frequency of up to 1 Hz [108].

3.3.1. Protein Samples

Proteins are diverse and complex amphoteric molecules. Their charge characteristics, structure and interaction with a surface can vary substantially with pH. The proteins used in this study were selected to have a range of p*I* values: lysozyme (p*I* 11.1), cytochrome *c* (p*I* 10.2), ribonuclease A (p*I* 9.3) and myoglobin (p*I* 7.3). They were injected into the CE system at different concentrations (0.5, 1.0, 2.0, and 2.5 mg/ml) and at two different pH's, 6.91 and 9.1. Figure 3.1 shows the EOF versus time after injections of lysozyme at pH 9.1 at several concentrations. For an injection of just buffer (top trace), the EOF was constant (1.0% RSD) over the course of the run. When samples containing lysozyme were injected, the EOF rates decreased at the beginning of the run and became constant for the rest of the run. The drop in EOF increased in magnitude from 3.3% to 24% as the lysozyme concentration increased from 0.5 to 2.5 mg/mL as shown in Table 3.1. The decrease in EOF rate is not surprising since the buffer pH is below the p*I* of lysozyme, and the protein has a net positive charge at this pH. Positively charged protein molecules adsorb to the negatively charged silanol groups on the capillary surface, which alters the zeta potential and reduces the EOF.

Additionally, the time over which the EOF decreased was concentration dependent. The EOF drop time increased from 25 s to 100 s before reaching a relatively constant value as the lysozyme concentration was increased from 0.5 mg/ml to 2.5 mg/ml. This is an indication of a

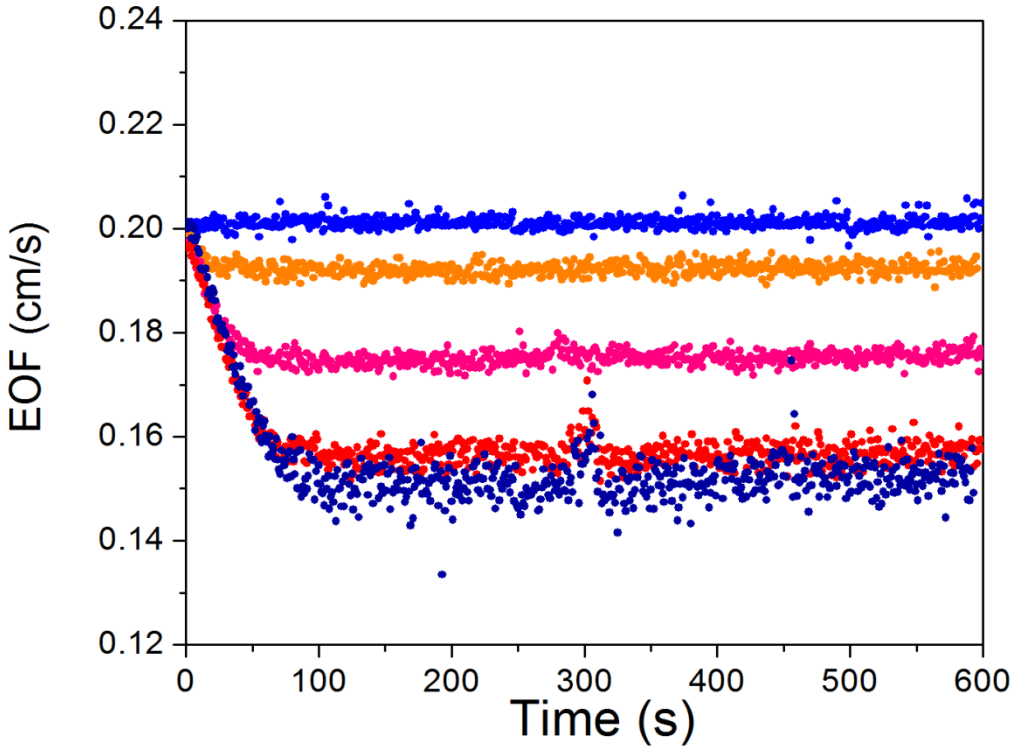

Figure 3.1. EOF rate versus time plots for experiments in which lysozyme samples were electrokinetically injected for 5.0 s. The plots are for lysozyme concentrations of 0, 0.5, 1.0, 2.0 and 2.5 mg/ml from top to bottom. The separation buffer and the sample solution was 20.0 mM borate buffer at pH 9.1. All solutions contained 50 nM coumarin 334. The applied potential was 277 V/cm, and the current was 17.8 µA. The bleaching pulse duration was 50 ms every 1.0 s, and the bleaching beam power was 54.2 mW at F1, and the detection power at F2 was 10.0 mW.

time that is required for zeta potential to reach a steady state which was also observed by Lee et al. in Figure 7 in ref [107]. Cytochrome *c* and ribonuclease A both have p*I*'s above this buffer pH, and the results for these proteins were similar to those for lysozyme as shown in Table 3.1. The relation between the percent changes in EOF rates with protein concentration is presented in Figure 3.2.

At pH 6.91, injections of lysozyme also caused significant changes in EOF as expected (see Figure 3.3). As at pH 9.1, EOF rates decreased at the beginning of the run; however, the EOF continued to decrease slowly after the initial sharp drop unlike the experiments at pH 9.1.

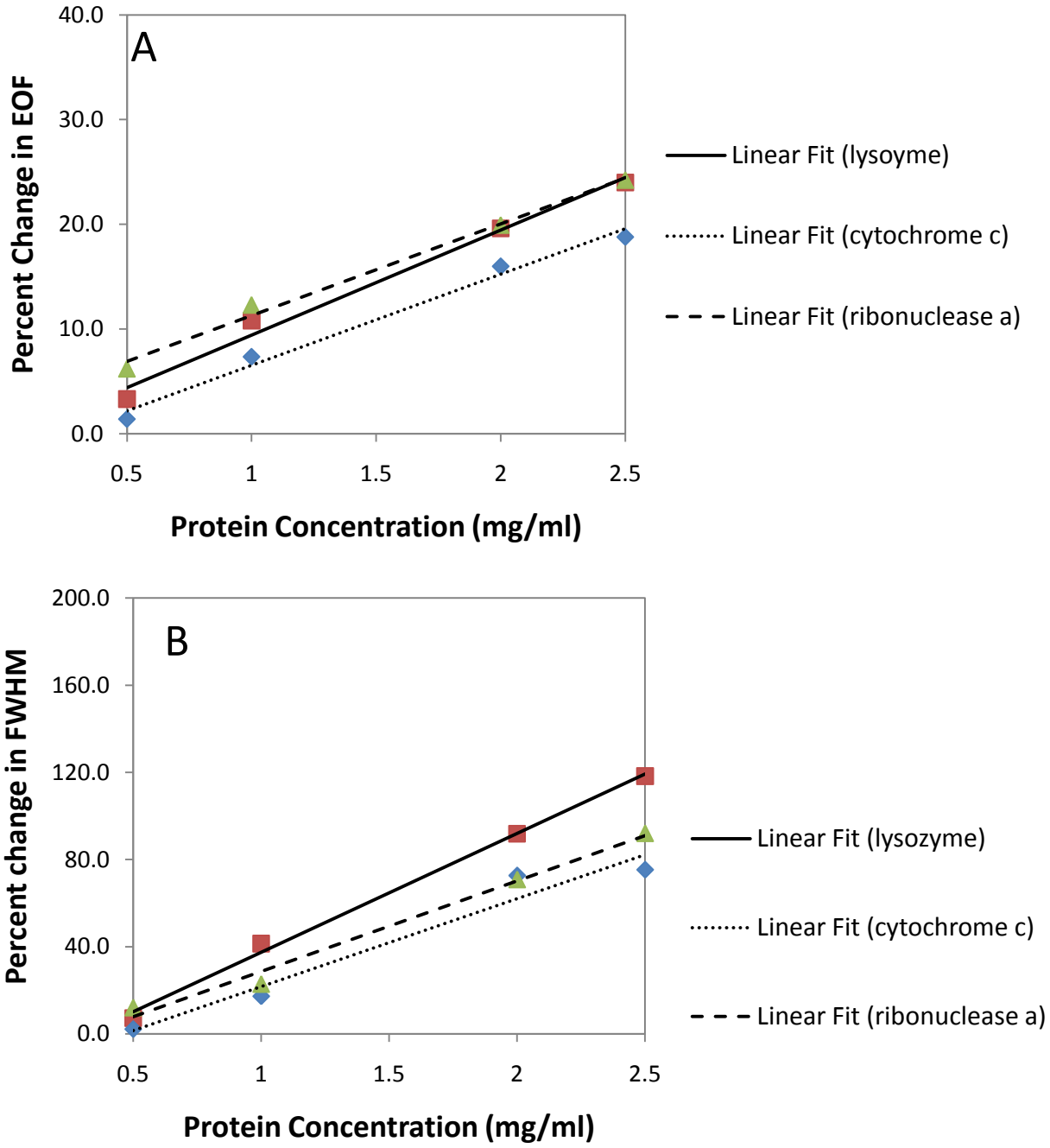

Figure 3.2. Plots presenting the relation between the percent changes in A) EOF rates and B) FWHM values of the photobleaching peaks due to model protein runs for the experiments with pH 9.1.

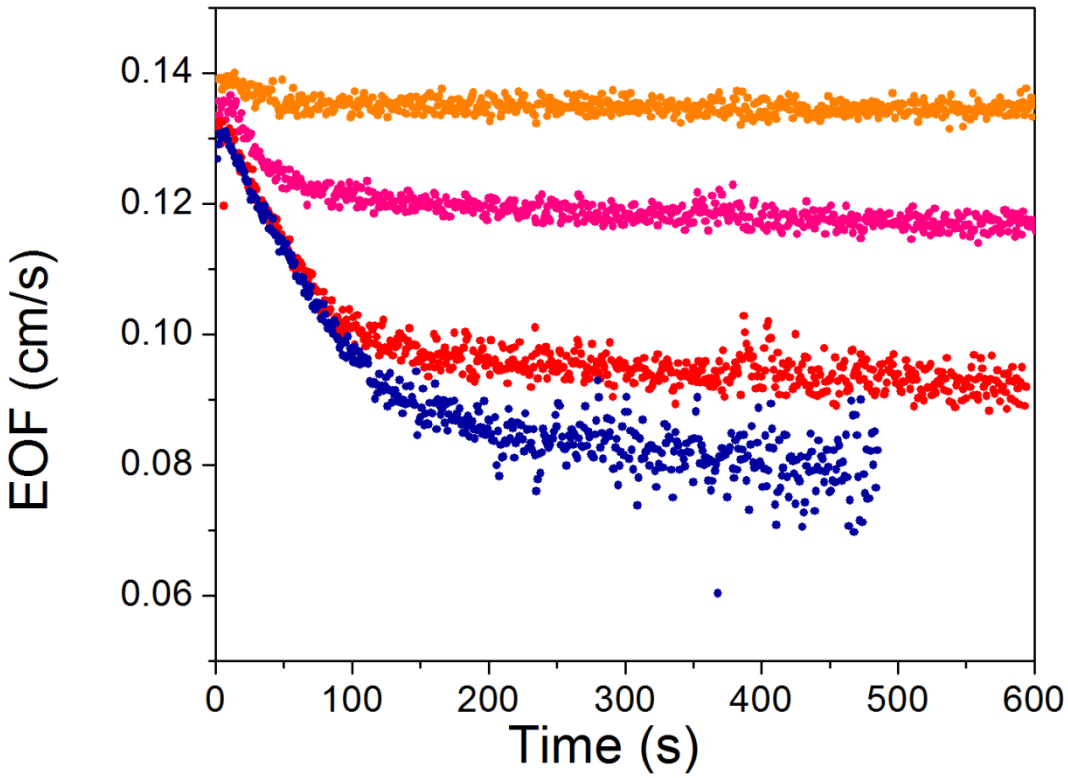

Figure 3.3. EOF rate versus time plots for experiments in which lysozyme samples with various concentrations were electrokinetically injected for 5 s. The plots are for lysozyme concentrations of 0.5, 1.0, 2.0 and 2.5 mg/ml from top to bottom. For the separation buffer and the sample solution, 20.1 mM borate buffer at pH 6.91 was used (electrophoretic current was 5.4 µA)

The initial, more rapid drop in EOF increased from 2.5% to 26.7% as the lysozyme concentration increased from 0.5 to 2.5 mg/mL, and the magnitude of the overall EOF decrease ranged from 2.8% to 37.0%, again increasing with concentration as shown in Table 3.2. The times of the initial decrease in EOF were longer at pH 6.91, compared to pH 9.1 ranging from 45 s to 120 s. The differences in EOF dynamics observed between lysozyme injections at pH 6.91 and 9.1 are likely caused by increased electrostatic interaction for more positively charged proteins due to the larger difference between the p*I* and buffer pH, and consequently, more adsorption to the capillary wall [56]. The first sharp decrease in the EOF rates is presumably caused by the adsorption of available protein molecules; however, the continuing EOF decrease could indicate

Table 3.1. Summary of changes in EOF rates and FWHM for protein injections at pH 9.1*

protein	*lysozyme*			*cytochrome c*			*ribonuclease A*		
concentration	EOF rate decrease percentage	drop time (s)	FWHM increase percentage	EOF rate decrease percentage	drop time (s)	FWHM increase percentage	EOF rate decrease percentage	drop time (s)	FWHM increase percentage
0.5 mg/ml	3.3 ± 2.2	25-35 s	7.2 ± 4.1	1.4 ±0.2	16-20 s	2.2 ±0.7	6.2 ± 0.5	34-39 s	12.0 ± 4.6
1.0 mg/ml	10.8 ± 3.0	67-72 s	41.4 ± 18.8	7.4 ± 0.5	39-44 s	17.3 ± 1.3	12.3 ± 3.2	66-71 s	22.8 ± 6.4
2.0 mg/ml	19.6 ± 0.4	73-78 s	91.8 ± 11.6	16.0 ± 0.5	80-85 s	72.7 ± 6.4	19.9 ± 1.3	90-100 s	70.8 ± 7.2
2.5 mg/ml	24 ± 1.6	100-110 s	118.3 ± 7.8	18.8 ± 1.1	94-100 s	75.4 ± 5.1	24.2 ± 3.4	164-171 s	92.0 ± 27.3

* Error values are standard deviations in three runs.

Table 3.2. Summary of changes in EOF rates during the experiments with buffer at pH 6.91*

protein	*lysozyme*			*cytochrome c*			*ribonuclease A*		
concentration	Initial EOF decrease percentage	Overall EOF decrease percentage	drop time (s)	Initial EOF decrease percentage	Overall EOF decrease percentage	drop time (s)	Initial EOF decrease percentage	Overall EOF decrease percentage	drop time (s)
0.5 mg/ml	2.5 ± 0.7	2.8 ± 0.6	47-52 s	-0.6	-0.7	-	2.4	7.9 ± 1.1	70-73 s
1.0 mg/ml	8.7 ± 0.6	12.5 ± 1.1	70-75 s	4.2 ± 1.2	5.2 ± 1.6	40-45 s	12.7 ± 9.0	14.8 ± 1.4	100-103 s
2.0 mg/ml	20.2 ± 0.5	26.3 ± 3.3	97-102 s	14.0 ± 0.7	18.4 ± 0.5	68-73 s	59.1 ± 17.0	27.7 ± 2.8	170-173 s
2.5 mg/ml	26.7 ± 1.2	37.0 ± 5.0	120-125 s	19.4 ± 0.5	22.0 ± 0.2	97-102 s	92.2 ± 9.1	34.6 ± 1.5	200-203 s

* Error values are standard deviations in three runs.

changes in the structure of the already adsorbed protein molecules. On the other hand, as the charge on the protein molecules increase, the repulsion of adsorbed molecules with same charge also increases. In addition, less ionized silanol groups at the lower pH on the capillary wall decreases the electrostatic attraction and thus the degree of adsorption. When all of these factors are considered, the overall effect on the EOF rates is a combination of couple opposing effects and apparently, electrostatic interaction between counter charged capillary wall and protein molecules overcomes the other factors. Towns and Regnier [56] have provided insightful information and set a milestone to understand the protein adsorption in CE experiments. They have reported that biggest EOF change occurred at longer times of the CE experiment, however, we should point out that in our case, the most dramatic EOF change happened at the beginning of the experiments.

The three model compounds (lysozyme, cytochrome *c* and ribonuclease A) for protein molecules presented similarities since they all caused decrease in the EOF rates. However, the degree of EOF change differs for each protein which has different structures, p*I* values, charged sites on the surface etc. which means the protein-capillary surface interaction is protein dependent [152]. For instance, the change in EOF rates occurred over a longer period of time for the ribonuclease A results (see Tables 3.1 and 3.2). But, the overall percent change in EOF rates is similar to the other protein results. Another interesting point for ribonuclease A is that even though, the buffer pH (9.1) is very close its p*I* value (9.3) the adsorption effects are still observed. Overall net charge of the protein molecule is zero, the adsorption is still achieved due to electrostatic attraction of local positively charged regions of the protein molecules with unequal charge distribution to the negatively charged capillary wall [153]. In addition, repulsion between the protein molecules is diminished since the overall charge is zero, thus the adsorption

is further supported [154]. It has also been reported in the literature that the adsorption process, otherwise an electrostatic interaction, becomes hydrophilic attachment when pH is close to the p*I* value of the protein [155].

The results for the experiments with myoglobin differed substantially from those with the other three proteins tested. At pH 9.1, injection of myoglobin resulted in no significant changes with EOF, suggesting that the protein was not adsorbing to the capillary surface under these conditions (see Figure 3.4). At 6.91, myoglobin has a net positive charge (p*I* is 7.3), and adsorption effect was expected. However, the flow profile was also constant with only 1.1% RSD in EOF rates as a verification of unchanged capillary wall chemistry. Similar observation was noticed in the report by Towns and Regnier that myoglobin presented very little adsorption effects when the buffer pH was varied (see Figure 3 in ref [56]). In addition, the myoglobin structure reveals that it is mostly neutral with a few charged sites [155]. It was reported that the myoglobin adsorbed the most at pH 6.5, not at the pH values above this.

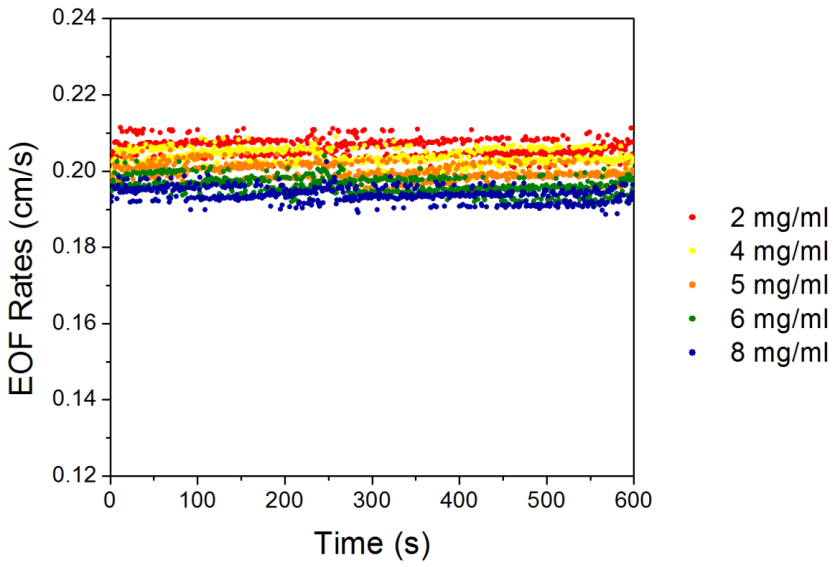

Figure 3.4. Changes in the EOF rates as a function of time for 5 s injections of myoglobin in 20.1 mM phosphate buffer at pH 9.1.

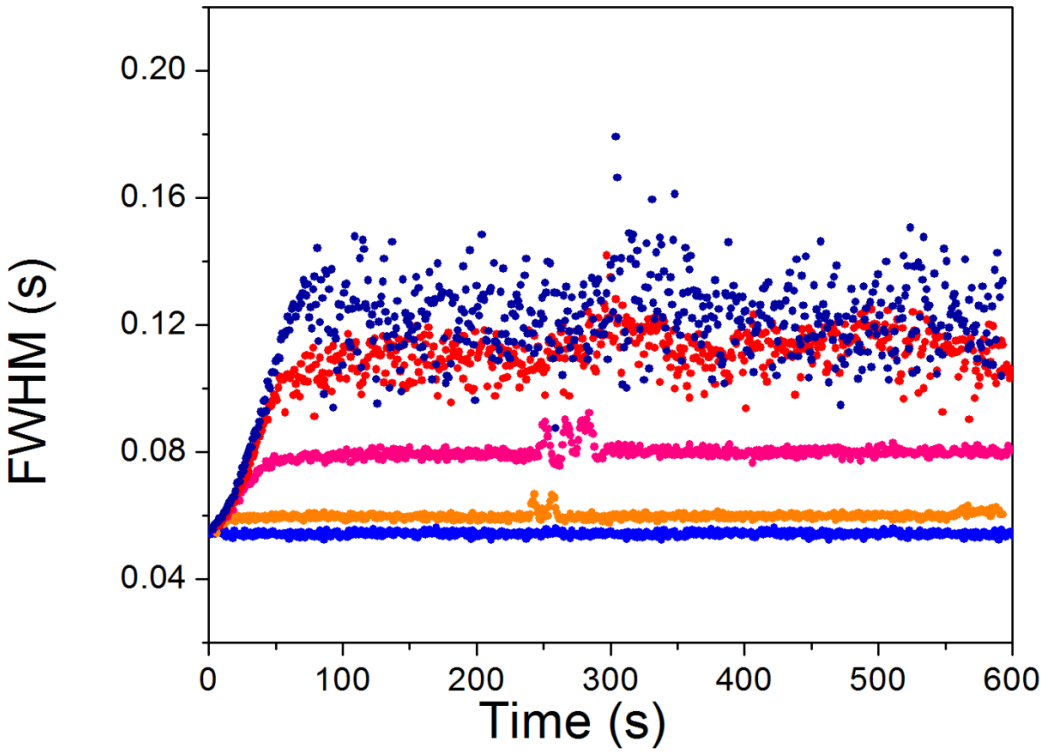

Figure 3.5. FWHM versus time plots for experiments in which lysozyme samples with various concentrations were electrokinetically injected for 5 s. The traces are for lysozyme concentrations of 2.5, 2.0, 1.0, 0.5 mg/ml from the top and the bottom trace is for blank sample. All other experimental conditions are the same as those in Figure 3.1.

As the EOF decreased after injection of lysozyme, broadening of the fluorescence vacancy peaks used for EOF measurement was apparent. Figure 3.5 shows the full width at half maximum (FWHM) values of these vacancy peaks versus time for different lysozyme concentrations at pH 9.1. Examples of EOF monitoring peaks for these experiments are presented in the Figure 3.6. Such broadening has been observed previously during EOF monitoring and has been attributed to a parabolic flow profile developing in the capillary due to a mismatch in zeta potential down the length of a capillary [110, 111] . Towns and Regnier reported hydrodynamic flow profile, band broadening and peak tailing when sample molecules adsorb to the capillary wall [56]. The EOF monitoring method used here allows for the

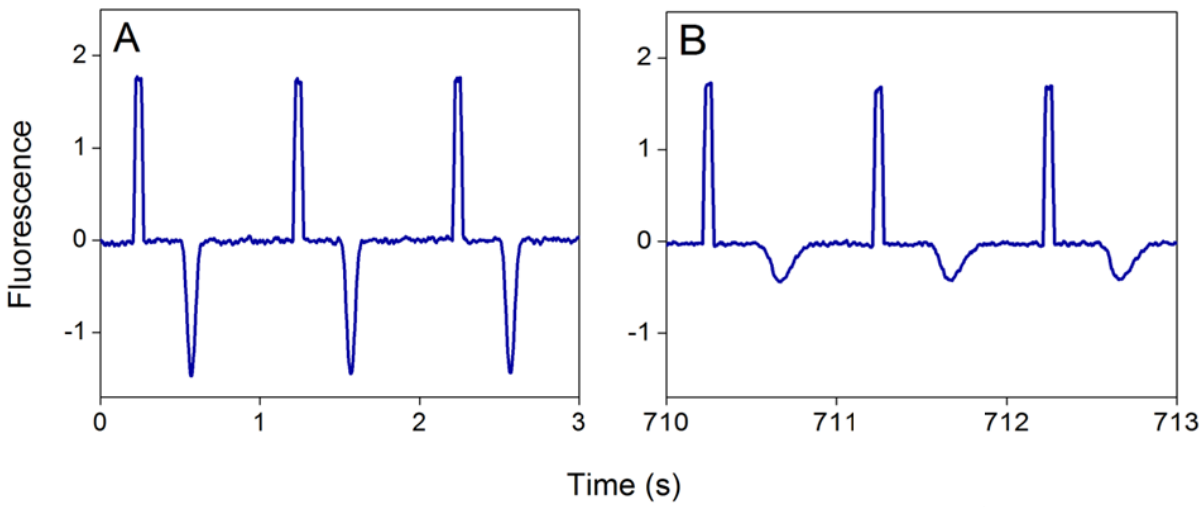

Figure 3.6. Development of band broadening due to protein injection to the CE system. Figure A presents photobleaching peaks at the beginning and Figure B shows the end of the experiment where 2.0 mg/ml lysozyme was injected for 5s in 20.0 mM borate buffer at pH 9.1.

observation of this effect as a function of time. The FWHM values increased at the beginning of the runs and then became constant, following the pattern of changes for the EOF. The FWHM values increased 7.2%, 41.4%, 91.8% and 118.3% as protein concentration increased from 0.5 to 2.5 mg/mL. Peak broadening was also observed in similar fashion for cytochrome *c* and ribonuclease A as a result of sample adsorption as seen in Table 3.1.

Although it is natural to conclude that the observed broadening was primarily due to a mismatch in the zeta potential down the length of the capillary due to protein adsorption, diffusional broadening will also increase as the EOF decreases and the migration times of the vacancy peaks increases. The vacancy peak broadening was evaluated quantitatively in order to determine the importance of these two factors. Several factors are known to contribute to peak variance (σ_{Tot}^2) for CE experiments, including injection length (σ_{inj}^2), detection length (σ_{det}^2), longitudinal diffusion (σ_{LD}^2) and zone mismatch (σ_{mis}^2) as shown in Equation 3.1. [156]

$$\sigma_{Tot}^2 = \sigma_{inj}^2 + \sigma_{det}^2 + \sigma_{LD}^2 + \sigma_{mis}^2 \qquad (3.1)$$

For the EOF monitoring experiments, σ_{det}^2 is defined by the focused laser beam used for LIF detection and should be both negligible and unaffected by protein adsorption in the capillary. The EOF monitoring peaks are actually coumarin vacancy peaks, and (σ_{mis}^2) at the EOF monitoring area should be unaffected by protein adsorption near the injection end. The vacancy injection time (50 ms) was optimized to not impact the vacancy peaks widths, and (σ_{inj}^2), will actually decrease as EOF decreases. Only longitudinal diffusion (σ_{LD}^2) and the mismatch in zeta potential down the length of the capillary should contribute to significant changes in σ_{Tot}^2 in response to sample adsorption.

The total variance for the EOF monitoring peaks (coumarin 334 vacancy peaks) was calculated for injections of 2.0 mg/ml cytochrome *c* at pH 6.91 and is shown in Figure 3.7 (top trace). The changes in (σ_{LD}^2) were quantified by measuring the diffusion coefficient of coumarin by using a modified version of the stopped flow method that was developed by Walbroehl and Jorgenson [157]. The diffusion coefficient was then used to calculate (σ_{LD}^2) as the EOF decreased. This is plotted in Figure 3.7 (bottom trace), and is clear that longitudinal diffusion is not a significant contributor to the observed changes in the EOF monitoring peaks. The middle trace in Figure 3.7 is the difference between σ_{Tot}^2 and σ_{LD}^2, and large changes are due to the mismatch in capillary zeta potential caused by sample protein adsorption. any inhomogeneities in the axial direction cause an axial pressure gradient and hydrodynamic flow [158, 159].

Another potential contributor to the observed changes in EOF and vacancy peak broadening is solution viscosity due to high protein concentrations as indicated in Equation 1.4 in Chapter 1. The experiments with myoglobin injections at 2.0, 4.0, 5.0, 6.0 and 8.0 mg/ml indicate that the solution viscosity is not a significant factor (see Figure 3.4). Also the EOF rates

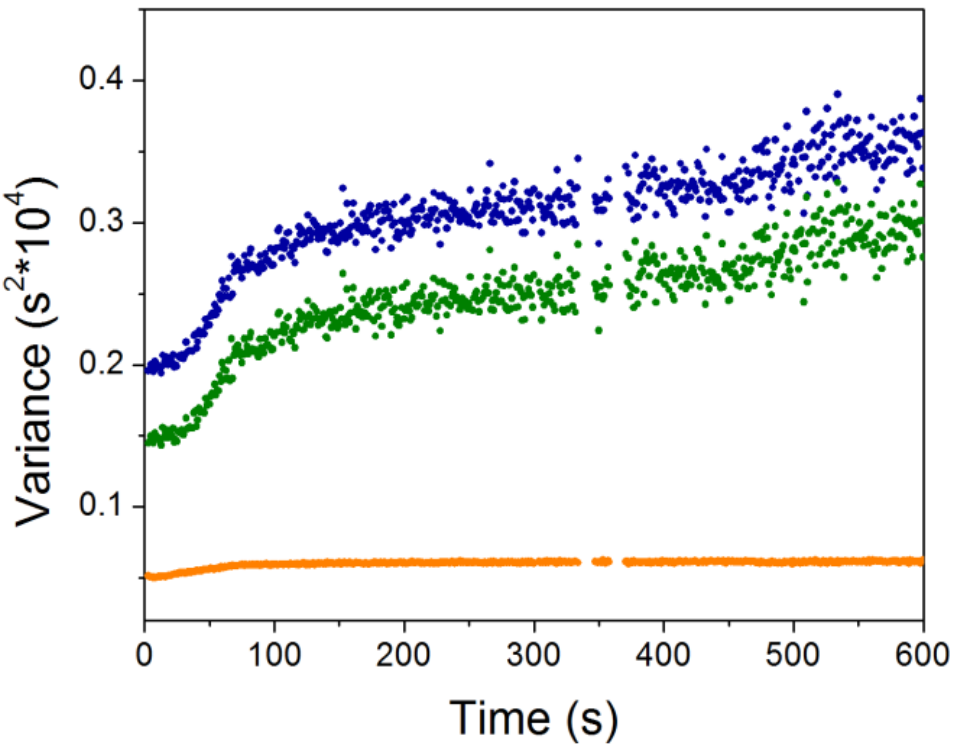

Figure 3.7. Contributions from different factors to the peak variance as a function of time for the run with 5 s electrokinetic injection of 2.0 mg/ml cytochrome *c* in 20.0 mM borate buffer at pH 9.1. Full blue circles (●), green circles (●), and orange circles (●) represent contributions from peak variance, mismatch factor and diffusion, respectively. All the other experimental conditions are the same as Figure 3.1.

do decrease at the very high protein concentrations used there, however, the changes are small relative to those observed at lower protein concentrations (Figure 3.1), and the dynamics of these changes are quite different qualitatively. The results from continuous EOF monitoring data presented very stable EOF flow profile which is an indication of unchanged capillary wall surface and a stable zeta potential.

Proteins are complex molecules that are composed of amino acids which have different structures, charges and degrees of polarity. Possible ways for protein molecules to interact with the capillary wall are through hydrophobic interaction, electrostatic interaction and formation of

hydrogen bonding [136]. Protein molecules favor to interact with a surface through hydrophobic relations, however, hydrophilic nature of the silanol groups on the capillary surface eliminates potential hydrophobic interactions [135, 160]. The formation of hydrogen bonds is dependent upon the degree of dissociation of hydroxyl groups on the silica which is related to pH of the separation medium. As the pH increases the dissociation increases which limits the hydrogen bond formation. Thus, the adsorption that was observed in this study is mostly due to the columbic attraction between negatively charged silanol groups on the capillary wall and positively charged sample molecules. The factors that affect the ionization of silanol groups and overall charge of the protein molecules will play important role in the degree of adsorption. Therefore, adsorption behavior of protein completely depends on the primary structure, conformation, availability of charged and polar sites on the surface of the protein, and pH of the solution. We should take into consideration the fact that once the protein molecules adsorb to the surface they will prevent further adsorption by other protein molecules due the repulsion effect of the same charges. The observed adsorption behavior of the protein molecules is a net result of these factors and it is specific to each protein. Therefore, it is hard to generalize these observations to every protein.

3.3.2. Carbohydrate, DNA, Cholesterol and Lipids

The effect of injection of some simple carbohydrates on EOF was studied using *d*-galactose, *d*-cellobiose, and maltoheptaose with concentrations 3.0, 6.0 and 12.0 mM at pH 6.91 and 9.1. The results of the experiments with the model compounds did not present any change in EOF rates or FWHM of the photobleached peaks (data not shown). Representative graphs for EOF and FWHM profiles for such experiments are shown in Figure 3.8. This was expected since

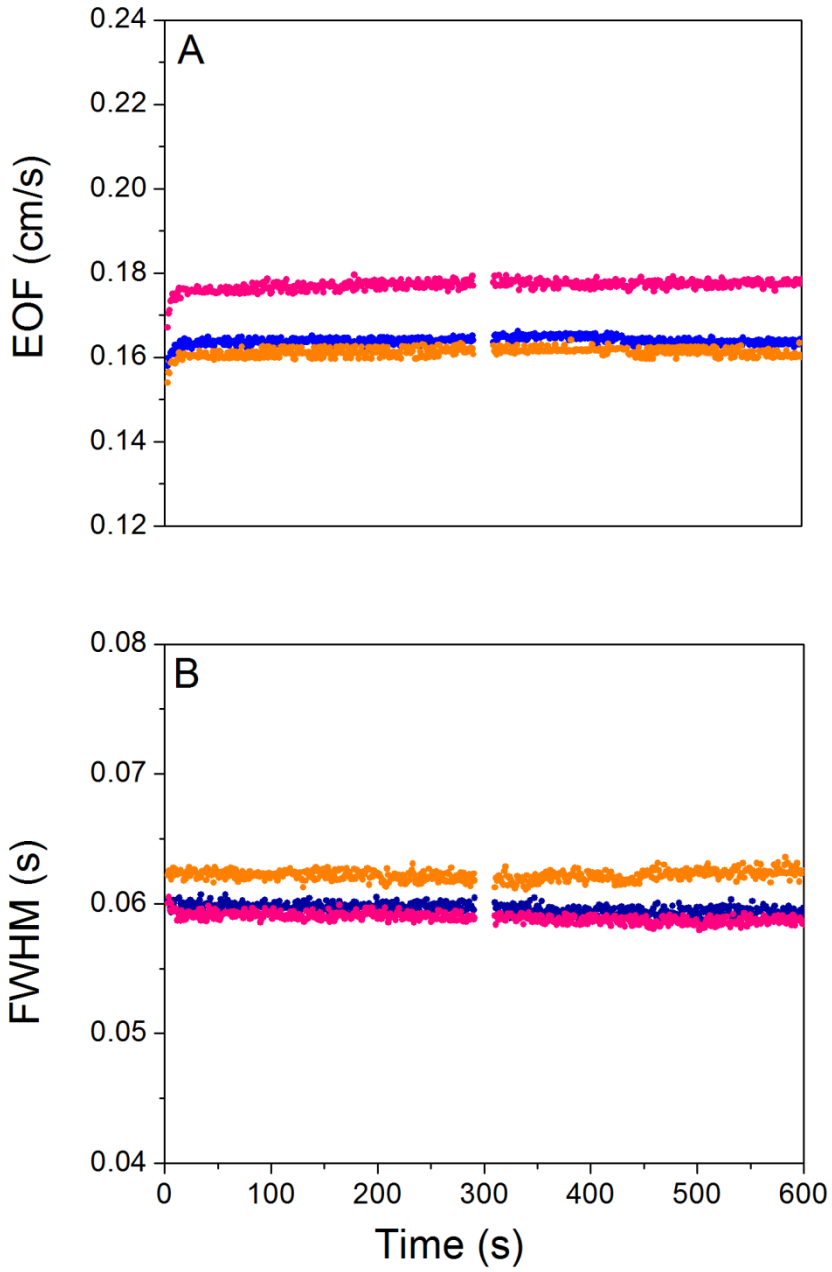

Figure 3.8. Plots of changes in A) EOF rates and B) FWHM values of the photobleaching peaks as a function of time to show sample plots for EOF and FWHM profiles for carbohydrate, liposome and DNA samples. The data of the plots are from the experiments with 5 s injection of DPPC/DPPG liposomes at 20.1 mM phosphate buffer at pH 6.91 with various concentrations (electrophoretic current was 5.4 µA). Blue circles (●), orange circles (●), and pink circles (●) represent samples with 5%, 10% and 20% (v/v) DPPC/DPPG liposomes, respectively. All the other experimental conditions are the same as Figure 3.1.

carbohydrates are neutral compounds, thus they do not interact with the negatively charged capillary wall.

For our study, dsDNA samples were prepared at 15, 30, 60 and 120 µg/ml concentrations in different buffers with neutral and basic pHs, and after injection to the capillary the EOF rates were monitored. Figure 4 is a representation of the EOF rates and FWHM results for the samples that did not change the capillary wall chemistry. The EOF rates remained constant throughout the runs as expected as the negative charges on the DNA molecules prevent any interaction with the negatively charged capillary wall.

It is often assumed that substance in a cell wall will adsorb to a capillary surface and significantly impact EOF for CE analysis of biological samples. We examined this hypothesis using samples containing lipids. Cholesterol which is part of the lipid family and cell membrane was dissolved in 62.5% THF and mixed with 37.5% ACN to improve miscibility of the two phases in concentrations of 2.0, 4.0 and 8.0 mg/ml. A blank solution containing the same ratio of THF and ACN as the sample solution was injected first. The results demonstrated that cholesterol does not affect the EOF.

Phospholipids typically are not soluble in water and are often dissolved in organic solvents (like chloroform) that are known to cause problems for CE separations [161, 162]. To overcome this, liposomes of DPPC/DPPG and DOTAP were prepared. This is appropriate for overall objective to understand how different components of a biological sample contribute to changes in EOF due sample adsorption since most phospholipids can be expected to be present in cell walls, the wall of organelles or other structures similar to liposomes. Liposomes of DPPC/DPPG (3.24 mM DPPC and 0.36 mM DPPG) were prepared according to Zuidam et al. [163] and solutions of 5%, 10%, 20% (v/v) in pHs 6.91 and 9.1. The sizes of the liposomes were

determined to be 5 μm by an optical microscope (Nikon Microphot-FXA) and TEM (JEOL 100CX). Injection of these liposomes did not significantly change the EOF rate. The outer surfaces of the liposomes are negatively charged based on the structures of the lipids, and it is not surprising that these intact liposomes might not interact with the negatively charged capillary surface. In order to disrupt the liposomes and expose the surface to the hydrophobic part of the molecules, acetonitrile was injected immediately after the liposome samples. The zone of acetonitrile will partially mix with the liposomes after injection due to diffusion, and the acetonitrile zone will overtake the liposomes after electrophoresis begins. The injection of acetonitrile after the liposomes did not result in significant changes to the EOF. Next, a positively charged liposome, DOTAP was prepared [149] and injected at different concentrations (0.275 mM, 0.55 mM, and 1.1 mM). Injection of these liposomes also did not affect the EOF rates both with and without injection of acetonitrile to disrupt the liposomes. The DOTAP liposomes were studied at pH 6.91 only since they will not form liposomes at pH 9.1.

3.3.3. Cell Samples

Samples containing cultured mammalian cells were injected in order to study the effects of sample adsorption on EOF. Even the injection of single cells is known to impact the EOF and CE separations, presumably due to adsorption of components of the cells. Two types of cultured human adipocyte cells with different lipid content (low and high) were used. Injections without lysing did not affect the EOF dynamics. Therefore, the cells were lysed just before injection to the CE system by using a freeze-thaw method [150]. The cell lysate sample did have a smaller effect (8% decrease) on the EOF rates when the separation was carried out immediately following injection. To increase the effect a 1.0 min incubation time was included immediately after injection of the cells. The plots of EOF and EOF monitoring peak FWHM values are shown

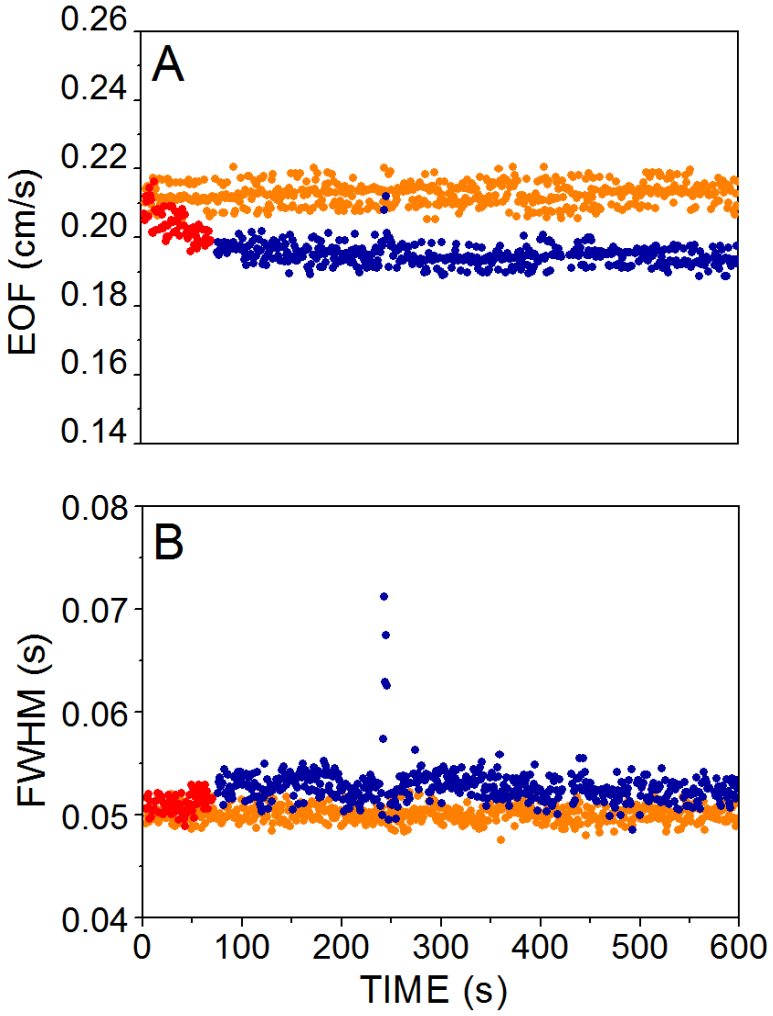

Figure 3.9. Plots presenting changes in A) EOF rates and B) FWHM values as a function of time for the adipocyte cell sample (with less fat content) with 20.0 mM borate buffer at pH 9.1 buffer. Blank sample (orange circle (●)), cell lysate sample before incubation (red circle (●)) and cell lysate sample after incubation (blue circle (●)) are presented in the plots. All the other experimental conditions are the same as Figure 3.1.

in Figure 3.9A and 3.9B, respectively, for the low lipid content adipocytes at pH 9.1. The top trace in Figure 5A and bottom trace in Figure 5B present the results for control experiments (injection of separation buffer without cells). The results are qualitatively and quantitatively

similar to the experiments with proteins (lysozyme, cytochrome *c*, ribonuclease A). The EOF rates decreased 11% and FWHM increased 7% after the sample injection. The difference in lipid

Table 3.3. EOF rate and FWHM value changes due to complex biological sample injections

	pH 6.91		pH 9.1	
Sample	**EOF Decrease**	**FWHM increase**	**EOF Decrease**	**FWHM increase**
Cell sample with low fat content	3%	4%	6%	2%
Cell sample with high fat content	6%	2%	11%	7%
12.5% FB Serum	1%	1%	2%	4%
25% FB Serum	4%	3%	5%	14%
50% FB Serum	12%	15%	8%	30%
75% FB Serum	16%	21%	19%	67%

content did not seem to have a significant impact on the EOF decrease for the results of pH 6.91 experiments as indicated in Table 3.3. However, a small difference is noticed for the pH 9.1 results between cells with low fat content and high fat content which resulted in more changes in the EOF rates and FWHM values. Proteins and enzymes play important role in the pathway of expressing lipid molecules for adipocyte cells [164]. Differences in lipid content could cause differences in the content of lipid-binding proteins such as ALBP/aP2 which has p*I* value of 9.0 [165]. Strong adsorption effects were observed when pH is close to the protein's p*I* value during the experiments with ribonuclease A. This could be one of the factors that affected the observed different results for the cell sample with higher fat content at pH 9.1. Overall, the changes in the EOF rate are very similar for both types of cells which indicate fat content of the cell sample

does not affect the adsorption to the capillary wall. This is consistent with the results for injection of lipid samples (Section 3.3.2).

3.3.4. Serum Samples

Fetal bovine serum (FBS) was used to study the impact of serum on EOF. Diluted solutions 12.5%, 25%, 50%, and 75% (v/v**)** solutions were studies at both pH 6.91 and 9.1. The results for EOF rates and FWHM values for experiments at pH 6.91 are presented in Figures 3.10A and 3.10B, respectively. The EOF rates decreased (1%, 4%, 12%, and 16% for increasing FBS concentrations) and FWHM values increased (1%, 3%, 15%, and 21% for increasing FBS concentrations) as an indication of sample adsorption to the capillary wall, the results are summarized in the Table 3.3. For the runs with pH 9.1 buffer, decrease in the EOF rates and apparent band broadening were observed with the increasing serum concentration in a similar fashion to the results at pH 6.91 (see Table 3.3). As it was noted from the model protein runs, these observations are indications of sample adsorption to the capillary wall, and serum proteins are suspected to be responsible for this adsorption effect. The serum solution consists of various protein molecules with different structures and p*I* values in a range of 3.75-10.0 [166]. At the pH values that the experiments were conducted, there is a mixture of positively and negatively charged proteins in the serum sample. The apparent adsorption effects are caused by these protein molecules.

In addition to the observation of sample absorption, the serum sample results exhibited unusual features in the EOF and FWHM plots as clearly seen in the Figures 3.10A and 3.10B (also see Figure 3.11). EOF rates decreased and FWHM values increased during these features

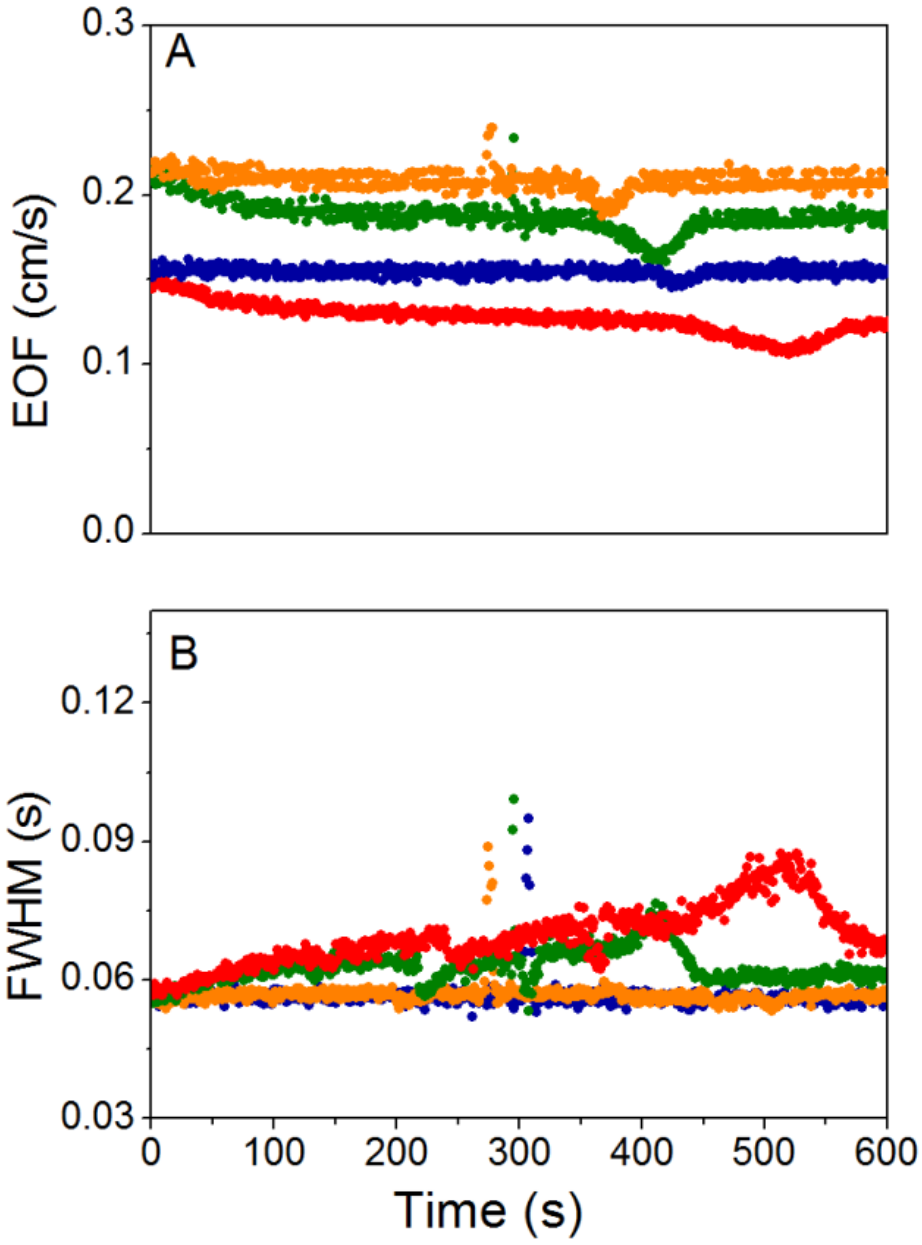

Figure 3.10. Plots of changes in A) EOF rates and B) FWHM values of the photobleaching peaks as a function of time for 5 s injection of serum samples results with varying concentrations in 20.0 mM phosphate buffer at pH 6.91 (electrophoretic current was 5.4 µA). Red circle (●), green circle (●), orange circle (●), and blue circle (●) represent 75%, 50%, 25% and 12.5% FBS samples, respectively. All the other experimental conditions are as same as in Figure 3.1.

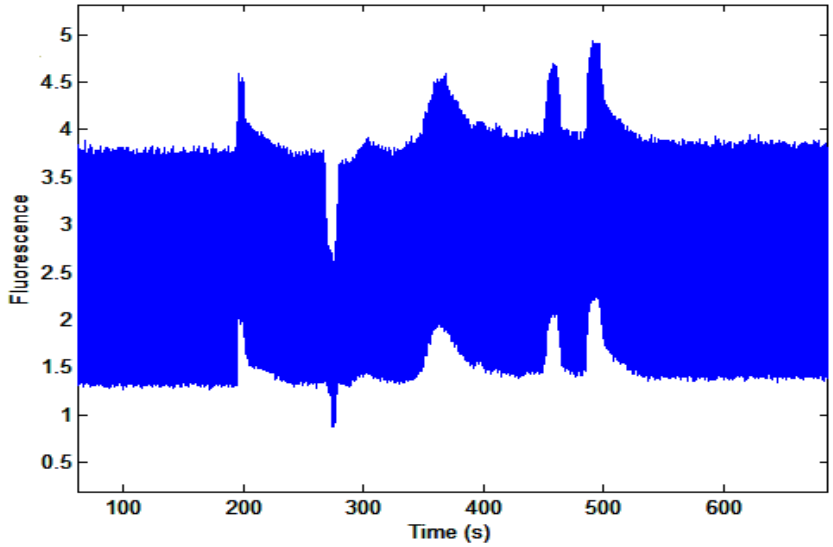

Figure 3.11. Raw data of 5 s injection of FBS sample at 12.5% dilution

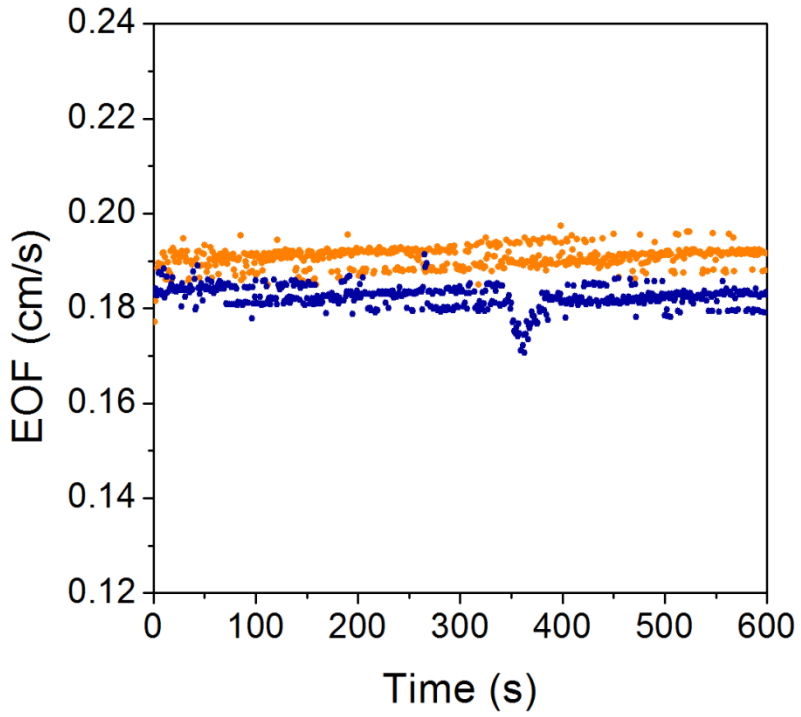

Figure 3.12. Changes in EOF rates as a function of time for 5 s injections of 15.1 mM NaCl (top trace) and FBS sample at 12.5% dilution (bottom trace) in 20.1 mM phosphate buffer at pH 6.91.

and then the values went back to the earlier values. Serum sample is a complex sample with various components, therefore, these features could be due to any of the components of the sample. The salt content is one of the major constituents of the serum. The salt ions can cause some changes in EOF due to the difference in their conductivity. In order to determine if the salt content of serum was responsible for the peaks, first the salt concentration in the FBS sample was determined, and then a conductivity study was carried out. The capillary was filled with several NaCl standards and12.5% (v/v) FBS solution then, the current in the capillary was measured for each sample. By using a calibration plot, the salt concentration in the serum sample was determined to be 121 mM. The runs with 121 mM NaCl had a very stable EOF profile, which shows that the salt content was not the cause of the unusual features that were observed in the FBS results (see the comparison of EOF rates for the experiments with NaCl and FBS sample in Figure 3.12). Possibly, the peaks were caused by other ions in the FBS sample, but they did not cause any adsorption effects.

3.4. Conclusion

Effects of biological samples on the EOF dynamics and capillary wall surface chemistry have been monitored using the continuous EOF monitoring method. Model compounds to represent biological cell components were used at two pH values (6.91 and 9.1). Protein molecules affected the EOF rates the most by adsorbing to the capillary wall which results in nonuniform zeta potential and slower EOF rates. The adsorption behavior is protein dependent. In addition, band broadening of the photobleaching peaks were observed as a direct result of sample adsorption. Similar adsorption effects were observed in the experiments with the cell lysate and serum samples. The continuous EOF monitoring method proved to be a useful and suitable tool to investigate such effects since it provided a real-time EOF profile for the CE runs.

CHAPTER 4
EXPERIMENTAL AND COMPUTATIONAL INVESTIGATION OF ELECTROOSMOTIC FLOW AND ELECTRIC FIELD DYNAMICS FOR CAPILLARY ELECTROPHORESIS WITH DISCONTINUOUS SOLUTIONS

4.1. Introduction

Capillary electrophoresis experiments are usually carried out using the same buffer for the sample and the separation. However, discontinuous systems are also part of CE applications, in which the sample is introduced to a CE system in a solution that differs from the separation buffer in terms of ionic strength, pH and composition. Discontinuous systems arise upon injection of any sample into an otherwise homogenous system. In electrophoretically mediated microanalysis (EMMA), there are often multiple discontinuities as zones enzyme and/or substrate are injected and then mixed by differences in their electrophoretic mobilities. The products and reactants then separate electrophoretically and products are detected [167]. In addition, sample stacking techniques employ discontinuous systems to increase the analyte concentration and lower the limit of detection [168-170]. Such systems have been used for applications in various fields such as biological, environmental, toxicology, food analysis and pharmaceutical fields [171, 172]. Several approaches have been implemented to achieve sample stacking. In field amplified sample stacking, the sample is prepared in a buffer that has a lower concentration than the separation buffer [173-175]. Whereas, for the isotachophoresis technique, the sample solution consists of leading and terminating buffer solutions with different mobilities than the separation buffer, in addition to analyte molecules [176-178]. Another approach uses a sample with a different pH than the buffer, generating a pH junction, so that the analyte molecules are stacked based on their isoelectric points [179-181]. In addition to sample stacking applications, discontinuous systems are observed when the sample is prepared in a matrix that includes an organic modifier. The organic additives are used to lower the conductivity of the

sample solution, to increase analyte solubility or to affect the acid-base properties of the sample components [182].

Ionic discontinuities within an electrophoretic system cause non-uniform field distribution which give rise to dynamic changes in local ionic migration rates yielding sample concentration changes that would not occur in conditions of uniform electric field and EOF. This phenomenon is based on the basic principles of Ohm's law and adjustment of the Kouhlrasch regulation function (KRF). According to Ohm's law (Equation 4.1), the current density (j) is constant through the capillary column. The changes in zone conductivity, σ, is compensated by the electric field (E), therefore, the low conductivity zone has a relatively high electric field.

$$j = E\sigma \tag{4.1}$$

The Kouhlrasch regulation function (KRF) should be a constant value at any given point x along the migration path. This value (ω) depends on the concentration (c_i) of the ions, their mobilities (μ_i) and relative charge (z_i) as seen in Equation 4.2. [183]

$$\omega = \sum_i \frac{c_i(x) z_i}{|\mu_i|} \tag{4.2}$$

This function requires adjustment of the concentration of ions when there are changes in the ionic content and concentration in solution. If the KRF value of the sample plug, ω_S, is lower than the KRF value of separation buffer, ω_{BGE}, sample ions will stack at the boundary between the two zones. Additionally, the velocity of the analyte ions in the sample zone is higher than its velocity in the buffer zone, due to the higher field intensity in the sample zone, which has lower conductivity. With the influence of an applied field, the analyte molecules pass the boundary between the sample and the buffer, and then they are concentrated to a sharp zone to adjust to the KRF value of the buffer. The sharp sample zone migrates with its electrophoretic mobility and is detected at the detection point. Peak broadening occurs due to the normal dispersive factors

present in CE plus a pressure gradient that is caused by the mismatch between the low field and high field, which in time counteracts the zone sharpening effect of stacking. The concentration boundaries between the buffer and sample zones move with the EOF through the capillary. They can be detected as a peak if $\omega_S > \omega_{BGE}$ or as a dip in the baseline if $\omega_S < \omega_{BGE}$ [183].

In 2003, Pittman et al. investigated EOF dynamics for sample stacking conditions experimentally by monitoring the EOF rates continuously [110]. The method is based on periodic photobleaching of a neutral dye which is added to the separation buffer and sample solution. A UV absorbance detector was employed to detect the analytes and observe sample stacking. The EOF dynamics were monitored using a laser induced fluorescence (LIF) detection system. This report showed that EOF rates decreased and peak widths broadened as a result of mismatch between different parts of the capillary. The EOF monitoring method was found to be an efficient method to obtain time-resolved EOF data and observe changes in the EOF dynamics during every second of a CE experiment. In addition, it was shown in recent reports that the EOF monitoring method can be employed to improve the reproducibility of CE and study fundamental aspects of CE.

In this study, we propose using two marker compounds to monitor field changes in discontinuous systems. The continuous EOF monitoring system that was used to investigate EOF dynamics during sample stacking experiments can be easily modified to monitor the field changes during a CE experiment. Two marker compounds, one neutral and one negatively charged, are added to the background electrolyte and sample solution. The neutral compound migrates only with the EOF and its migration data is used to calculate the EOF rates. A negatively charged compound has a negative electrophoretic velocity at the buffer pH, and its apparent velocity is a vectoral sum of the EOF rate and its own electrophoretic velocity. The

electrophoretic behavior is directly related to the electric field strength, so when the time resolved migration behavior of the negatively charged compound is obtained, it will provide some information about the field dynamics in the system. Obtaining this information allows us to learn more about complex systems in CE, which are part of every common application of CE. In this study, a continuous field and the EOF monitoring method was presented and applied during discontinuous system conditions. The results were compared to the simulation results of the same experimental conditions.

4.2. Material and Methods

4.2.1. Chemicals

Sodium phosphate (monobasic), fluorescein (sodium salt), ACES (N-[2-acetamido]-2-aminoethanesulfonic acid), and acetonitrile were obtained from Sigma-Aldrich (St. Louis, MO). Sodium hydroxide was purchased from Fisher Scientific (Fair Lawn, New Jersey). Laser grade coumarin 334 was obtained from Acros Organics (Morris Plains, NJ). All aqueous solutions were prepared in ultrapure water (> 18 MΩ-cm, ModuLab water purification system, United States Filter Corp.; Palm Desert, CA). Coumarin 334 was dissolved in methanol and diluted with ultrapure water to 100 µM. Working stock solutions of coumarin 334 (500 nM) were prepared by diluting the 100 µM solution with the separation buffer. A fluorescein stock solution (1.94 mM) was prepared in ultrapure water and diluted to 500 nM with the separation buffer to be used as working stock solutions.

4.2.2. Capillary Electrophoresis

The general design of the CE system was described previously [108]. Fused-silica capillary (50-µm id/360-µm od) was purchased from Polymicro Technologies (Phoenix, AZ) and cut to 72.0 cm. The polyimide coating was removed (~1 cm) to make a detection window at 49.1

cm from the injection end of the capillary. All separation buffers used were filtered with a 0.2 μm nylon filter (Whatman, Oregon) prior to use. In order to monitor EOF and the electric field, all solutions contained 100 nM coumarin 334 and 25 nM fluorescein. Injections of solutions for discontinuous solution measurements were performed hydrodynamically by lowering the detection end of the capillary 11.4 cm below the injection end. The injection length is calculated by using Pouiselle equation for hydrodynamic injection. An electrophoretic potential of 30.0 kV (417 V/cm) was applied with a Spellman CZE 1000R high voltage power supply (Hauppauge, NY) for all experiments.

4.2.3. Electroosmotic Flow Monitoring

The instrument for CE with EOF monitoring is similar to one described previously [108]. The 488.0-nm line of an argon ion laser (Melles Griot 543-AP-A01; Carlsbad, CA) was used as the light source. The laser beam was split with a broadband cubic beam splitter, and then the beams were focused on the capillary at two different positions, F1 and F2. The bleaching portion of the beam (35.0 mW) was directed through a computer controlled shutter (Uniblitz LS6Z2; Rochester, NY) and focused at the F1 position on the capillary. The shutter was opened for 50 ms every 1.0 s to generate photobleached zones. Additionally, a small portion of the light passing through the capillary at F1 was directed to a photomultiplier tube (PMT) (Hamamatsu HC 170; Bridgewater, NJ) by a fiber optic to mark the beginning of each individual flow and field measurement. The detection portion of the beam was attenuated to 8.4 mW by a neutral density filter and focused on the capillary at F2 by a microscope objective, which was used to collect fluorescence emission. The emitted light was directed through a dichroic mirror (505DRLPXR; Omega Optical; Brattleboro, VT), band-pass filter (520BP10; Omega Optical; Brattleboro, VT) and pinhole (1.0 cm) to the PMT biased at 850 V. The PMT signal was filtered with a 200 Hz

low-pass filter. A program written in LabView (National Instruments; Austin, TX) was used to control the shutter and to collect the data using a National Instruments PCI-6299 (Austin, TX) data acquisition board at a 1000 Hz scan rate. The distance between the bleaching and detection points (d_{F1-F2}) was determined to be 1066 ± 2 μm using a previously described method [108].

4.2.4. Data Analysis

Data for the EOF monitoring experiments were analyzed with a program written in Matlab 6.1 (Natick, MA), which was used for data smoothing, baseline subtraction, peak picking, and calculation of EOF rates and electrophoretic mobilities based on the migration times for the neutral marker and fluorescein vacancy peaks. The program also provided FWHM values for both photobleached peaks. Microsoft Excel (Microsoft Corp.; Redmond, WA) and Origin 7.5 (Northampton, MA) were also used to plot and present the data.

4.2.5. Computer Simulations

The program, Simul 5.0, was used to perform the simulations, and was downloaded from www.natur.cuni.cz/gas [184]. Consistent with other work with computer simulations, to avoid mathematical instability and oscillations in the simulated concentrations, the field strength used in the simulations were much lower 0.857 V/cm, than the corresponding wet experiments, so the effects of diffusion are exaggerated in the simulated results. The simulated capillary was 35.0 cm in total length but only 72 mm of the tube was actively modeled (278 mm in "fake" length), and the EOF was disabled to allow the observation of the developments of local changes within the modeled window. The initial injection zone was 8.5 mm in width. The electrophoretic mobility of sodium was available from the Simul 5.0 program which obtained from ref. [185]. The value of electrophoretic mobility of 10.0 mM ACES at pH 7.43 used was 24.9×10^{-9}mm^2/Vs. It was determined by injecting sample zone containing different concentration of ACES. These mobility

experiments were performed using a P/ACE MDQ with 32 Karat version 5.0 software from Beckman Coulter, Inc. and the UV absorbance wavelength was 230 nm. 10.0 mM and 1.0 mM ACES at pH 7.43 were injected hydrodynamically for 0.5 s at 5 psi into a capillary filled with 5.0 mM ACES at pH 7.43. The ACES mobility was determined based on the migration time of the sample zone. The electrophoretic mobility of fluorescein in 10.0 mM ACES buffer at pH 7.43 was determined based on the migration time of fluorescein in CE experiments using the same CE instrument described in section 2.2.

4.3. Results and Discussion

4.3.1. Development of a Two-Marker System for EOF and Electric Field Measurement

The goal of this study was to develop a two-marker technique to simultaneously monitor EOF and electric field dynamics during CE experiments when the capillary contained discontinuous solutions. A discontinuous system consists of zones with different conductivity which could be caused by difference in ionic strength, composition and pH of the sample zone compared to the separation zone. Low ionic strength buffers generate low conductivity, high resistivity and high electric field, and the opposite is true for the high ionic strength buffers. The differences in the ionic strength result in discrete zones within local electric field. Equations 4.3 and 4.4 show the relationship between field strength and differing resistivities of two buffers, where E_1 and E_2 are the field strengths of the high and low resistance solutions, respectively. E_0 is the field strength in a system of only buffer 1 or 2, γ is the ratio of the resistivities of the low concentration buffer to that of the high, and x is the fraction of the capillary filled with low resistance buffer.

$$E_1 = \gamma E_0/[\gamma x + (1 - x)] \quad (4.3)$$

$$E_2 = E_0/[\gamma x + (1 - x)] \quad (4.4)$$

In CE, net velocity of an analyte, v_{net}, includes contributions of the analyte's electrophoretic velocity, v_{ep}, and the velocity of EOF, v_{eof}, as shown in Equation 4.5. The electrophoretic and electroosmotic velocity are directly proportional to E and analyte's electrophoretic mobility, μ_{ep}, and electroosmotic mobility, μ_{eof}, respectively, as shown in Equations 4.6 and 4.7.

$$v_{ep} = v_{net} - v_{eof} \tag{4.5}$$

$$v_{ep} = \mu_{ep} E \tag{4.6}$$

$$v_{eof} = \mu_{eof} E \tag{4.7}$$

The information about the EOF dynamics obtained from one marker (neutral) is an indication of EOF of the whole capillary system. However, the second marker's (charged) electrophoretic velocity provides information about changes in the local electric field as seen in Equation 4.6. A two-marker system is developed by using coumarin 334 and fluorescein dyes. Coumarin 334 is neutral over a wide range of pH values (3.5-11.0), therefore, its migration is only influenced by the EOF and it was used as an EOF marker in previous [110, 111] and recent research [126]. Fluorescein has pKa values of 6.4, 4.3 and 2.2 [186] with fluorescence properties that are sensitive to pH changes. At pH= 7.43, the buffer pH that was used, fluorescein is in its dianion form. Due to its charge, fluorescein's migration includes influences of EOF and electrophoretic mobility and it is possible to observe the field changes from its migration behavior.

The successful development of the two-marker system was accomplished by performing continuous periodic photobleaching of these two dyes in a buffer solution. As a result, two negative peaks were generated in the electropherogram, along with a positive peak that was used as a time stamp as seen in Figure 4.1. Although EOF information is useful, the two-marker

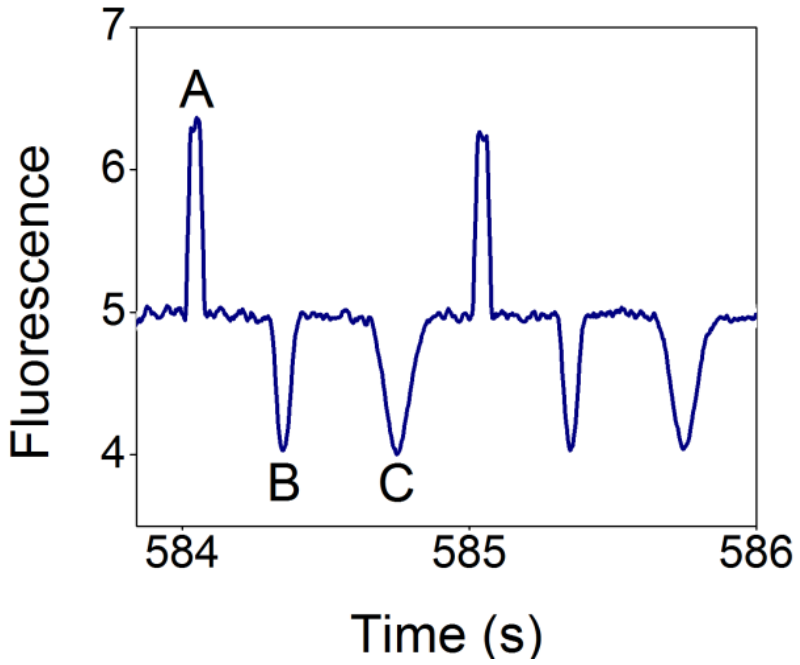

Figure 4.1. Data illustrating the EOF and electric field monitoring technique. The buffered solution filling the capillary (10.0 mM ACES at pH 7.43) contained 100 nM coumarin 334 (neutral) and 25 nM fluorescein (negatively charged). Photobleached zones were generated by opening a shutter for 50 ms to produce a pulse from an Ar^+ laser. The shutter was opened every 1.00 s. The photobleaching and fluorescence excitation beams were 35.0 and 8.4 mW, respectively at 457.9 nm. The positive peak (A) is due to light from the bleaching pulse. The negative peaks are due to coumarin 334 (B) and fluorescein (C) vacancy peaks and were used to monitor EOF and the local electric field, respectively. A second measurement cycle is shown after the first cycle. For the experiment shown here, the field was 417 V/cm, and the electrophoretic current was 5.6 μA.

system can be used to observe a charged compounds' migration behavior throughout an experiment which could provide more detailed information about CE separations.

4.3.2. Application to Discontinuous Solution Studies

A discontinuous system can be generated by preparing a sample in a more dilute buffer than the separation buffer. Changes in ionic strength of the sample zone result in a non-uniform electric field and the CE separation is affected by these changes. This type of discontinuous

system was used to investigate EOF dynamics during sample stacking conditions in a previous study by Pittman et al [110] with only one marker (neutral) compound. Preparing the sample solution in a more dilute buffer than the separation buffer to generate sample stacking is a common approach. In the previous study, the phosphate buffer system was used. In this study, an ACES buffer system was used to compare the EOF profile of such systems to a theoretical study performed by Thormann et al [187]. The sample with lower ionic strength buffer is introduced into the capillary by hydrodynamic injection to prevent sampling bias on negatively charged ions. EOF is sensitive to even small changes in the ionic strength of the sample introduced, so the bulk EOF will show that change in the flow. The sample was prepared in 0.1 mM ACES buffer at pH 7.43 where the separation buffer is 10.0 mM ACES buffer at pH 7.43. Both solutions contained 100 nM coumarin 334 and 25 nM fluorescein for EOF and field monitoring. The sample zone filled 4% of the capillary. Figure 4.2 presents the EOF for this experiment. As was observed by Pittman et al [110] for experiments with phosphate buffer and predicted by Thormann et al. [187] for the same solutions using computer simulation, the EOF decreased sharply at the beginning of the experiment, became constant for a time that corresponded to the time that it takes for the sample zone to leave the capillary, and then decreased and became constant again. The EOF rates increase in the low ionic strength buffer because the Debye layer thickness is inversely proportional to the buffer concentration. Then, the sample plug mixes with the separation buffer, which has high ionic strength, resulting in a decrease in the EOF rates due to this dilution. Finally, when the sample plug leaves the capillary, the EOF rates are slower because the high ionic strength buffer fills the capillary. These results with monitoring of EOF

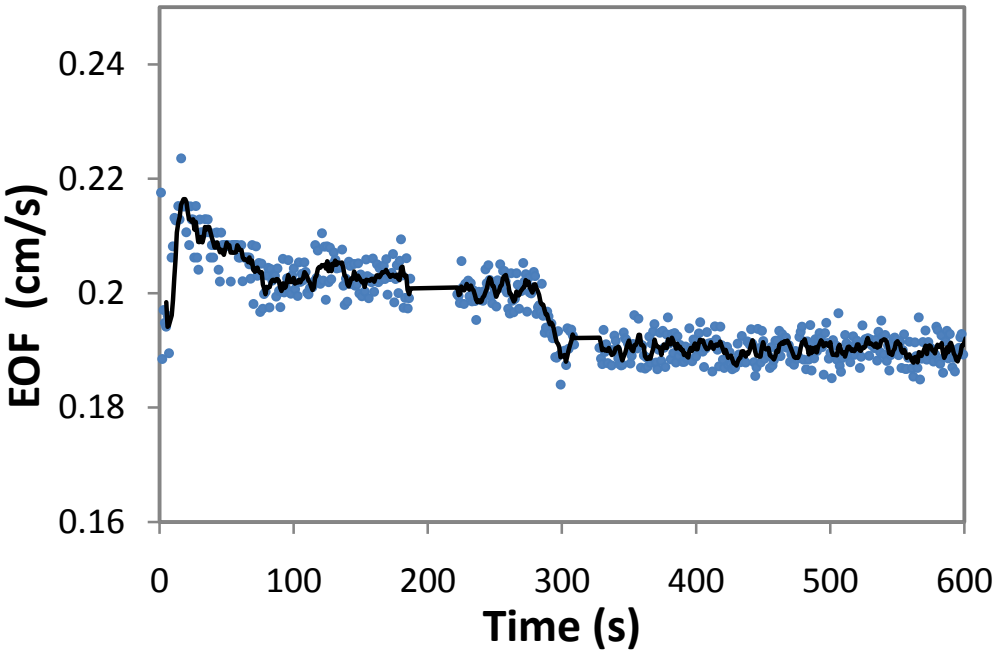

Figure 4.2. EOF versus time for a zone of dilute buffer solution (0.1 mM ACES at pH 7.43) in a capillary filled with 10.0 mM ACES at pH 7.43. The dilute solution was injected hydrodynamically for 240 s to fill 4% of the capillary. Both solutions contained 100 nM coumarin 334 and 25 nM fluorescein. The applied field was 417 V/cm. The solid line is a 5-point moving average of the individual data points. Conditions for EOF and field monitoring were the same as in Figure 4.1.

dynamics reaffirm the simulation results of Thormann et al. using ACES buffer as well as the earlier measurements by Pittman et al. using a phosphate buffer system. More importantly for this work, they serve as a starting point to apply the two-marker system to study both EOF dynamics and electric field dynamics for discontinuous solution conditions commonly used by CE practitioners.

The electrophoretic velocity of fluorescein is monitored simultaneously along with the EOF, and this allows for the observation of local field changes in the system. The velocity is

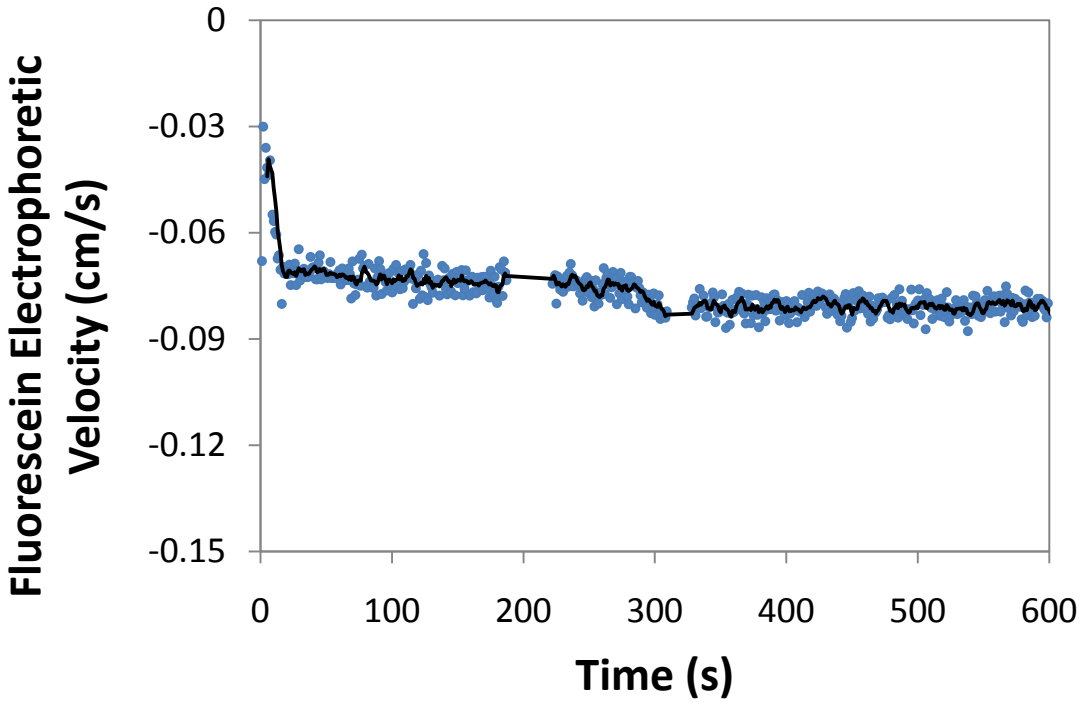

Figure 4.3. Fluorescein electrophoretic velocity versus time for the same experiment shown in Figure 4.2.The solid line is a 5-point moving average of the individual data points.

calculated based on fluorescein's migration time between the photobleaching point (F1) and the detection point (F2) for every second of the experiment. Using Equation 4.5 and the observed velocity can be converted into a voltage field, and results like those presented in Figure 4.3 can be obtained. The data for field strength shown in Figure 4.3 are for the same experimental conditions as for Figure 4.2. As seen in Figure 4.3, the electrophoretic velocity of fluorescein followed a similar trend in comparison to Figure 4.2. The existence of the discontinuous zone in the capillary causes a decrease in the fluorescein's electrophoretic velocity values overall. As the discontinuous zone leaves the capillary, the velocity goes back its original value in high ionic strength buffer. The slow fluorescein velocities in the first section (0-13 s) of the plot are caused by slow increase of the electrophoretic current. The time constant of the system with uniform field is 1.3 s, but in the system where a discontinuous zone existed, the current accelerated at a

slower pace after an initial rapid increase, which resulted in longer times for current to reach its full value. Due to the time constant of the current, first couple seconds (0-3 s) of the electropherogram, electrophoretic current data are not available which was also observed in Pittman et al [110]. Additionally, because of the mismatch between the high field and low field regions, and the resulting pressure-driven flow, the two vacancy peaks are broadened to the extent that they are unresolved at the beginning of the electropherogram.

The data in Figures 4.2 and 4.3 for both EOF and the fluorescein velocity include two regions (between 187-222 s and 309-328 s) where data were not plotted. Those regions correspond to time when the dilute buffer and fluorescein zones to pass the detector. The regions provide important information since the local electric fields in these zones are expected to differ from the BGE. The electropherograms for this experiment and expanded plots for these two regions are presented in the Figure 4.4. At the time where the dilute buffer zone passed the detector, the fluorescence signal dropped and no bleaching peaks were observed for coumarin 334 and fluorescein. When the fluorescein zone passed the detector, the fluorescence signal increased off-scale, making it impossible to detect any photobleaching peaks. The length of these regions is directly proportional to the dilute sample zone's injection length. Pittman et al. [110] made similar observations during EOF monitoring with coumarin 334 and attributed the effect to high temperatures caused by locally increased Joule heating in the region of high resistance (dilute buffer, low conductivity).

In an attempt to mimic the Joule heating effect, solutions containing coumarin 334 (100 nM) and fluorescein (25 nM) were brought to boil on a hot plate for a few seconds. Injection of these samples into the CE system with LIF detection did not indicate significant degradation of

Figure 4.4. A) Fluorescence versus time for a capillary containing a zone of dilute buffer (0.11 mM ACES at pH 7.43) in a capillary filled with 10.0 mM ACES at pH 7.43. The dilute solution was injected hydrodynamically for 240 s to fill 4% of the capillary. Both solutions contained 100 nM coumarin 334 (neutral) and 25 nM fluorescein (negatively charged). Expanded views of the regions in plot A show a broad negative peak (B) and a broad positive peak (C). Photobleached zones were generated by opening a shutter for 50 ms to produce a pulse from an Ar^+ laser. The shutter was opened every 1.0 s. The photobleaching and fluorescence excitation beams were 35.0 and 8.4 mW, respectively at 457.9 nm. The relatively narrow positive peaks are due to light from the bleaching pulse. The relatively narrow negative peaks are due to coumarin 334 and fluorescein vacancy peaks and were used to monitor EOF and the local electric field, respectively. For the experiment shown here, the applied field was 417 V/cm, and the average electrophoretic current was 4.4 μA.

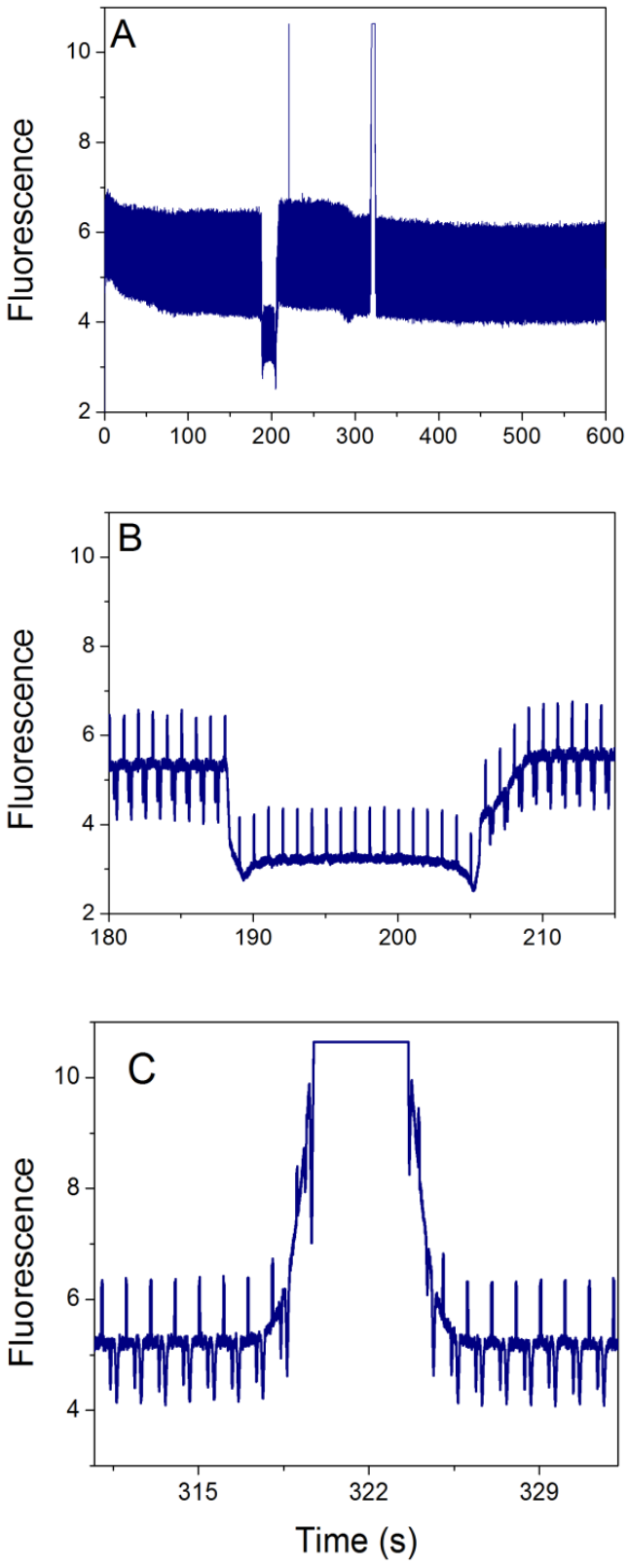
A
B
C
Fluorescence
Time (s)

either molecule compared to samples that were not boiled. Thermal degradation cannot be completely ruled out since higher temperatures and pressures could be present inside the capillary during electrophoresis. On the other hand, the temperature of the boiled sample is limited by the boiling point of the buffer which could be well under the real temperatures occurring during electrophoresis. Therefore, it is still possible that the high temperatures change fluorescence properties of the dyes.

The primary objective of this study was to investigate electric field and EOF dynamics in discontinuous systems. However, the limitations mentioned above make doing so difficult with normal injection conditions. To further study the dynamics, the effect of small changes in the resistivities of a "sample zone" were investigated by injecting diluted separation buffer that also contained the same concentration of the fluorogenic agents as in the BGE. The change is related to the ratio of the resistivities of the sample zone and the separation buffer and the ratio of capillary length filled with the low ionic strength buffer, as seen in Equations 4.3 and 4.4. A sample plug consisting of a lower ionic strength buffer has lower conductivity, higher resistivity and correspondingly higher local electric field than the rest of the capillary. The opposite is true for a sample zone comprising higher ionic strength buffer than the BGE. The degree of change in the EOF rates and fluorescein mobility was enhanced as the length of the capillary filled increased (data not shown). In addition, as the ionic strength difference between the sample and buffer was increased, the EOF rates and fluorescein electrophoretic velocity values were affected to a greater extent. The ionic strength of the sample zone was increased to 1.0 mM, 5.0 mM, 7.5 mM and 9.0 mM, it was not possible to detect photobleaching peaks when the sample was <9 mM ACES buffer. However, with an injection of 9.0 mM ACES at pH 7.43 filling only 4% of

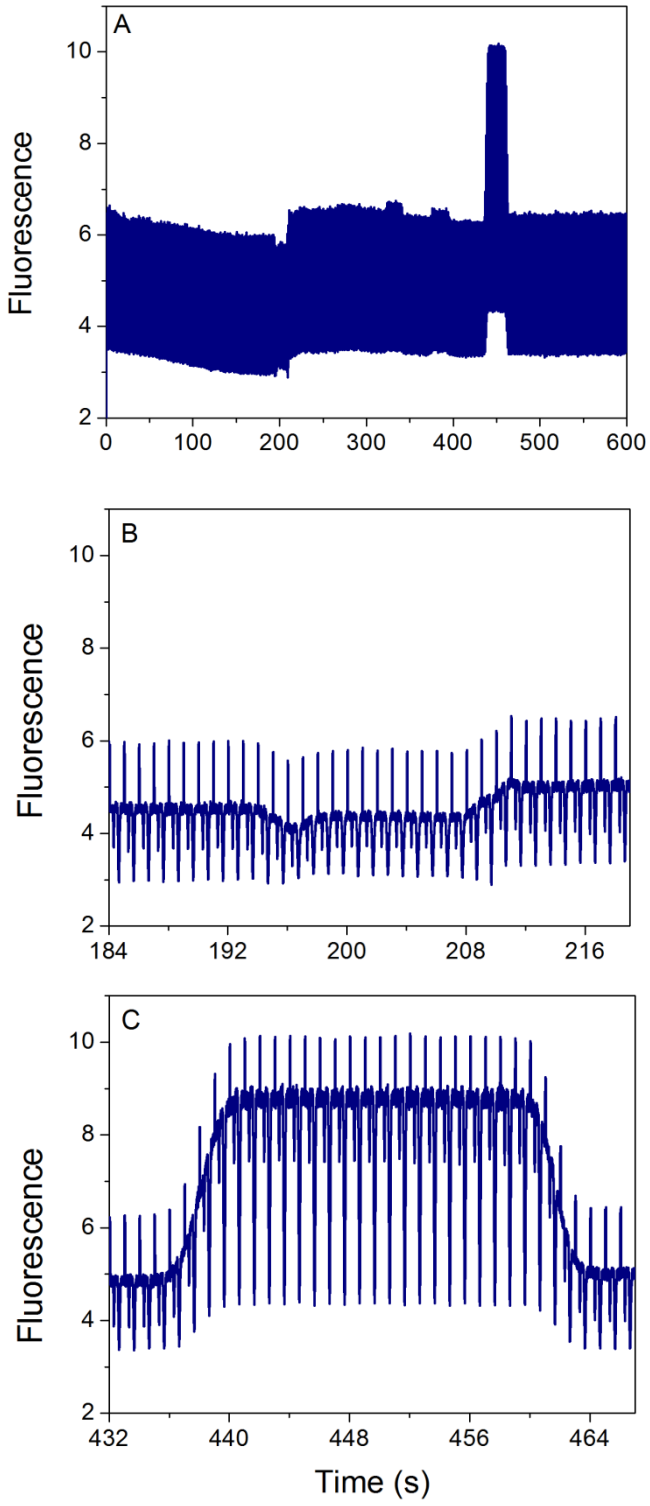

Figure 4.5. A) Electropherogram for a capillary 4% filled with 9.0 mM ACES at pH 7.43 (injected hydrodynamically for 240 s) with the remainder of the capillary filled with 10.0 mM ACES at pH 7.43. Expanded views of the regions in plot A show a broad negative peak (B) and a broad positive peak (C). All other experimental conditions are the same as those in Figure 4.4.

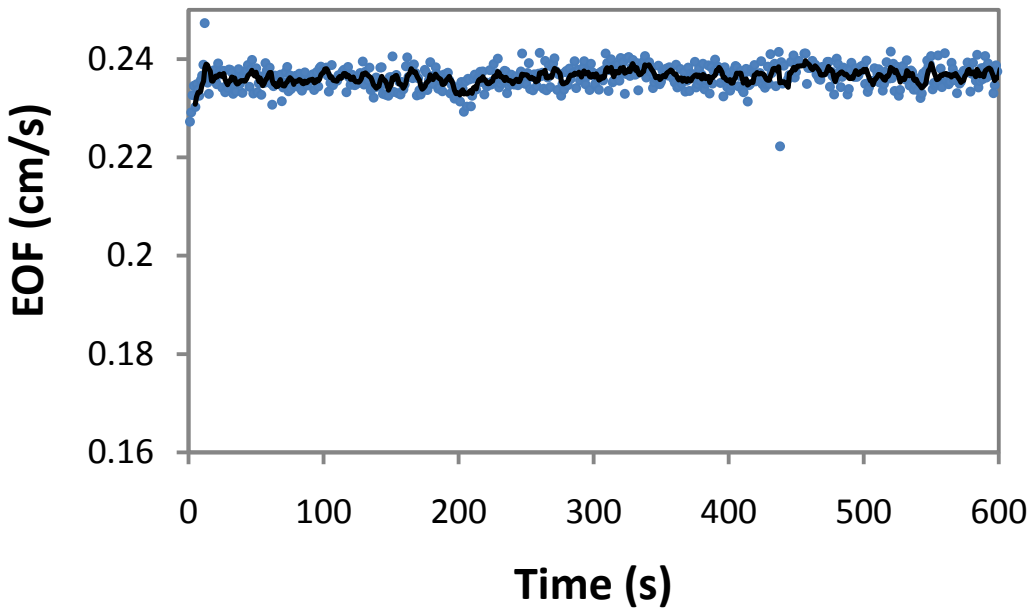

Figure 4.6. EOF versus time for a capillary 4% filled with 9.0 mM ACES at pH 7.43 (injected hydrodynamically for 240 s) with the remainder of the capillary filled with 10.0 mM ACES at pH 7.43. All other experimental conditions are the same as those in Figure 4.4. The solid line is a 5-point moving average of the individual data points.

the capillary otherwise filled with 10.0 mM ACES buffer at pH 7.43 allows well-resolved vacancy peaks. Figure 4.5 presents the electropherogram and the detailed views of the trough and the peak observed providing EOF and fluorescein velocity values for the whole experiment. The EOF rates were constant during the experiment, as might be expected with the small injection plug that does not significantly affect the overall EOF as seen in Figure 4.6. The electrophoretic velocity for fluorescein from the same experiment is presented in Figure 4.7. A small increase (% 5.4) in the fluorescein electrophoretic velocity was observed during the region of interest, seen as a dip at about 200 s in Figure 4.7. The low ionic strength buffer gave rise to a high electric field in the sample plug, which resulted in a higher observed velocity for fluorescein as the injection plug passed the detection region.

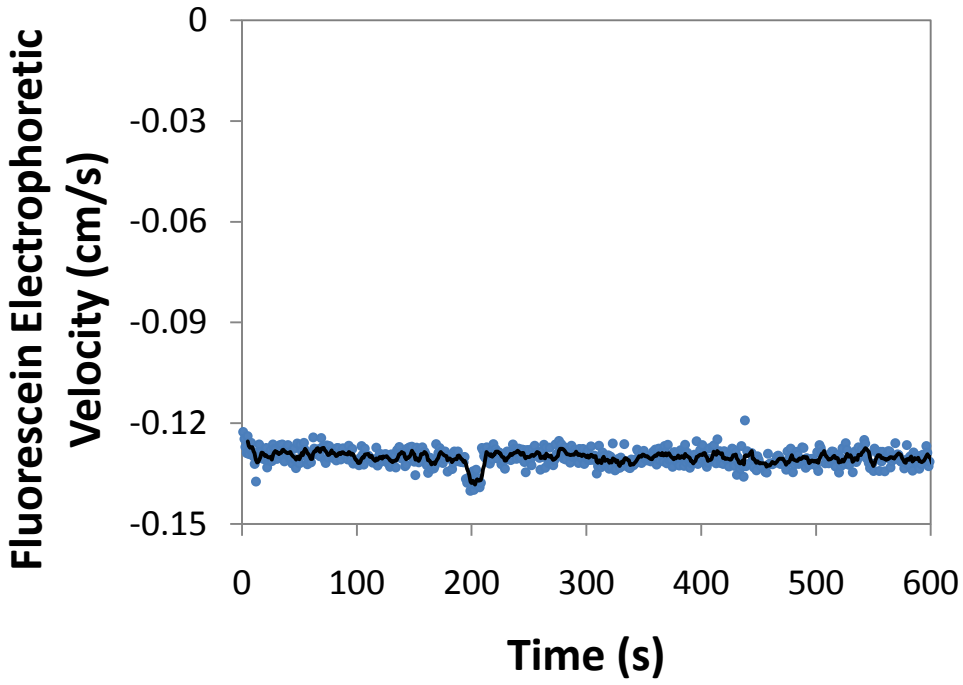

Figure 4.7. Fluorescein electrophoretic velocity versus time for the same experiment shown in Figures 4.5 and 4.6.

In the details of the electropherogram shown in the Figure 4.5, a decrease in the fluorescence signal was noticed when the low concentration buffer zone passed the detector, which is an indication of a low fluorescein concentration. In addition, a peak was observed at the point that matches the elution time of fluorescein, which suggests detection of a high fluorescein concentration. This was unexpected, since the separation and sample zones contained the same compounds, coumarin 334 and fluorescein. This pattern was observed with all experiments in which the sample zone was more dilute than the BGE. Injection of a zone of higher ionic strength buffer (but with the same concentration of the fluorophores as the BGE) gave rise the opposite effect: a peak in fluorescence marking the flow (as the sample plug passed the detector)

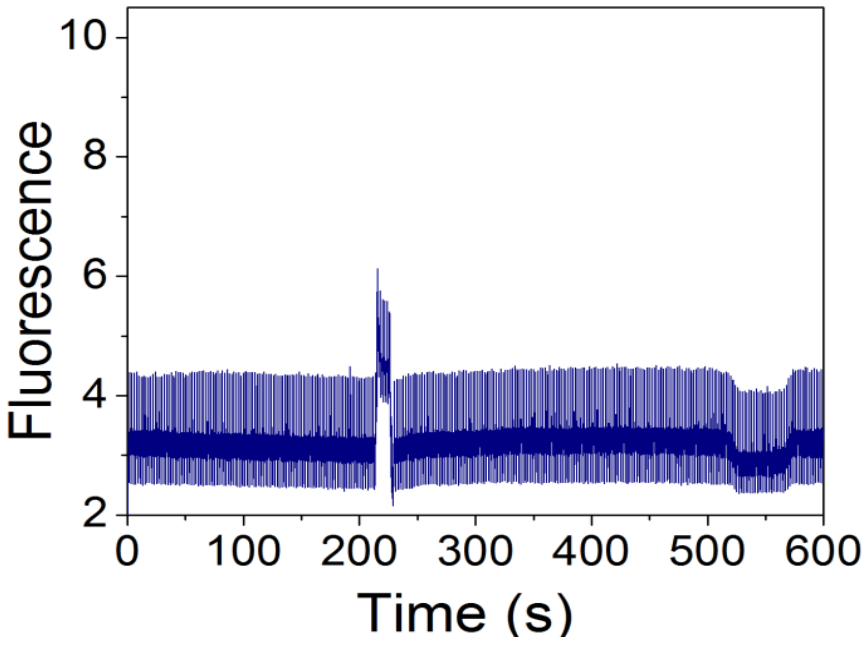

Figure 4.8. Electropherogram showing fluorescence versus time for a capillary 4% filled with 12.5 mM ACES at pH 7.43 (injected hydrodynamically for 240 s) with the remainder of the capillary filled with 10.0 mM ACES at pH 7.43. The nature of the relatively narrow positive and negative peaks used for EOF and field monitoring are described in Figure 4.1. All other experimental conditions are the same as those in Figure 4.1.

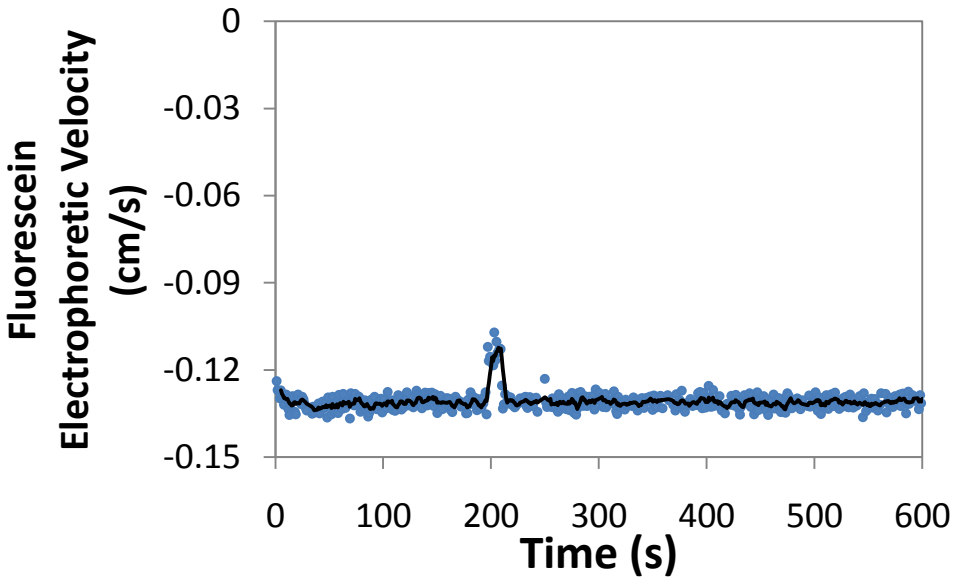

Figure 4.9. Fluorescein electrophoretic velocity versus time for the same experiment shown in Figure 4.8. The solid line is a 5-point moving average of the individual data points.

and a trough at the expected migration time for fluorescein (Figure 4.8). The EOF rate results demonstrated a constant EOF; however, as shown in Figure 4.9, the observed fluorescein electrophoretic velocity decreased as the high concentration buffer "sample" zone passed the detection point. The low electric field strength in the sample plug resulted in lower field strength and velocity values for fluorescein. These results clearly demonstrate proof of concept for the continuous monitoring of electric field monitoring by this methodology; however, the method cannot currently be used for large concentration differences.

4.3.3. Computer Simulations

A comprehensive molecular-level description of any CE experiment is difficult to achieve owing to the complexities of considering the many ionic constituents and the very dynamic processes that occur during the separation [188]. Although the dynamic evolution of a CE separation is not linear or easily internalized, mathematical descriptions of ionic migration are available and rationalization of some complex electrophoretic phenomena such as system peaks [189, 190] has been achieved via aid of computer simulation [191, 192]. These computer programs have proven to be valuable tools for the investigation of electrokinetic separations because they can predict the complex and often unpredictable movement of ions in a solution under the influence of an electric field. The dynamic models are composed of a set of balance laws governing the transport of components in electrophoretic separations, and the mathematical solutions involve a series of non-linear differential equations. It is possible to obtain an electropherogram of a separation by using the simulations. More importantly, monitoring the entire separation at every second is feasible; this provides insightful information about the complex electrokinetic processes that occur during the separation. The simulations have been

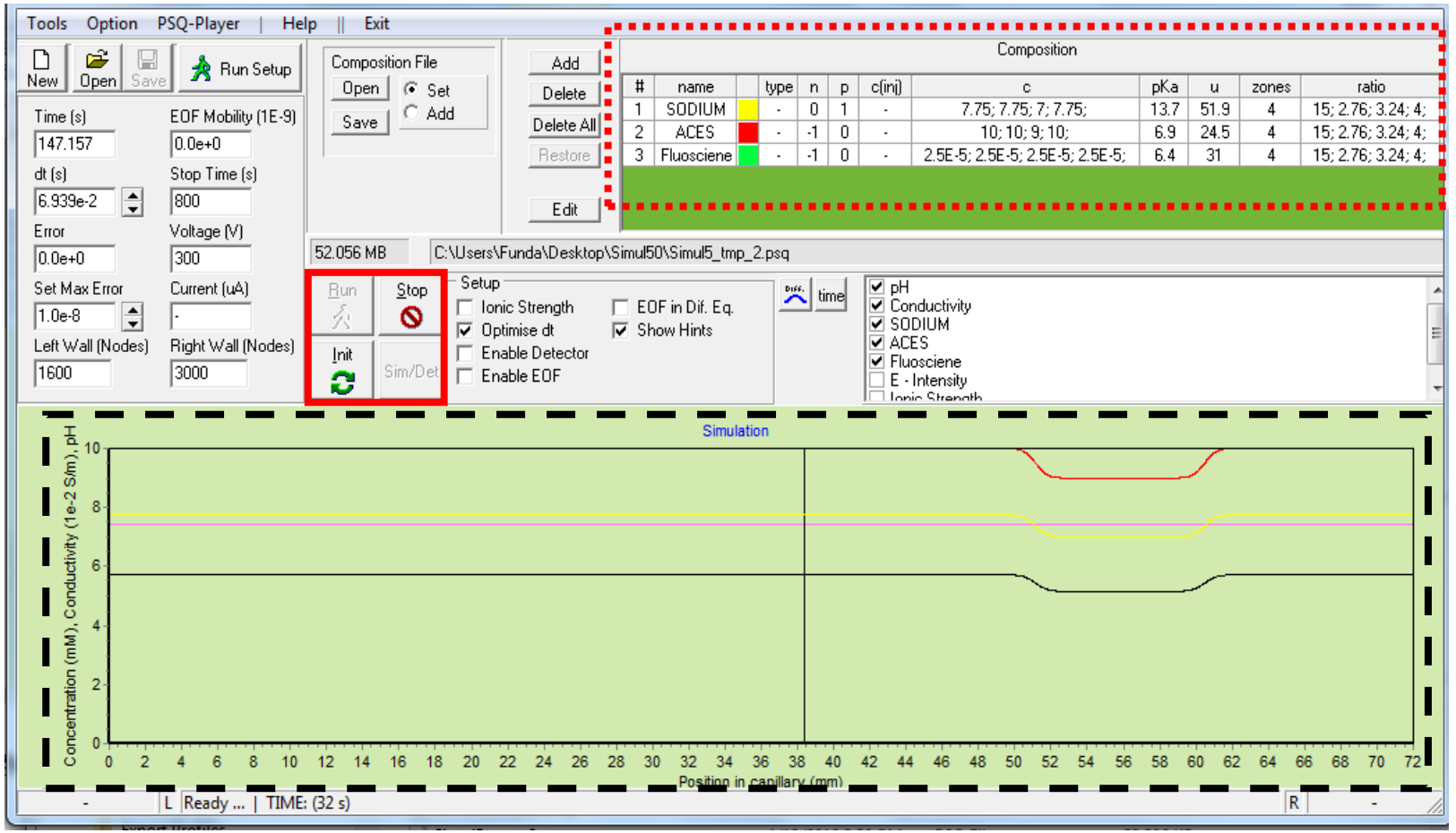

Figure 4.10. View of Simul 5.0 page for a simulation in which a capillary 4% filled with 9.0 mM ACES at pH 7.43 with the remainder of the capillary filled with 10.0 mM ACES at pH 7.43. The main page has a window (dashed rectangle) to demonstrate the changes in pH, conductivity, concentration of sodium (added to adjust pH), ACES buffer and fluorescein during the simulation. The composition window (red dotted rectangle) contains the list of constituents and their pKa, concentration, electrophoretic mobility values and zone ratios. The main page also includes the simulation buttons (re rectangle) to control the simulation.

used in many modes of CE, such as moving boundary electrophoresis (MBE), isotachophoresis (ITP) [178, 193, 194], isoelectric focusing (IEF) [195, 196] and electrokinetic capillary chromatography (EKC) [197, 198] to explain chemical and physical processes in detail by simulating the same conditions used in the experiments.

Here, computer simulations were carried out by using the Simul 5.0 program [184] in order to further examine our unexpected results. The development of low and high concentration zones due the injection of 9.0 mM ACES into a capillary filled with 10 mM ACES buffer was investigated by the program. The simulation zones and buffer concentration (see Figure 4.10) were set to match the experimental conditions in Figures 4.5 and 4.7. The simulation results are plotted as change of fluorescein concentration vs. position in the capillary and the flow is from right to left (which is the reverse of a regular electropherogram). To more clearly present the development of zones, the x axis is reversed in Figures 4.11, 4.12 and 4.13 so that the simulated data follow the same trends as the experimental data. Figure 4.11 presents plots of simulated fluorescein concentration in the capillary at different times. Two peaks were generated as a result of differences in the ionic strength of the sample and separation zones. A decrease in the fluorescein concentration was observed as a negative peak, and a positive peak was observed as an indication of increase in the fluorescein concentration. Development of low and high concentration zones was clear at the beginning of the separation, and a corresponding trough and peak developed at the boundaries between the sample and buffer zones. At the final stage of the simulation (260 s), the zones were fully formed and distinguished clearly. The formation of depleted and enhanced zones was also observed during the wet experiments (Figures 4.4, 4.5 and 4.8). This very interesting observation shows that modulation of ionic sample concentration occurs even when the difference in the ionic strength is as small as 10%.

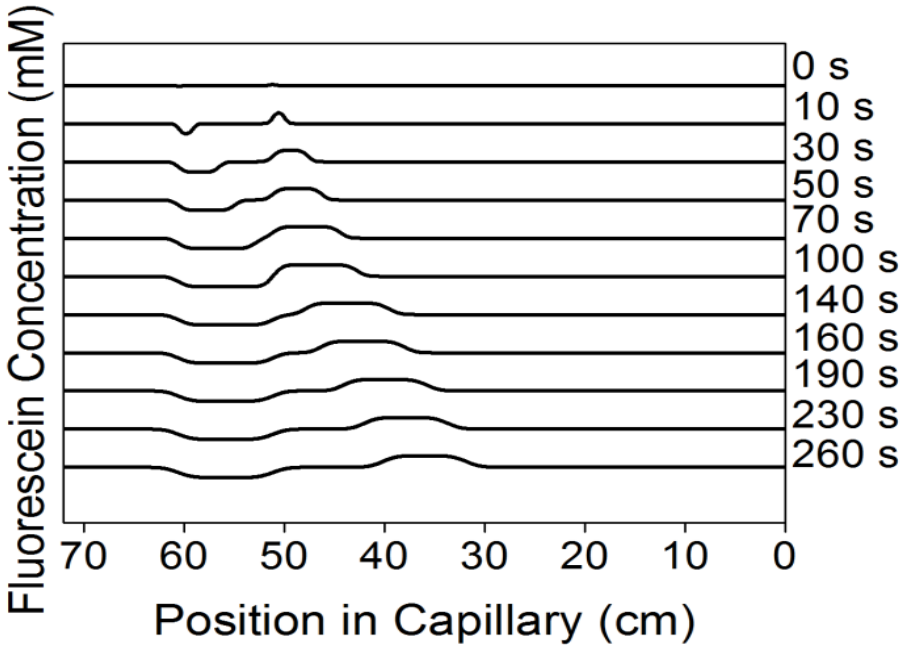

Figure 4.11. Simulation results at different migration times for injection of 9.0 mM ACES buffer at pH 7.43 (4% of the total capillary length) into a capillary filled with 10.0 mM ACES buffer at pH 7.43. Both solutions in the simulation contained 25 nM fluorescein. The simulation was designed to match the experimental conditions shown in Figure 4.5. The simulations were vertically offset for clarity. The x axis was reversed to show the flow from left to right.

The sample zone ionic strength was varied in the simulations from 0.01 mM to 100 mM to observe the changes in the fluorescein zones while the capillary was filled with 10.0 mM ACES at pH 7.43. Results for simulations at all of the concentrations studied are presented in Figure 4.12. Similar to Figure 4.11, two peaks were observed as a result of the differences in the ionic strength of the sample and separation zones. The order of these two peaks was switched as the ionic strength of the sample zone was increased. In addition, the change in the fluorescein concentration was more pronounced as the difference in the ionic strength between the two zones increased. Formation of negative and positive zones, the changes in the zone shapes in relation to the difference in ionic strength of the sample zone to the buffer zone and the change in the order in the electropherogram were observed in all the experiments as shown in Figures 4.4, 4.5 and

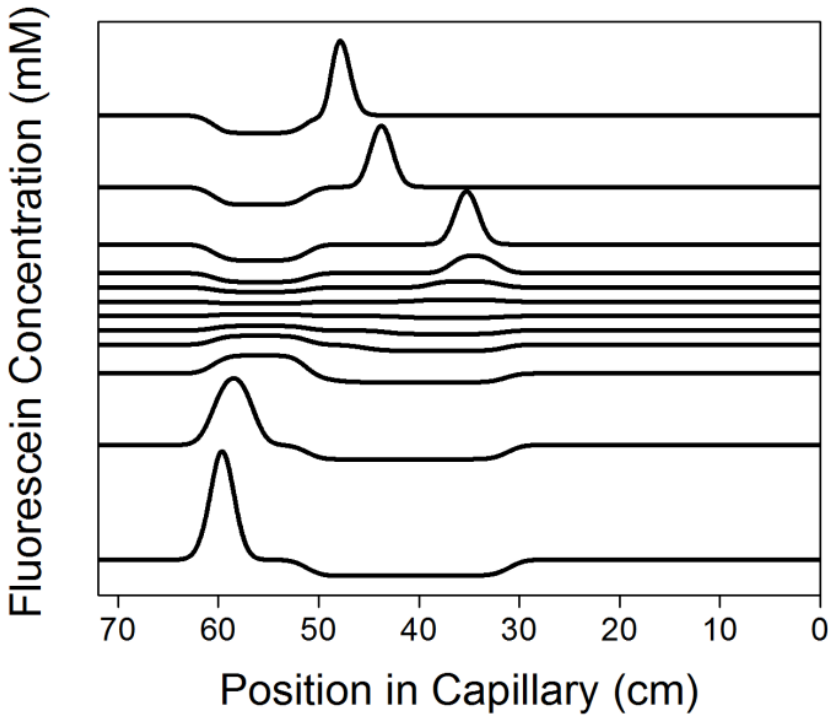

Figure 4.12. Simulation results that demonstrate the development of positive and negative peaks by injection of different ionic strength samples. Sample zone concentrations increase from the top to the bottom simulation (at the concentrations of 0.01, 0.1, 1.0, 5.0, 7.5, 9.0, 11.0, 12.5, 15.0, 20.0, 50.0, and 100.0 mM ACES). The results show final point (260 s) of the simulation experiment. Buffer (10 mM ACES, pH 7.43) and sample zones (sample length is 4% of the capillary) contained 25 nM fluorescein and they were set to match the experimental conditions in Figure 4.2. The simulations were offset for clarity. The x axis was reversed to show the flow from left to right.

4.8. Figure 4.13 presents a detailed plot for the transition from the negative peak to the positive peak for the injections of 5 mM to 15 mM ACES. The changes in fluorescein concentration due to the injection of dilute (or concentrated) sample zone are remarkable indications of the effect of field changes to the whole separation even though both zones contain fluorescein. The simulation results validate this behavior and bring valuable insight into the changes that happen during electrophoresis with discontinuous system.

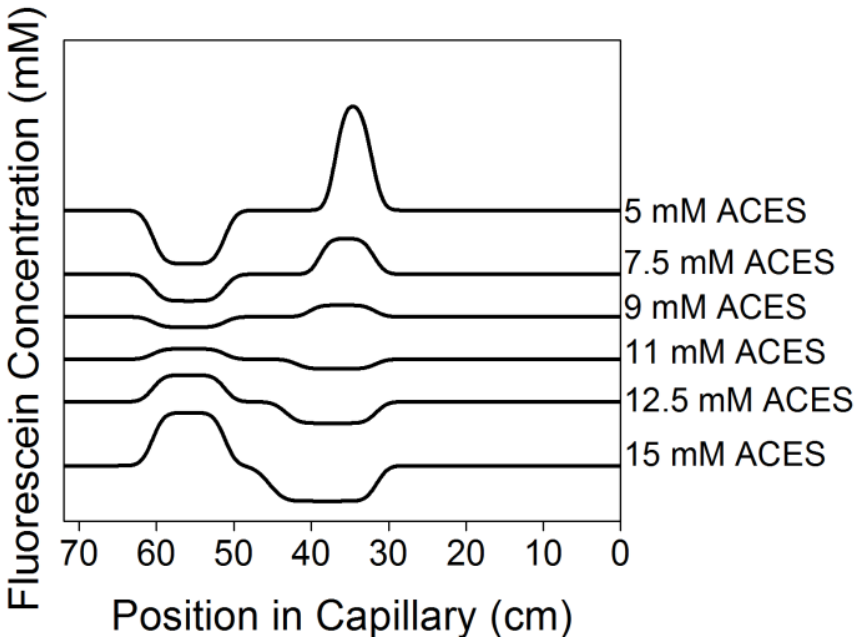

Figure 4.13. Detailed view of the simulation results for injection (4% of the total capillary length) of solutions with different ACES concentrations into a capillary containing 10.0 mM ACES at pH 7.43. All simulation details are same as in Figure 4.12. The plots were vertically offset for clarity. The x axis was reversed to show the flow from left to right.

4.4. Conclusion

Changes in EOF and field dynamics in a separation where discontinuous systems exist have been monitored by periodic photobleaching of neutral and charged dyes added to the separation buffer and sample solutions. Injections of sample prepared in a 1:100 dilution of separation buffer, resulted in high electric field zone in the sample plug, corresponding to increased EOF rates in the capillary and increased electrophoretic velocity of fluorescein within the sample plug. When the difference between the separation buffer and sample buffer is 10% in ionic strength, the continuous EOF and field monitoring method was able to provide insightful details about the discontinuous system. The changes in the fluorescence signal indicating a fluorescein concentration adjustment during the experiments could not be easily explained.

Computer simulations have been used in the literature to understand fundamental behaviors of electrophoretic separation principles, chemical and physical processes involved in the separation [199], and allow the visualization of the reactant migration velocities and zone shapes [200]. With the aid of Simul 5.0, the experimental results presented here were supported by simulation results which also demonstrated the same changes in fluorescein concentration. The simulations proved to be an important and useful tool to obtain information about the sample zone behavior during CE separations with discontinuous systems.

CHAPTER 5
CONCLUSION

The research presented in this dissertation focuses on investigations of electroosmotic flow (EOF) dynamics in capillary electrophoresis (CE) experiments. A continuous EOF monitoring method developed by Gilman and coworkers was employed to investigate changes in EOF during CE experiments as a function of time. In Chapter 2, the continuous EOF monitoring method was used to improve migration reproducibility, which is a fundamental and significant issue for any CE experiment. This study demonstrates that the continuous EOF monitoring method can be used to significantly improve migration reproducibility for CE experiments; however, direct experimental comparison of this method to several alternate approaches for improving migration reproducibility in the literature (neutral marker method, multiple marker method, migration time ratio method, and adjusted migration index method) indicate that this new technique is not broadly superior when both improvements in migration reproducibility and method complexity are considered. Nevertheless, the dynamic EOF data provided by the continuous monitoring method can be a useful tool to observe and study changes in EOF that may occur during the CE separations. In addition, direct experimental comparison between methods for improving CE migration reproducibility is valuable for CE practitioners and rarely has been reported in the literature. One of the most important and surprising conclusions from Chapter 2 is that for most of the separation conditions studied in this work, the simple and older neutral marker method provides results that are comparable to those obtained with more complicated and sophisticated techniques for improving CE migration reproducibility.

In Chapter 3, effects of injection of biological samples on the EOF dynamics and capillary wall surface chemistry were investigated using the continuous EOF monitoring method. Specific biological molecules representing cell components (proteins, lipids, carbohydrates and

DNA) were injected at different concentrations and at two pH values (neutral and basic). Injection of basic proteins had the largest impact on EOF since they adsorbed to the negatively charged silanol groups on the capillary surface, which resulted in a non-uniform zeta potential down the length of the capillary. The EOF rates decreased at the beginning of an experiment and then became constant for the rest of the run. Furthermore, broadening of the vacancy peaks used for EOF monitoring was observed due to parabolic flow caused by the mismatch of zeta potential in the capillary. As the concentration and basicity of the protein samples increased, the resulting effect on EOF and peak broadening increased. The model compounds for carbohydrates, DNA and lipids did not cause any significant changes in EOF in these experiments. The effects of injection of cell lysates (cultured adipocytes) and serum samples on EOF were also studied. Two types of cells with different lipid content (low and high) presented similar results, which indicate that the fat content of the cell sample does not affect EOF due to sample adsorption. This observation is in agreement with the results for injection of lipid samples, which resulted in no significant changes in EOF, and this is consistent with the hypothesis that protein adsorption is the major source of EOF changes after injection of these cells. In addition, large fluctuations were observed in the fluorescence signal without an indication of adsorption due to constant EOF rates during these experiments with fetal bovine serum (FBS). Possible effects of salts in the FBS sample were investigated; however, a very stable EOF profile indicated that the salt content was not the cause of the unusual fluctuations that were observed in the FBS results.

In Chapter 4, the continuous EOF monitoring method was expanded to simultaneously monitor both the local electric field and EOF by periodic photobleaching of two markers, coumarin 334 (neutral) and fluorescein (negatively charged). The addition of the charged marker (fluorescein) was used to determine the local electric field (between the photobleaching and

detection zones) based on the electrophoretic velocity of the fluorescein vacancy zone. The improved method was employed to investigate EOF dynamics and local electric field changes during CE with discontinuous solutions, which were generated by introducing a low ionic strength buffer zone into the capillary. The EOF decreased sharply at the beginning of the experiment, stayed constant until the discontinuous zone left the capillary, and then decreased before becoming constant again. The fluorescein electrophoretic velocity values decreased in magnitude overall due to the discontinuous zone in the capillary, and they increased as the zone left the capillary. The velocity values were higher in magnitude when the low ionic strength buffer zone passed the detection point due to high electric field within the zone.

Unexpected fluorescein concentration changes were observed during the experiments in Chapter 4. When the low ionic strength buffer zone passed the detector, a decrease in the fluorescence signal was observed, whereas an unexpected increase in the signal was noticed at the elution time of fluorescein. The photobleached vacancy peaks were not observable during these broader decreases and increases in fluorescence, and EOF and electric field information could not be obtained at these times. The vacancy peaks within the broader fluorescence increases and decreases were observed only when the difference in ionic strength between the sample zone and the buffer zone was decreased from 99% to 10%. We were unable to explain these changes in fluorescein concentration in a simple fashion based on typical electrophoretic behavior; however, these changes in fluorescein concentration could be reproduced by computer simulation using the program Simul5.0. Overall, both experiments and simulations produced these unexpected increases and decreases in fluorescein concentration even though the sample and buffer zones contained fluorescein and coumarin 334 at the same concentration. Overall, the study in Chapter 4 demonstrated principle of using neutral and charged markers for monitoring

both EOF and local electric field; however, for solutions with different ionic strengths, the technique only worked for small differences (e.g. 10%), and ultimately the application of this approach is limited by the interesting and unexpected electrophoretic behavior of the charged marker.

REFERENCES

1. Stellan, H., Free Zone Electrophoresis. *Chromatographic reviews* **1967,** *9* (2), 122-219.

2. Virtanen, R., Zone Electrophoresis in a Narrow-Bore Tube Employing Potentiometric Detection - Theoretical and Experimental Study. *Acta Polytechnica Scandinavica-Chemical Technology Series* **1974,** (123), 1-67.

3. Mikkers, F. E. P.; Everaerts, F. M.; Verheggen, T. P. E. M., High-Performance Zone Electrophoresis. *Journal of Chromatography A* **1979,** *169* (0), 11-20.

4. Jorgenson, J. W.; Lukacs, K. D., Zone Electrophoresis in Open-Tubular Glass Capillaries. *Analytical Chemistry* **1981,** *53* (8), 1298-1302.

5. Issaq, H. J., The Role of Separation Science in Proteomics Research. *Electrophoresis* **2001,** *22* (17), 3629-3638.

6. Weinberger, R., *Practical Capillary Electrophoresis*. 2nd ed.; Academic Press: Florida, 2000; p 462.

7. Landers, J. P.; Editor, *Capillary and Microchip Electrophoresis and Associated Microtechniques*. CRC Press LLC: 2008; p 1565.

8. Carrilho, E., DNA Sequencing by Capillary Array Electrophoresis and Microfabricated Array Systems. *ELECTROPHORESIS* **2000,** *21* (1), 55-65.

9. Frost, N. W.; Jing, M.; Bowser, M. T., Capillary Electrophoresis. *Analytical Chemistry* **2010,** *82* (12), 4682-4698.

10. Kostal, V.; Katzenmeyer, J.; Arriaga, E. A., Capillary Electrophoresis in Bioanalysis. *Analytical Chemistry* **2008,** *80* (12), 4533-4550.

11. Mikus, P.; Marakova, K., Advanced Ce for Chiral Analysis of Drugs, Metabolites, and Biomarkers in Biological Samples. *ELECTROPHORESIS* **2009,** *30* (16), 2773-2802.

12. Bruin, G. J. M.; Stegeman, G.; Van Asten, A. C.; Xu, X.; Kraak, J. C.; Poppe, H., Optimization and Evaluation of the Performance of Arrangements for Uv Detection in High-

Resolution Separations Using Fused-Silica Capillaries. *Journal of Chromatography A* **1991,** *559* (1-2), 163-181.

13. Altria, K. D., Key Points for Validating Ce Methods, Particularly in Pharmaceutical Analysis. *Lc Gc North America* **2001,** *19* (5), 498-+.

14. Johnson, M. E.; Landers, J. P., Fundamentals and Practice for Ultrasensitive Laser-Induced Fluorescence Detection in Microanalytical Systems. *ELECTROPHORESIS* **2004,** *25* (21-22), 3513-3527.

15. Garcia-Campana, A. M.; Taverna, M.; Fabre, H., Lif Detection of Peptides and Proteins in Ce. *ELECTROPHORESIS* **2007,** *28* (1-2), 208-232.

16. Watzig, H.; Degenhardt, M.; Kunkel, A., Strategies for Capillary Electrophoresis: Method Development and Validation for Pharmaceutical and Biological Applications. *ELECTROPHORESIS* **1998,** *19* (16-17), 2695-2752.

17. Smyth, W. F.; Brooks, P., A Critical Evaluation of High Performance Liquid Chromatography-Electrospray Ionisation-Mass Pectrometry and Capillary Electrophoresis-Electrospray-Mass Spectrometry for the Detection and Determination of Small Molecules of Significance in Clinical and Forensic Science. *ELECTROPHORESIS* **2004,** *25* (10-11), 1413-1446.

18. Harvey, D. J., Derivatization of Carbohydrates for Analysis by Chromatography; Electrophoresis and Mass Spectrometry. *Journal of Chromatography B-Analytical Technologies in the Biomedical and Life Sciences* **2011,** *879* (17-18), 1196-1225.

19. Kusmierek, K.; Chwatko, G.; Glowacki, R.; Kubalczyk, P.; Bald, E., Ultraviolet Derivatization of Low-Molecular-Mass Thiols for High Performance Liquid Chromatography and Capillary Electrophoresis Analysis. *Journal of Chromatography B-Analytical Technologies in the Biomedical and Life Sciences* **2011,** *879* (17-18), 1290-1307.

20. Foret, F., Capillary Electrophoresis of Small Ions Using Complex Formation and Indirect Detection. *ELECTROPHORESIS* **2009,** *30*, S34-S39.

21. Ragozina, N.; Pütz, M.; Faubel, W.; Pyell, U., Indirect Laser-Induced Fluorescence Detection for Capillary Electrophoresis Using a Frequency-Doubled Diode Laser. *ELECTROPHORESIS* **2003,** *24* (3), 567-574.

22. Shihabi, Z. K.; Hinsdale, M. E., Some Variables Affecting Reproducibility in Capillary Electrophoresis. *ELECTROPHORESIS* **1995,** *16* (1), 2159-2163.

23. Goodall, D. M.; Williams, S. J.; Lloyd, D. K., Quantitative Aspects of Capillary Electrophoresis. *TrAC Trends in Analytical Chemistry* **1991,** *10* (9), 272-279.

24. Mayer, B. X., How to Increase Precision in Capillary Electrophoresis. *Journal of Chromatography A* **2001,** *907* (1-2), 21-37.

25. Faller, T.; Engelhardt, H., How to Achieve Higher Repeatability and Reproducibility in Capillary Electrophoresis. *Journal of Chromatography A* **1999,** *853* (1-2), 83-94.

26. Strege, M. A.; Lagu, A. L., Studies of Migration Time Reproducibility of Capillary Electrophoretic Protein Separations. *Journal of Liquid Chromatography* **1993,** *16* (1), 51-68.

27. Labat, L.; Kummer, E.; Dallet, P.; Dubost, J. P., Comparison of High-Performance Liquid Chromatography and Capillary Zone Electrophoresis for the Determination of Parabens in a Cosmetic Product. *Journal of Pharmaceutical and Biomedical Analysis* **2000,** *23* (4), 763-769.

28. Aurora Prado, M. S.; Steppe, M.; Tavares, M. F. M.; Kedor-Hackmann, E. R. M.; Santoro, M. I. R. M., Comparison of Capillary Electrophoresis and Reversed-Phase Liquid Chromatography Methodologies for Determination of Diazepam in Pharmaceutical Tablets. *Journal of Pharmaceutical and Biomedical Analysis* **2005,** *37* (2), 273-279.

29. Velikinac, I.; Čudina, O.; Janković, I.; Agbaba, D.; Vladimirov, S., Comparison of Capillary Zone Electrophoresis and High Performance Liquid Chromatography Methods for Quantitative Determination of Ketoconazole in Drug Formulations. *Il Farmaco* **2004,** *59* (5), 419-424.

30. Altria, K., Essential Peak Area Normalisation for Quantitative Impurity Content Determination by Capillary Electrophoresis. *Chromatographia* **1993,** *35* (3), 177-182.

31. Gaona-Galdos, A. A.; Zanolli, L. A.; Maggi Tavares, M. F.; Aurora-Prado, M. S.; Santoro, M.; Kedor-Hackmann, E. R. M., Development and Validation of a Method for Quantitative Determination of Econazole Nitrate in Cream Formulation by Capillary Zone Electrophoresis. *Journal of Chromatography A* **2008,** *1192* (2), 301-305.

32. Curiel, H.; Vanderaerden, W.; Velez, H.; Hoogmartens, J.; Van Schepdael, A., Analysis of Underivatized Gentamicin by Capillary Electrophoresis with Uv Detection. *Journal of Pharmaceutical and Biomedical Analysis* **2007,** *44* (1), 49-56.

33. Heinig, K.; Vogt, C., Determination of Surfactants by Capillary Electrophoresis. *ELECTROPHORESIS* **1999,** *20* (15-16), 3311-3328.

34. Altria, K. D.; Elgey, J.; Lockwood, P.; Moore, D., An Overview of the Applications of Capillary Electrophoresis to the Analysis of Pharmaceutical Raw Materials and Excipients. *Chromatographia* **1996,** *42* (5-6), 332-342.

35. Navratil, M.; Poe, B. G.; Arriaga, E. A., Quantitation of DNA Copy Number in Individual Mitochondrial Particles by Capillary Electrophoresis. *Analytical Chemistry* **2007,** *79* (20), 7691-7699.

36. Glatz, Z., Determination of Enzymatic Activity by Capillary Electrophoresis. *Journal of Chromatography B-Analytical Technologies in the Biomedical and Life Sciences* **2006,** *841* (1-2), 23-37.

37. Shen, Y. F.; Smith, R. D., Proteomics Based on High-Efficiency Capillary Separations. *ELECTROPHORESIS* **2002,** *23* (18), 3106-3124.

38. Belin, G. K.; Krahenbuhl, S.; Hauser, P. C., Direct Determination of Valproic Acid in Biological Fluids by Capillary Electrophoresis with Contactless Conductivity Detection. *Journal of Chromatography B-Analytical Technologies in the Biomedical and Life Sciences* **2007,** *847* (2), 205-209.

39. Boone, C. M.; Franke, J.-P.; de Zeeuw, R. A.; Ensing, K., Intra- and Interinstrument Reproducibility of Migration Parameters in Capillary Electrophoresis for Substance Identification in Systematic Toxicological Analysis. *ELECTROPHORESIS* **2000,** *21* (8), 1545-1551.

40. Lacunza, I.; Lara-Quintanar, P.; Moya, G.; Sanz, J.; Diez-Masa, J. C.; de Frutos, M., Selection of Migration Parameters for a Highly Reliable Assignment of Bands of Isoforms of Erythropoietin Separated by Capillary Electrophoresis. *ELECTROPHORESIS* **2004,** *25* (10-11), 1569-1579.

41. Palmer, C. P.; Vandeginste, B. G. M., Statistical Evaluation of Various Qualitative Parameters in Capillary Electrophoresis. *Journal of Chromatography A* **1995,** *718* (1), 153-165.

42. Vespalec, R.; Gebauer, P.; Boček, P., Identification of Peaks in Capillary Zone Electrophoresis Based on Actual Mobilities. *ELECTROPHORESIS* **1992,** *13* (1), 677-682.

43. Beckers, J. L.; Everaerts, F. M.; Ackermans, M. T., Determination of Absolute Mobilities, Pk Values and Separation Numbers by Capillary Zone Electrophoresis : Effective Mobility as a Parameter for Screening. *Journal of Chromatography A* **1991,** *537*, 407-428.

44. Yang, J.; Bose, S.; Hage, D. S., Improved Reproducibility in Capillary Electrophoresis through the Use of Mobility and Migration Time Ratios. *Journal of Chromatography A* **1996,** *735* (1-2), 209-220.

45. Issaq, H. J.; Janini, G. M.; Atamna, I. Z.; Muschik, G. M., Separations by High-Performance Liquid-Chromatography and Capillary Zone Electrophoresis - a Comparative Study. *Journal of Liquid Chromatography* **1991,** *14* (5), 817-845.

46. Wätzig, H.; Kaupp, S.; Graf, M., Inner Surface Properties of Capillaries for Electrophoresis. *TrAC Trends in Analytical Chemistry* **2003,** *22* (9), 588-604.

47. Kunkel, A.; Degenhardt, M.; Schirm, B.; Wätzig, H., Performance of Instruments and Aspects of Methodology and Validation in Quantitative Capillary Electrophoresis an Update. *Journal of Chromatography A* **1997,** *768* (1), 17-27.

48. B. J. Radola, F. F., L. Krivankova, P. Bocek, *Capillary Zone Electrophoresis*. 1st edition ed.; VCH Verlagsgesellschaft mbH: Weinheim, **1993**; p 346.

49. Cohen, N.; Grushka, E., Influence of the Capillary Edge on the Separation Efficiency in Capillary Electrophoresis. *Journal of Chromatography A* **1994,** *684* (2), 323-328.

50. Bean, S. R.; Lookhart, G. L., Optimizing Quantitative Reproducibility in High-Performance Capillary Electrophoresis (Hpce) Separations of Cereal Proteins. *Cereal Chemistry* **2001,** *78* (5), 530-537.

51. Schaeper, J. P.; Sepaniak, M. J., Parameters Affecting Reproducibility in Capillary Electrophoresis. *Electrophoresis* **2000,** *21* (7), 1421-1429.

52. Doherty, E. A. S.; Meagher, R. J.; Albarghouthi, M. N.; Barron, A. E., Microchannel Wall Coatings for Protein Separations by Capillary and Chip Electrophoresis. *ELECTROPHORESIS* **2003,** *24* (1-2), 34-54.

53. Robb, C. S., Applications of Physically Adsorbed Polymer Coatings in Capillary Electrophoresis. *Journal of Liquid Chromatography & Related Technologies* **2007,** *30* (5-7), 729-759.

54. Masliyah, J. H.; Bhattacharjee, S., *Electrokinetic and Colloid Transport Phenomena*. Wiley-Interscience: New Jersey, 2006.

55. Hjertén, S., High-Performance Electrophoresis : Elimination of Electroendosmosis and Solute Adsorption. *Journal of Chromatography A* **1985,** *347*, 191-198.

56. Towns, J. K.; Regnier, F. E., Impact of Polycation Adsorption on Efficiency and Electroosmotically Driven Transport in Capillary Electrophoresis. *Analytical Chemistry* **1992,** *64* (21), 2473-2478.

57. Jorgenson, J. W.; Lukacs, K. D., Capillary Zone Electrophoresis. *Science* **1983,** *222* (4621), 266-272.

58. Zhu, M.; Rodriguez, R.; Hansen, D.; Wehr, T., Capillary Electrophoresis of Proteins under Alkaline Conditions. *Journal of Chromatography A* **1990,** *516* (1), 123-131.

59. Altria, K.; Fabre, H., Approaches to Optimisation of Precision in Capillary Electrophoresis. *Chromatographia* **1995,** *40* (5), 313-320.

60. Valko, I. E.; Siren, H.; Riekkola, M. L.; Jumppanen, J. H., Effect of Buffering and Buffer Replenishment on Repeatability in Capillary Electrophoresis. *Journal of Microcolumn Separations* **1996,** *8* (6), 421-426.

61. Kelly, M. A.; Altria, K. D.; Clark, B. J., Approaches Used in the Reduction of the Buffer Electrolysis Effects for Routine Capillary Electrophoresis Procedures in Pharmaceutical Analysis. *Journal of Chromatography A* **1997,** *768* (1), 73-80.

62. Bello, M. S., Electrolytic Modification of a Buffer During a Capillary Electrophoresis Run. *Journal of Chromatography A* **1996,** *744* (1-2), 81-91.

63. Shaafati, A., Clark, B. J., Development of a Capillary Zone Electrophoresis Method for Atenolol and Its Related Impurities in a Tablet Preparation. *Analytical Proceedings* **1993,** *30* (12), 481-483.

64. Zhu, T.; Sun, Y.-l.; Zhang, C.-x.; Ling, D.-k.; Sun, Z.-p., Variation of the Ph of the Background Electrolyte as a Result of Electrolysis in Capillary Electrophoresis. *Journal of High Resolution Chromatography* **1994,** *17* (7), 563-564.

65. Rathore, A. S., Joule Heating and Determination of Temperature in Capillary Electrophoresis and Capillary Electrochromatography Columns. *Journal of Chromatography A* **2004,** *1037* (1-2), 431-443.

66. Boughtflower, R.; Underwood, T.; Paterson, C., Capillary Electrochromatography — Some Important Considerations in the Preparation of Packed Capillaries and the Choice of Mobile Phase Buffers. *Chromatographia* **1995,** *40* (5), 329-335.

67. Ali, I.; Aboul-Enein, H.; Gupta, V., Precision in Capillary Electrophoresis. *Analytical Letters* **2006,** *39* (11), 2345-2357.

68. Altria, K. D., Improved Performance in Capillary Electrophoresis Using Internal Standards. *Lc Gc Europe* **2002,** *15* (9), 588-594.

69. Kunkel, A.; Günter, S.; Dette, C.; Wätzig, H., Quantitation of Insulin by Capillary Electrophoresis and High-Performance Liquid Chromatography Method Comparison and Validation. *Journal of Chromatography A* **1997,** *781* (1-2), 445-455.

70. Lux, J.; Yin, H.; Schomburg, G., Construction, Evaluation and Analytical Operation of a Modular Capillary Electrophoresis Instrument. *Chromatographia* **1990,** *30* (1), 7-15.

71. Evenhuis, C. J.; Guijt, R. M.; Macka, M.; Marriott, P. J.; Haddad, P. R., Variation of Zeta-Potential with Temperature in Fused-Silica Capillaries Used for Capillary Electrophoresis. *ELECTROPHORESIS* **2006,** *27* (3), 672-676.

72. Lukacs, K. D.; Jorgenson, J. W., Capillary Zone Electrophoresis: Effect of Physical Parameters on Separation Efficiency and Quantitation. *Journal of High Resolution Chromatography* **1985,** *8* (8), 407-411.

73. Evenhuis, C. J.; Haddad, P. R., Joule Heating Effects and the Experimental Determination of Temperature During Ce. *ELECTROPHORESIS* **2009,** *30* (5), 897-909.

74. Kurosu, Y.; Hibi, K.; Sasaki, T.; Saito, M., Influence of Temperature Control in Capillary Electrophoresis. *Journal of High Resolution Chromatography* **1991,** *14* (3), 200-203.

75. Rush, R. S.; Cohen, A. S.; Karger, B. L., Influence of Column Temperature on the Electrophoretic Behavior of Myoglobin And .Alpha.-Lactalbumin in High-Performance Capillary Electrophoresis. *Analytical Chemistry* **1991,** *63* (14), 1346-1350.

76. Grushka, E.; McCormick, R. M.; Kirkland, J. J., Effect of Temperature Gradients on the Efficiency of Capillary Zone Electrophoresis Separations. *Analytical Chemistry* **1989,** *61* (3), 241-246.

77. Knox, J.; McCormack, K., Temperature Effects in Capillary Electrophoresis 2: Some Theoretical Calculations and Predictions. *Chromatographia* **1994,** *38* (3), 215-221.

78. Gobie, W. A.; Ivory, C. F., Thermal Model of Capillary Electrophoresis and a Method for Counteracting Thermal Band Broadening. *Journal of Chromatography A* **1990,** *516* (1), 191-210.

79. Altria, K. D., Quantitative Aspects of the Application of Capillary Electrophoresis to the Analysis of Pharmaceuticals and Drug Related Impurities. *Journal of Chromatography A* **1993,** *646* (2), 245-257.

80. Wätzig, H.; Dette, C., Precise Quantitative Capillary Electrophoresis : Methodological and Instrumental Aspects. *Journal of Chromatography A* **1993,** *636* (1), 31-38.

81. Grushka, E.; McCormick, R. M., Zone Broadening Due to Sample Injection in Capillary Zone Electrophoresis. *Journal of Chromatography A* **1989,** *471*, 421-428.

82. Dose, E. V.; Guiochon, G., Problems of Quantitative Injection in Capillary Zone Electrophoresis. *Analytical Chemistry* **1992,** *64* (2), 123-128.

83. Yin, H.; Keely-Templin, C.; McManigill, D., Preparative Capillary Electrophoresis with Wide-Bore Capillaries. *Journal of Chromatography A* **1996,** *744* (1-2), 45-54.

84. Tsuda, T.; Zare, R. N., Split Injector for Capillary Zone Electrophoresis. *Journal of Chromatography A* **1991,** *559* (1-2), 103-110.

85. Rose, D. J.; Jorgenson, J. W., Characterization and Automation of Sample Introduction Methods for Capillary Zone Electrophoresis. *Analytical Chemistry* **1988,** *60* (7), 642-648.

86. Wei, H.; Ang, K. C.; Li, S. F. Y., Minimization of Sample Discrimination Introduced by on-Column Fracture/Electrokinetic Injection in Capillary Electrophoresis. *Analytical Chemistry* **1998,** *70* (11), 2248-2253.

87. Engelhardt, H.; Beck, W.; Kohr, J.; Schmitt, T., Capillary Electrophoresis - Methods and Scope. *Angewandte Chemie-International Edition in English* **1993,** *32* (5), 629-649.

88. Krivácsy, Z.; Gelencsér, A.; Hlavay, J.; Kiss, G.; Sárvári, Z., Electrokinetic Injection in Capillary Electrophoresis and Its Application to the Analysis of Inorganic Compounds. *Journal of Chromatography A* **1999,** *834* (1-2), 21-44.

89. Huang, X.; Gordon, M. J.; Zare, R. N., Bias in Quantitative Capillary Zone Electrophoresis Caused by Electrokinetic Sample Injection. *Analytical Chemistry* **1988,** *60* (4), 375-377.

90. Terabe, S.; Otsuka, K.; Ichikawa, K.; Tsuchiya, A.; Ando, T., Electrokinetic Separations with Micellar Solutions and Open-Tubular Capillaries. *Analytical Chemistry* **1984,** *56* (1), 111-113.

91. Köller, G.; Rolle-Kampczyk, U.; Lehmann, I.; Popp, P.; Herbarth, O., Determination of Ochratoxin a in Small Volumes of Human Blood Serum. *Journal of Chromatography B* **2004,** *804* (2), 313-317.

92. Jumppanen, J. H.; Riekkola, M.-L., Marker Techniques for High-Accuracy Identification in Cze. *Analytical Chemistry* **1995,** *67* (6), 1060-1066.

93. Boone, C. M.; Franke, J.-P.; de Zeeuw, R. A.; Ensing, K., Evaluation of Capillary Electrophoretic Techniques Towards Systematic Toxicological Analysis. *Journal of Chromatography A* **1999,** *838* (1–2), 259-272.

94. Chen, N.; Wang, L.; Zhang, Y. K., Electrophoretic Selectivity as a Function of Operating Parameters in Free Solution Capillary Electrophoretic Separation of Dipeptides. *Journal of Liquid Chromatography* **1993,** *16* (17), 3609-3622.

95. Lee, T. T.; Yeung, E. S., Facilitating Data Transfer and Improving Precision in Capillary Zone Electrophoresis with Migration Indexes. *Analytical Chemistry* **1991,** *63* (24), 2842-2848.

96. Natsuki, I.; Yuji, Y.; Takeshi, H., Electropherogram of Capillary Zone Electrophoresis with Effective Mobility Axis as a Transverse Axis and Its Analytical Utility I. Transformation Applying the Hypothetical Electroosmotic Flow. *Electrophoresis* **2000,** *21* (2), 360-366.

97. Philippe, S.-K.; Andrej, V. G.; Alexey, V. K.; Franz, M.; Irina, V. P.; Norbert, H.; Dieter, F.; Valery, S. P.; Antonius, K., Quantitative and Qualitative Precision Improvements by Effective Mobility-Scale Data Transformation in Capillary Electrophoresis Analysis. *Electrophoresis* **2001,** *22* (1), 77-87.

98. Picou, R.; Moses, J. P.; Wellman, A. D.; Kheterpal, I.; Gilman, S. D., Analysis of Monomeric Aβ Peptide by Capillary Electrophoresis. *Analyst* **2010,** *135* (7), 1631-1635.

99. Schmitt-Kopplin, P.; Garmash, A. V.; Kudryavtsev, A. V.; Menzinger, F.; Perminova, I. V.; Hertkorn, N.; Freitag, D.; Petrosyan, V. S.; Kettrup, A., Quantitative and Qualitative Precision Improvements by Effective Mobility-Scale Data Transformation in Capillary Electrophoresis Analysis. *Electrophoresis* **2001,** *22* (1), 77-87.

100. Ikuta, N.; Yamada, Y.; Yoshiyama, T.; Hirokawa, T., New Method for Standardization of Electropherograms Obtained in Capillary Zone Electrophoresis. *Journal of Chromatography A* **2000,** *894* (1-2), 11-17.

101. Iwata, T.; Koshoubu, J.; Kurosu, Y., Electropherograms in Capillary Zone Electrophoresis Plotted as a Function of the Quantity of Electric Charge. *Journal of Chromatography A* **1998,** *810* (1-2), 183-191.

102. Mammen, M.; Colton, I. J.; Carbeck, J. D.; Bradley, R.; Whitesides, G. M., Representing Primary Electrophoretic Data in the 1/Time Domain: Comparison to Representations in the Time Domain. *Analytical Chemistry* **1997,** *69* (11), 2165-2170.

103. Markov, D. A.; Bornhop, D. J., Nanoliter-Scale Non-Invasive Flow-Rate Quantification Using Micro-Interferometric Back-Scatter and Phase Detection. *Fresenius Journal of Analytical Chemistry* **2001,** *371* (2), 234-237.

104. StClaire, J. C.; Hayes, M. A., Heat Index Flow Monitoring in Capillaries with Interferometric Backscatter Detection. *Analytical Chemistry* **2000,** *72* (19), 4726-4730.

105. Saito, R. M.; Neves, C. A.; Lopes, F. S.; Blanes, L.; Brito-Neto, J. G. A.; do Lago, C. L., Monitoring the Electroosmotic Flow in Capillary Electrophoresis Using Contactless Conductivity Detection and Thermal Marks. *Analytical Chemistry* **2007,** *79* (1), 215-223.

106. Seiman, A.; Vaher, M.; Kaljurand, M., Monitoring of the Electroosmotic Flow of Ionic Liquid Solutions in Non-Aqueous Media Using Thermal Marks. *Journal of Chromatography A* **2008,** *1189* (1-2), 266-273.

107. Lee, T. T.; Dadoo, R.; Zare, R. N., Real-Time Measurement of Electroosmotic Flow in Capillary Zone Electrophoresis. *Analytical Chemistry* **1994,** *66* (17), 2694-2700.

108. Pittman, J. L.; Gilman, S. D.; Schrum, K. F., On-Line Monitoring of Electroosmotic Flow for Capillary Electrophoretic Separations. *The Analyst* **2001,** *126* (8), 1240-1247.

109. Schrum, K. F.; Lancaster, J. M.; Johnston, S. E.; Gilman, S. D., Monitoring Electroosmotic Flow by Periodic Photobleaching of a Dilute, Neutral Fluorophore. *Analytical Chemistry* **2000,** *72* (18), 4317-4321.

110. Pittman, J. L.; Gessner, H. J.; Frederick, K. A.; Raby, E. M.; Batts, J. B.; Gilman, S. D., Experimental Studies of Electroosmotic Flow Dynamics During Sample Stacking for Capillary Electrophoresis. *Analytical Chemistry* **2003,** *75* (14), 3531-3538.

111. Pittman, J. L.; Henry, C. S.; Gilman, S. D., Experimental Studies of Electroosmotic Flow Dynamics in Microfabricated Devices During Current Monitoring Experiments. *Analytical Chemistry* **2003,** *75* (3), 361-370.

112. Huang, X.; Coleman, W. F.; Zare, R. N., Analysis of Factors Causing Peak Broadening in Capillary Zone Electrophoresis. *Journal of Chromatography A* **1989,** *480*, 95-110.

113. Leube, J.; Roeckel, O., Quantification in Capillary Zone Electrophoresis for Samples Differing in Composition from the Electrophoresis Buffer. *Analytical Chemistry* **1994,** *66* (7), 1090-1096.

114. Hettiarachchi, K.; Cheung, A. P., Precision in Capillary Electrophoresis with Respect to Quantitative Analysis of Suramin. *Journal of Chromatography A* **1995,** *717* (1-2), 191-202.

115. Fujiwara, S.; Honda, S., Determination of Cinnamic Acid and Its Analogs by Electrophoresis in a Fused-Silica Capillary Tube. *Analytical Chemistry* **1986,** *58* (8), 1811-1814.

116. Huang, X. H.; Luckey, J. A.; Gordon, M. J.; Zare, R. N., Qunatitative-Analysis of Low-Molecular Weight Carboxylic-Acids by Capillary Zone Electrophoresis Conductivity Detection. *Analytical Chemistry* **1989,** *61* (7), 766-770.

117. Williams, S. J.; Goodall, D. M.; Evans, K. P., Analysis of Anthraquinone Sulphonates : Comparison of Capillary Electrophoresis with High-Performance Liquid Chromatography. *Journal of Chromatography A* **1993,** *629* (2), 379-384.

118. Dose, E. V.; Guiochon, G. A., Internal Standardization Technique for Capillary Zone Electrophoresis. *Analytical Chemistry* **1991,** *63* (11), 1154-1158.

119. Altria, K. D.; Harden, R. C.; Hart, M.; Hevizi, J.; Hailey, P. A.; Makwana, J. V.; Portsmouth, M. J., Inter-Company Cross-Validation Exercise on Capillary Electrophoresis : I. Chiral Analysis of Clenbuterol. *Journal of Chromatography A* **1993,** *641* (1), 147-153.

120. Gilman, S. D.; Chapman, P. J., Measuring Electroosmotic Flow in Microchips and Capillaries. *Methods Mol. Biol. (Totowa, NJ, U. S.)* **2006,** *339* (Microchip Capillary Electrophoresis), 187-201.

121. Smith, S. C.; Strasters, J. K.; Khaledi, M. G., Influence of Operating Parameters on Reproducibility in Capillary Electrophoresis. *Journal of Chromatography A* **1991,** *559* (1-2), 57-68.

122. Radim, V.; Petr, G.; Petr, B., Identification of Peaks in Capillary Zone Electrophoresis Based on Actual Mobilities. *Electrophoresis* **1992,** *13* (1), 677-682.

123. K. D. Lukacs, J. W. J., Capillary Zone Electrophoresis: Effect of Physical Parameters on Separation Efficiency and Quantitation. *Journal of High Resolution Chromatography* **1985,** *8* (8), 407-411.

124. Li, X.-F.; Ren, H.; Le, X.; Qi, M.; Ireland, I. D.; Dovichi, N. J., Migration Time Correction for the Analysis of Derivatized Amino Acids and Oligosaccharides by Micellar Capillary Electrochromatography. *Journal of Chromatography A* **2000,** *869* (1-2), 375-384.

125. Wanders, B. J.; van de Goor, T. A. A. M.; Everaerts, F. M., On-Line Measurement of Electroosmosis in Capillary Electrophoresis Using a Conductivity Cell. *Journal of Chromatography A* **1993,** *652* (1), 291-294.

126. O'Grady, J. F.; Noonan, K. Y.; McDonnell, P.; Mancuso, A. J.; Frederick, K. A., Detecting Deviations from Pure Eof During Ce Separations. *Electrophoresis* **2007,** *28* (14), 2385-2390.

127. Kraly, J.; Fazal, M. A.; Schoenherr, R. M.; Bonn, R.; Harwood, M. M.; Turner, E.; Jones, M.; Dovichi, N. J., Bioanalytical Applications of Capillary Electrophoresis. *Analytical Chemistry* **2006,** *78* (12), 4097-4110.

128. Xue, Q.; Yeung, E. S., Indirect Fluorescence Determination of Lactate and Pyruvate in Single Erythrocytes by Capillary Electrophoresis. *Journal of Chromatography A* **1994,** *661* (1-2), 287-295.

129. Chen, F.-T. A.; Sternberg, J. C., Characterization of Proteins by Capillary Electrophoresis in Fused-Silica Columns: Review on Serum Protein Analysis and Application to Immunoassays. *ELECTROPHORESIS* **1994,** *15* (1), 13-21.

130. Hogan, B. L.; Yeung, E. S., Determination of Intracellular Species at the Level of a Single Erythrocyte Via Capillary Electrophoresis with Direct and Indirect Fluorescence Detection. *Analytical Chemistry* **1992,** *64* (22), 2841-2845.

131. Gordon, M. J.; Lee, K. J.; Arias, A. A.; Zare, R. N., Protocol for Resolving Protein Mixtures in Capillary Zone Electrophoresis. *Analytical Chemistry* **1991,** *63* (1), 69-72.

132. Jorgenson, J. W.; Lukacs, K. D., Free-Zone Electrophoresis in Glass-Capillaries. *Clinical Chemistry* **1981,** *27* (9), 1551-1553.

133. Yu, M.; Dovichi, N. J., Attomole Amino Acid Determination by Capillary Zone Electrophoresis with Thermooptical Absorbance Detection. *Analytical Chemistry* **1989,** *61* (1), 37-40.

134. Felhofer, J. L.; Blanes, L.; Garcia, C. D., Recent Developments in Instrumentation for Capillary Electrophoresis and Microchip-Capillary Electrophoresis. *ELECTROPHORESIS* **2010,** *31* (15), 2469-2486.

135. Stutz, H., Protein Attachment onto Silica Surfaces - a Survey of Molecular Fundamentals, Resulting Effects and Novel Preventive Strategies in Ce. *Electrophoresis* **2009,** *30* (12), 2032-2061.

136. Rodriguez, I.; Li, S. F. Y., Surface Deactivation in Protein and Peptide Analysis by Capillary Electrophoresis. *Analytica Chimica Acta* **1999,** *383* (1-2), 1-26.

137. Ghosal, S., Effect of Analyte Adsorption on the Electroosmotic Flow in Microfluidic Channels. *Analytical Chemistry* **2002,** *74* (4), 771-775.

138. Graf, M.; García, R. G.; Wätzig, H., Protein Adsorption in Fused-Silica and Polyacrylamide-Coated Capillaries. *Electrophoresis* **2005,** *26* (12), 2409-2417.

139. Lee, T. T.; Yeung, E. S., Quantitative Determination of Native Proteins in Individual Human Erythrocytes by Capillary Zone Electrophoresis with Laser-Induced Fluorescence Detection. *Analytical Chemistry* **1992,** *64* (23), 3045-3051.

140. Ghosal, S., Band Broadening in a Microcapillary with a Stepwise Change in the Zeta-Potential. *Analytical Chemistry* **2002,** *74* (16), 4198-4203.

141. Fang, N.; Zhang, H.; Li, J.; Li, H.-W.; Yeung, E. S., Mobility-Based Wall Adsorption Isotherms for Comparing Capillary Electrophoresis with Single-Molecule Observations. *Analytical Chemistry* **2007,** *79* (16), 6047-6054.

142. Salim, M.; O'Sullivan, B.; McArthur, S. L.; Wright, P. C., Characterization of Fibrinogen Adsorption onto Glass Microcapillary Surfaces by Elisa. *Lab on a Chip* **2007,** *7* (1), 64-70.

143. Lionello, A.; Josserand, J.; Jensen, H.; Girault, H. H., Protein Adsorption in Static Microsystems: Effect of the Surface to Volume Ratio. *Lab on a Chip* **2005,** *5* (3), 254-260.

144. Rossier, J. S.; Gokulrangan, G.; Girault, H. H.; Svojanovsky, S.; Wilson, G. S., Characterization of Protein Adsorption and Immunosorption Kinetics in Photoablated Polymer Microchannels. *Langmuir* **2000,** *16* (22), 8489-8494.

145. Wojciechowski, P.; Ten Hove, P.; Brash, J. L., Phenomenology and Mechanism of the Transient Adsorption of Fibrinogen from Plasma (Vroman Effect). *Journal of Colloid and Interface Science* **1986,** *111* (2), 455-465.

146. Salim, M.; Wright, P. C.; McArthur, S. L., Studies of Electroosmotic Flow and the Effects of Protein Adsorption in Plasma-Polymerized Microchannel Surfaces. *ELECTROPHORESIS* **2009,** *30* (11), 1877-1887.

147. Swords, K. E.; Bartline, P. B.; Roguski, K. M.; Bashaw, S. A.; Frederick, K. A., Assessment of Polyelectrolyte Coating Stability under Dynamic Buffer Conditions in Ce. *Journal of Separation Science* **2011,** *34* (18), 2427-2432.

148. Burns, S. T.; Agbodjan, A. A.; Khaledi, M. G., Characterization of Solvation Properties of Lipid Bilayer Membranes in Liposome Electrokinetic Chromatography. *Journal of Chromatography A* **2002,** *973* (1-2), 167-176.

149. Bordi, F.; Cametti, C.; Diociaiuti, M.; Gaudino, D.; Gili, T.; Sennato, S., Complexation of Anionic Polyelectrolytes with Cationic Liposomes:Â€‰ Evidence of Reentrant Condensation and Lipoplex Formation. *Langmuir* **2004,** *20* (13), 5214-5222.

150. Shin, J. H.; Lee, G. M.; Kim, J. H., Comparison of Cell Disruption Methods for Determining B-Galactosidase Activity Expressed in Animal Cells. *Biotechnology Techniques* **1994,** *8* (6), 425-430.

151. Ermakov, S. V.; Zhukov, M. Y.; Capelli, L.; Righetti, P. G., Wall Adsorption in Capillary Electrophoresis Experimental Study and Computer Simulation. *Journal of Chromatography A* **1995,** *699* (1-2), 297-313.

152. Gray, J. J., The Interaction of Proteins with Solid Surfaces. *Current Opinion in Structural Biology* **2004,** *14* (1), 110-115.

153. Haynes, C. A.; Norde, W., Globular Proteins at Solid/Liquid Interfaces. *Colloids and Surfaces B: Biointerfaces* **1994,** *2* (6), 517-566.

154. Malmsten, M., Formation of Adsorbed Protein Layers. *Journal of Colloid and Interface Science* **1998,** *207* (2), 186-199.

155. Essa, H.; Magner, E.; Cooney, J.; Hodnett, B. K., Influence of Ph and Ionic Strength on the Adsorption, Leaching and Activity of Myoglobin Immobilized onto Ordered Mesoporous Silicates. *Journal of Molecular Catalysis B: Enzymatic* **2007,** *49* (1–4), 61-68.

156. Moore, A. W.; Jorgenson, J. W., Study of Zone Broadening in Optically Gated High-Speed Capillary Electrophoresis. *Analytical Chemistry* **1993,** *65* (24), 3550-3560.

157. Walbroehl, Y.; Jorgenson, J. W., Capillary Zone Electrophoresis for the Determination of Electrophoretic Mobilities and Diffusion Coefficients of Proteins. *Journal of Microcolumn Separations* **1989,** *1* (1), 41-45.

158. Ghosal, S., Fluid Mechanics of Electroosmotic Flow and Its Effect on Band Broadening in Capillary Electrophoresis. *Electrophoresis* **2004,** *25* (2), 214-228.

159. Ren, L.; Li, D., Electroosmotic Flow in Heterogeneous Microchannels. *Journal of Colloid and Interface Science* **2001,** *243* (1), 255-261.

160. Vogler, E. A., Structure and Reactivity of Water at Biomaterial Surfaces. *Advances in Colloid and Interface Science* **1998,** *74* (1-3), 69-117.

161. Valkó, I. E.; Sirén, H.; Riekkola, M.-L., Characteristics of Electroosmotic Flow in Capillary Electrophoresis in Water and in Organic Solvents without Added Ionic Species. *Journal of Microcolumn Separations* **1999,** *11* (3), 199-208.

162. Cottet, H.; Struijk, M. P.; Van Dongen, J. L. J.; Claessens, H. A.; Cramers, C. A., Non-Aqueous Capillary Electrophoresis Using Non-Dissociating Solvents: Application to the Separation of Highly Hydrophobic Oligomers. *Journal of Chromatography A* **2001,** *915* (1–2), 241-251.

163. Zuidam, N. J.; Versluis, C.; Vernooy, E. A. A. M.; Crommelin, D. J. A., Gamma-Irradiation of Liposomes Composed of Saturated Phospholipids. Effect of Bilayer Composition, Size, Concentration and Absorbed Dose on Chemical Degradation and Physical Destabilization of Liposomes. *Biochimica et Biophysica Acta (BBA) - Biomembranes* **1996,** *1280* (1), 135-148.

164. Richard, A. J.; Stephens, J. M., Emerging Roles of Jak-Stat Signaling Pathways in Adipocytes. *Trends in Endocrinology and Metabolism* **2011,** *22* (8), 325-332.

165. Simpson, M. A.; LiCata, V. J.; Ribarik Coe, N.; Bernlohr, D. A., Biochemical and Biophysical Analysis of the Intracellular Lipid Binding Proteins of Adipocytes. *Molecular and Cellular Biochemistry* **1999,** *192* (1), 33-40.

166. Jenkins, M. A.; Guerin, M. D., Optimization of Serum Protein Separation by Capillary Electrophoresis. *Clinical Chemistry* **1996,** *42* (11), 1886-1886.

167. Van Dyck, S.; Kaale, E.; Nováková, S.; Glatz, Z.; Hoogmartens, J.; Van Schepdael, A., Advances in Capillary Electrophoretically Mediated Microanalysis. *Electrophoresis* **2003,** *24* (22-23), 3868-3878.

168. Shihabi, Z. K., Stacking in Capillary Zone Electrophoresis. *Journal of Chromatography A* **2000,** *902* (1), 107-117.

169. Osbourn, D. M.; Weiss, D. J.; Lunte, C. E., On-Line Preconcentration Methods for Capillary Electrophoresis. *Electrophoresis* **2000,** *21* (14), 2768-2779.

170. Shihabi, Z. K., Stacking and Discontinuous Buffers in Capillary Zone Electrophoresis. *Electrophoresis* **2000,** *21* (14), 2872-2878.

171. Malá, Z.; Gebauer, P.; Boček, P., Contemporary Sample Stacking in Analytical Electrophoresis. *Electrophoresis* **2011,** *32* (1), 116-126.

172. Simpson Jr, S. L.; Quirino, J. P.; Terabe, S., On-Line Sample Preconcentration in Capillary Electrophoresis: Fundamentals and Applications. *Journal of Chromatography A* **2008,** *1184* (1–2), 504-541.

173. Chien, R.-L.; Burgi, D. S., Field Amplified Sample Injection in High-Performance Capillary Electrophoresis. *Journal of Chromatography A* **1991,** *559* (1-2), 141-152.

174. Albert, M.; Debusschere, L.; Demesmay, C.; Rocca, J. L., Large-Volume Stacking for Quantitative Analysis of Anions in Capillary Electrophoresis I. Large-Volume Stacking with Polarity Switching. *Journal of Chromatography A* **1997,** *757* (1–2), 281-289.

175. Zhu, L.; Lee, H. K., Field-Amplified Sample Injection Combined with Water Removal by Electroosmotic Flow Pump in Acidic Buffer for Analysis of Phenoxy Acid Herbicides by Capillary Electrophoresis. *Analytical Chemistry* **2001,** *73* (13), 3065-3072.

176. Schwer, C.; Gas, B.; Lottspeich, F.; Kenndler, E., Computer Simulation and Experimental Evaluation of on-Column Sample Preconcentration in Capillary Zone Electrophoresis by Discontinuous Buffer Systems. *Analytical Chemistry* **1993,** *65* (15), 2108-2115.

177. Foret, F.; Szoko, E.; Karger, B. L., On-Column Transient and Coupled Column Isotachophoretic Preconcentration of Protein Samples in Capillary Zone Electrophoresis. *Journal of Chromatography A* **1992,** *608* (1–2), 3-12.

178. Li, T.; Booker, C. J.; Yeung, K. K. C., Migration Behaviour of Discontinuous Buffers in Capillary Electrophoresis During Protein Enrichment. *Analyst* **2012,** *137* (20), 4766-4773.

179. Nesbitt, C. A.; Lo, J. T. M.; Yeung, K. K. C., Over 1000-Fold Protein Preconcentration for Microliter-Volume Samples at a Ph Junction Using Capillary Electrophoresis. *Journal of Chromatography A* **2005,** *1073* (1–2), 175-180.

180. Arnett, S. D.; Lunte, C. E., Enhanced Ph-Mediated Stacking of Anions for Ce Incorporating a Dynamic Ph Junction. *Electrophoresis* **2007,** *28* (20), 3786-3793.

181. Foret, F.; Fanali, S.; Bocek, P., Applicability of Dynamic Change of Ph in the Capillary Zone Electrophoresis of Proteins. *Journal of Chromatography A* **1990,** *516* (1), 219-222.

182. Schwer, C.; Kenndler, E., Electrophoresis in Fused-Silica Capillaries: The Influence of Organic Solvents on the Electroosmotic Velocity and The .Zeta. Potential. *Analytical Chemistry* **1991,** *63* (17), 1801-1807.

183. Urbánek, M.; Křivánková, L.; Boček, P., Stacking Phenomena in Electromigration: From Basic Principles to Practical Procedures. *Electrophoresis* **2003,** *24* (3), 466-485.

184. Hruška, V.; Jaroš, M.; Gaš, B., Simul 5 – Free Dynamic Simulator of Electrophoresis. *Electrophoresis* **2006,** *27* (5-6), 984-991.

185. Beckers, J. L.; Verheggen, T. P. E. M.; Everaerts, F. M., Use of a Double-Detector System for the Measurement of Mobilities in Zone Electrophoresis. *Journal of Chromatography A* **1988,** *452* (0), 591-600.

186. Klonis, N.; Sawyer, W. H., Spectral Properties of the Prototropic Forms of Fluorescein in Aqueous Solution. *Journal of Fluorescence* **1996,** *6* (3), 147-157.

187. Thormann, W.; Zhang, C.-X.; Caslavska, J.; Gebauer, P.; Mosher, R. A., Modeling of the Impact of Ionic Strength on the Electroosmotic Flow in Capillary Electrophoresis with Uniform and Discontinuous Buffer Systems. *Analytical Chemistry* **1998,** *70* (3), 549-562.

188. Petr, J.; Maier, V.; Horáková, J.; Ševčík, J., Simultaneous Contactless Conductivity Detection and Uv Detection for the Study of Separation of Tamsulosin Enantiomers in Discontinuous Electrolyte Systems by Ce. *Electrophoresis* **2006,** *27* (23), 4735-4745.

189. Poppe, H., Overloading and Interaction Phenomena in Electrophoretic Separations. *Analytical Chemistry* **1992,** *64* (17), 1908-1919.

190. Štědrý, M.; Jaroš, M.; Hruška, V.; Gaš, B., Eigenmobilities in Background Electrolytes for Capillary Zone Electrophoresis: Iii. Linear Theory of Electromigration. *Electrophoresis* **2004,** *25* (18-19), 3071-3079.

191. Beckers, J. L.; Boček, P., System Zones in Capillary Zone Electrophoresis: Moving Boundaries Caused by Freely Migrating Hydrogen Ions. *Electrophoresis* **2005,** *26* (2), 446-452.

192. Malá, Z.; Gebauer, P.; Boček, P., System Effects in Sample Self-Stacking Cze: Single Analyte Peak Splitting of Salt-Containing Samples. *Electrophoresis* **2009,** *30* (5), 866-874.

193. Vítková, K.; Petr, J.; Maier, V.; Znaleziona, J.; Ševčík, J., Study of Electromigration Effects on a Ph Boundary During the on-Line Electrokinetic Preconcentration by Capillary Electrophoresis. *Electrophoresis* **2010,** *31* (16), 2771-2777.

194. Yu, J.-W.; Chou, Y.; Yang, R.-J., High-Resolution Modeling of Isotachophoresis and Zone Electrophoresis. *Electrophoresis* **2008,** *29* (5), 1048-1057.

195. Mosher, R. A.; Thormann, W.; Graham, A.; Bier, M., The Formation of Stable Ph Gradients with Weak Monovalent Buffers for Isoelectric Focusing in Free Solution. *Electrophoresis* **1985,** *6* (11), 545-551.

196. Mao, Q.; Pawliszyn, J.; Thormann, W., Dynamics of Capillary Isoelectric Focusing in the Absence of Fluid Flow: High-Resolution Computer Simulation and Experimental Validation with Whole Column Optical Imaging. *Analytical Chemistry* **2000,** *72* (21), 5493-5502.

197. Breadmore, M. C.; Quirino, J. P.; Thormann, W., High-Resolution Computer Simulations of Ekc. *Electrophoresis* **2009,** *30* (4), 570-578.

198. Dubský, P.; Svobodová, J.; Gaš, B., Model of Ce Enantioseparation Systems with a Mixture of Chiral Selectors: Part I. Theory of Migration and Interconversion. *Journal of Chromatography B* **2008,** *875* (1), 30-34.

199. Thormann, W.; Breadmore, M. C.; Caslavska, J.; Mosher, R. A., Dynamic Computer Simulations of Electrophoresis: A Versatile Research and Teaching Tool. *Electrophoresis* **2010,** *31* (5), 726-754.

200. Stahl, J. W.; Catherman, A. D.; Sampath, R. K.; Seneviratne, C. A.; Strein, T. G., Investigating the Effects of Conductivity on Zone Overlap with Emma: Computer Simulation and Experiment. *Electrophoresis* **2011,** *32* (12), 1492-1499.

APPENDIX: EQUATIONS USED IN DATA ANALYSIS

Neutral marker method

(from ref [120])

$$v_{eof} = \frac{L_d}{t_m} \quad \text{(A1)}$$

$$\mu_{eof} = \frac{v_{eof} * L_t}{V} \quad \text{(A2)}$$

$$v_{net} = \frac{L_d}{t_r} \quad \text{(A3)}$$

$$\mu_{net} = \mu_{ep} + \mu_{eof} \quad \text{(A4)}$$

$$v_{net} = \mu_{net} * E = (\mu_{ep} + \mu_{eof}) * E \quad \text{(A5)}$$

v_{eof}: electroosmotic flow velocity

L_d: capillary length to the detection point

t_m: migration time of EOF marker

μ_{eof}: electroosmotic flow mobility

L_t: total capillary length

V: applied voltage

v_{net}: net electrophoretic velocity

t_r: migration time of analyte

μ_{net}: net mobility

μ_{ep}: electrophoretic mobility

E: electric field

EOF monitoring method

$$\mu_{eof} = v_{ave(eof)}/E \quad \text{(A6)}$$

$v_{ave(eof)}$: average EOF velocity at the migration time of the analyte

Multiple marker method

(from ref [92])

$$a = \begin{matrix} \frac{1}{2}t_1^2 & t_1 & \mu_1 t_1 \\ \frac{1}{2}t_2^2 & t_2 & \mu_2 t_1 \\ \frac{1}{2}t_3^2 & t_3 & \mu_3 t_3 \end{matrix} \quad \text{(A7)}$$

$$b = \begin{matrix} L_{eff} \\ L_{eff} \\ L_{eff} \end{matrix} \quad \text{(A8)}$$

$$x = \begin{matrix} b \\ a \\ E \end{matrix} \quad \text{(A9)}$$

t_1: migration time of first marker

t_2: migration time of second marker

t_3: migration time of third marker

μ_1: electrophoretic mobility of first marker

μ_2: electrophoretic mobility of second marker

μ_3: electrophoretic mobility of third marker

$$\mu_{ep(x)} = ({}^{L_{eff}}/_{t_x} - {}^{bt_x}/_{2} - a)/E \quad \text{(A10)}$$

$\mu_{ep(x)}$: electrophoretic mobility of analyte x

t_x: migration time of analyte x

$$v_{eof} = bt + a \quad \text{(A11)}$$

Migration time ratio method

(from ref [44])

$$\text{Migration time ratio} = \frac{t_m}{t_r} \quad \text{(A12)}$$

t_m: migration time of EOF marker

t_r: migration time of analyte

Migration index method

(from ref [95])

$$MI = \int_0^t \frac{i}{L_t} dt \quad \text{(A13)}$$

$$AMI = \frac{(MI_{eof}) * MI}{MI_{eof} - MI} \quad \text{(A14)}$$

MI: migration index

i: current density

L_t: capillary length

AMI: adjusted migration index

MI_{eof}: migration index of EOF marker

VITA

Funda Kizilkaya was born in Ankara, Turkey. She graduated from 9 Eylul University with a Bachelor in Architecture degree in 1998. In 2005, she began graduate school at Louisiana State University in Department of Chemistry. She is currently a candidate for the degree of Doctor of Philosophy in analytical chemistry. She is married to Orhan Kizilkaya and they have two beautiful children.